March 1995
(Distributed: April 1995)

AFOSR-TR-95

0609

ANNUAL TECHNICAL REPORT
to

US AIR FORCE OFFICE OF SCIENTIFIC RESEARC.

Bolling Air Force Base
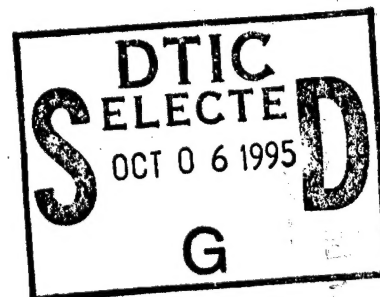Washington DC 20332-6448

AFOSR Grant No. 94-0143

TRANSPORT PHENOMENA AND INTERFACIAL KINETICS IN MULTIPHASE COMBUSTION SYSTEMS

Principal Investigator: **Daniel E. Rosner**

Period Covered: 15 February 1994 to 14 February 1995

Yale University

High Temperature Chemical Reaction Engineering Laboratory
Department of Chemical Engineering
PO Box 208286 YS, New Haven, CT 06520-8286 USA

DTIC
ELECTE
OCT 0 6 1995
G

LUX ET VERITAS

APPROVED FOR PUBLIC RELEASE: DISTRIBUTION UNLIMITED

19951004 150

DTIC QUALITY INSPECTED 8

TRANSPORT PHENOMENA AND INTERFACIAL KINETICS IN MULTIPHASE COMBUSTION SYSTEMS

Principal Investigator: Prof. **Daniel E. Rosner**

TABLE OF CONTENTS

Gokoglu, S.A., Stewart, G.D., Collins, J., and Rosner, D.E.,"Numerical Analysis of an Impinging Jet Reactor for the CVD and Gas Phase Nucleation of Titania", **Mat. Res. Sympos. Proc. Vol. 335**, 171-176 (1994)

Rosner, D.E. and Tandon, P., "Prediction and Correlation of 'Accessible' Area of Large Multi-particle Aggregates ", *AIChE J.* **40** (7), 1167-1182 (1994)

Rosner, D.E., Tandon, P. and Konstandopoulos, A.G., "Rational Prediction of Inertially Induced Particle Deposition Rates for a Cylindrical Target in Dust-Laden Streams",*Proc. 1st Int. Particle Technology Forum*, AIChE , **Vol. II,** 374-381 (1994).

REPORT DOCUMENTATION PAGE

Public reporting burden for this collection of information is estimated to average 1 hour per response, including the time for reviewing instructions, searching existing data sources, gathering and maintaining the data needed, and completing and reviewing the collection of information. Send comments regarding this burden estimate or any other aspect of this collection of information, including suggestions for reducing this burden, to Washington Headquarters Services, Directorate for Information Operations and Reports, 1215 Jefferson Davis Highway, Suite 1204, Arlington, VA 22202-4302, and to the Office of Management and Budget, Paperwork Reduction Project (0704-0188), Washington, DC 20503.

1. AGENCY USE ONLY (Leave blank)	2. REPORT DATE March 1995	3. REPORT TYPE AND DATES COVERED Annual Tech. Rep. 2/15/94 - 2/14/95

4. TITLE AND SUBTITLE

(U) TRANSPORT PHENOMENA AND INTERFACIAL KINETICS IN MULTIPHASE COMBUSTION SYSTEMS

5. FUNDING NUMBERS

PE - 61102F
PR - 2308
SA - BS
G - F49620-94-1-0143

6. AUTHOR(S)

Daniel E. Rosner

7. PERFORMING ORGANIZATION NAME(S) AND ADDRESS(ES)

Yale University
High Temperature Chemical Reaction Engineering Laboratory
Department of Chemical Engineering
PO Box 208286 YS, New Haven, CT 06520-8286 USA

8. PERFORMING ORGANIZATION REPORT NUMBER

9. SPONSORING/MONITORING AGENCY NAME(S) AND ADDRESS(ES)

AFOSR/NA
110 Duncan Avenue, Suite B115
Bolling AFB DC 20332-0001

10. SPONSORING/MONITORING AGENCY REPORT NUMBER

Accesion For
NTIS CRA&I ☒
DTIC TAB ☐
Unannounced ☐
Justification _____

By _____
Distribution /

Availability Codes

11. SUPPLEMENTARY NOTES

12a. DISTRIBUTION/AVAILABILITY STATEMENT

Approved for public release; distribution is unlimited

12b. DISTRIBUTION CODE

Dist	Avail and/or Special
A-1	

13. ABSTRACT (Maximum 200 words)

Rational pseudo-continuum methods were developed to predict the *sintering kinetics, and the associated evolution of transport properties* (eg., Brownian coagulation rate constant) for aggregated 'soot' particles (eg., Al_2O_3, TiO_2) containing N ($\gg$1) primary particles in high temperature combustion gases. Results show a much weaker N-dependence of the total time required for "collapse" than $N^{1/3}$ (resulting from theories based on collapse at constant fractal dimension). Using both laser light scattering and thermophoretic sampling/TEM image analysis, comprehensive experiments were initiated to understand how changes in seed level, flame stoichiometry and strain rate influence the nature of the particles formed in the HTCRE Lab counterflow laminar diffusion flame burner. In ancillary theoretical studies, rational yet remarkably convenient methods were developed to predict the *erosion rates* of metal and ceramic solid surfaces (eg., circular cylinders, leading "edges") in abrasive, high-speed streams. It was found that metal targets "sharpen" while ceramic targets become "blunter"! Yale HTCRE Lab experimental data motivated the development of quantitative methods for predicting/correlating the effects particle formation in CVD thermal boundary layers on the rate and surface roughness of vapor-deposited ceramic thin films. Finally, a Damkohler number-based rational correlation for the density of vapor-deposited solids was developed and shown to be successful using literature data for the vapor deposition of seven important solid materials (including graphite and boron nitride).

14. SUBJECT Soot, aggregated particles, mass transport, thermophoresis, particle inertia, Brownian diffusion, chemical vapor deposition, particle sampling, nano-particle synthesis in flames, deposit microstructure/properties, Brownian diffusion, erosion of metals and ceramics	15. NUMBER OF PAGES 45
	16. PRICE CODE

17. SECURITY CLASSIFICATION OF REPORT Unclassified	18. SECURITY CLASSIFICATION OF THIS PAGE Unclassified	19. SECURITY CLASSIFICATION OF ABSTRACT Unclassified	20. LIMITATION OF ABSTRACT UL

TRANSPORT PHENOMENA AND INTERFACIAL KINETICS IN MULTIPHASE COMBUSTION SYSTEMS

Principal Investigator: Prof. **Daniel E. Rosner**

1. INTRODUCTION

The performance of ramjets burning slurry fuels (leading to condensed oxide aerosols and liquid film deposits), gas turbine engines in dusty or marine atmospheres, or when using fuels from non-traditional sources, depends upon the formation and transport of small particles across non-isothermal combustion gas boundary layers (BLs). Even airbreathing engines burning "clean" hydrocarbon fuels can experience *soot* formation/deposition problems (*e.g.*, combustor liner burnout, accelerated turbine blade erosion and "hot" corrosion). Moreover, particle formation and transport are important in many chemical reactors used to synthesize or process aerospace materials (turbine blade coatings, optical waveguides, ceramic precursor powders, fibers for composites,...). Accordingly, our research is directed toward providing chemical propulsion systems engineers and materials-oriented engineers with new techniques and quantitative information on important particle- and vapor-mass transport mechanisms and rates.

The purpose of this report is to summarize our research methods and accomplishments under AFOSR Grant 94-0143 (Technical Monitor: J. M. Tishkoff) during the 1-year period: 15 February '94-14 February '95. Readers interested in greater detail than contained in Section 2 are advised to consult the published papers explicitly cited in Sections 2 and 5. Copies of any of these published papers (Section 5.2 and Appendix) or preprints (Section 5.3) can be obtained by writing to the PI: Prof. Daniel E. Rosner, at the Department of Chemical Engineering, Yale University, New Haven , CT 06520-8286 USA. Comments on, or examples of, the *applications* of our research (Section 3.4) will be especially welcome.

An interactive experimental/theoretical approach has been used to gain understanding of performance-limiting chemical-, and mass/energy transfer-phenomena at or near interfaces. This included the development and exploitation of seeded laboratory counterflow diffusion flame burners (Section 2.1), new optical diagnostic and particle characterization techniques (Section 2.2) and induction-heated flow reactors (Section 2.4). Resulting experimental rate data , together with the predictions of asymptotic theories , continue to be used as the basis for proposing and verifying simple viewpoints and effective engineering correlations with a rational basis for future design/optimization studies.

2. RESEARCH ACCOMPLISHMENTS

Most of the results obtained under Grant AFOSR 94-0143 during 2/94-2/95 can be divided into the subsections below:

2.1. FORMATION, TRANSPORT AND STABILITY OF COMBUSTION-GENERATED PARTICLES: SEEDED LAMINAR COUNTERFLOW DIFFUSION FLAME EXPERIMENTS

Based on our recent measurements of the *thermophoretic diffusivity* of flame-generated submicron "soot" particles using a $TiCl_4(g)$-seeded low strain-rate counterflow laminar diffusion flame (CDF-) technique (Gomez and Rosner, 1993) we showed that a knowledge of the relative positions of the gas and particle phase stagnation planes and the associated local chemical environments, can be used to control the composition and morphology of flame-synthesized particles. These factors will also influence particle production and *radiation* from *turbulent* non-premixed "sooting" flames.

To obtain fundamental information on the nucleation, growth and restructuring kinetics of flame-generated aggregates, during this past year we have exploited an improved "slot-type" burner seeded with the TiO_2(s) vapor precursor: titanium tetra-iso-propoxide (TTIP) or the Al_2O_3(s) vapor precursor trimethyl aluminum (TMA) (Fig. 1) to carry out *in situ* measurements of aggregate dynamics and morphology evolution. For the latter we use the morphology-insensitive *thermophoretic sampling* technique (Rosner, Mackowski and Garcia-Ybarra, 1991) with carbon film-coated copper grids to extract aggregates from various positions in the seeded-CDF for morphological analysis using transmission electron microscope (TEM-)images (Fig. 2a). Aggregate data obtained from CH_4 flames seeded with TTIP- or TMA-vapor are now being obtained and analyzed using the theoretical methods briefly outlined in Section 2. Apart from characterizing the *fractal dimension*, D_f, of aggregates sampled from various points within the CDF, we are currently examining other potentially instructive "fingerprints", such as the distribution of the angles between triplets of primary particles, based on their projected TEM images. When corrected for the fact that the centroids of the particles comprising the aggregate are not all in one plane, we believe these histograms will be useful to characterize the degree of aggregate restructuring of moderate size aggregates in high temperature flames (see Section 2, Cohen and Rosner,1993,1994, and Tandon and Rosner,1995). Our long range goal is to understand how changes in seed level, flame stoichiometry and strain rate influence the nature of the particles formed in this well-defined *laminar* mixing/reaction zone, and to assess the relevance of this information to *turbulent* non-premixed reactors.

2.2 TRANSPORT AND RESTRUCTURING PROPERTIES OF FLAME-GENERATED AGGREGATES: THEORY

The ability to reliably predict the transport properties and morphological stability of *aggregated* flame-generated *particles* (carbonaceous soot, Al_2O_3, SiO_2,...) is important to many technologies, including chemical propulsion and refractory materials fabrication. Needed are methods to anticipate coagulation and ultimate deposition rates of suspended populations of such particles in combustion systems. Toward this end we are developing efficient methods for predicting the transport properties of large 'fractal' aggregates *via* a spatially variable effective porousity pseudo-continuum model. Since "young" small aggregates are frequently "stringy" (fractal dimensions much less than 2) we are also introducing an aggregate statistical characterization based on the *pdf* of angles between triplets of primary particles (Fig. 3 a,b), and developing methods to predict the evolution of such *pdf*s due to the *restructuring* mechanisms of Brownian motion, surface energy driven viscous flow, and/or capillary-condensation (Cohen and Rosner, 1993,1994). Indeed, these factors determine the observed size of the apparent "primary" particles comprising soot particles, the "collapse" of surface area observed in some high temperature systems, and the associated evolution of particle transport properties (see, eg., Tandon and Rosner, 1995).

These new methods/results, together with our recent estimates of the *spread* of aggregate sizes in coagulating populations, are now being used to predict particle *capture rates* on solid surfaces by the mechanisms of convective-diffusion, turbulent eddy-impaction, and thermophoresis (Rosner, Tassopoulos and Tandon, 1993,1994). Also under development are methods to predict interactions between aggregates and their surrounding *vapor* environment---interactions which can lead to primary particle growth, or burn-out. Toward this end, we have also developed new and efficient methods to predict the "accessible surface area" of populations of aggregates (expressed as a fraction, η_{pop}, of the true total surface area (Rosner and Tandon,1994), including its dependence on mean aggregate size (N), probing molecule reaction probability α, and pressure level (*via* Knudsen number based on primary particle diameter) for aggregates of a prescribed structure (fractal dimension, D_f).

We are now carrying out theoretical studies on the structure of thin reaction-nucleation-coagulation 'sublayers' within laminar mixing- and boundary- layers (Fig.7 below), including stagnation flows similar to those achieved in our counterflow burner (Fig. 1) and CVD-impingement flow reactor (Fig. 5). An account of our recent studies of the *unusual population dynamics* of coagulating absorbing-emitting particles in strong *radiation fields* will be found in *Aerosol Sci. Tech.* (Mackowski *et.al.*, 1993). For an overview of our work on these effects (energy transfer on particle dynamics), see our *IEC-Research* paper: Rosner, *et. al.*, 1992.
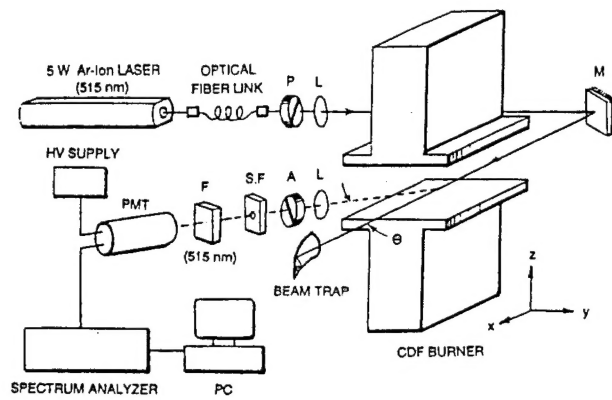
Fig.1 "Slot"-type laminar counterflow diffusion flame (CDF) burner set-up for *in situ* and extractive experimental studies of the nucleation, growth, transport and restructuring of aggregates in flames (after Albagli, Xing and Rosner,1995; see, also, Gomez and Rosner, 1993)
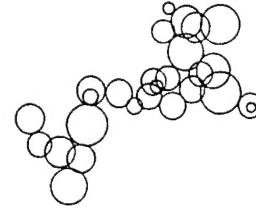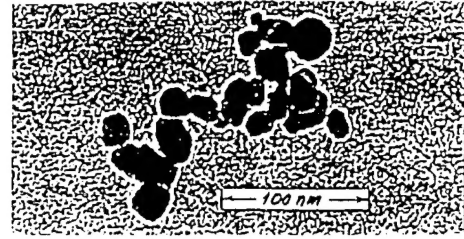
Fig. 2 Typical multi-particle aggregate thermophoretically extracted from laminar CDF ($CH_4/O_2/N_2$, equiv. ratio: 0.833, nom. strain rate 4 s^{-1}) seeded with TiO_2 precursor TTIP vapor. TEM image (a) compared with 'touching sphere' idealization (b) (after Albagli, Xing and Rosner, 1995)
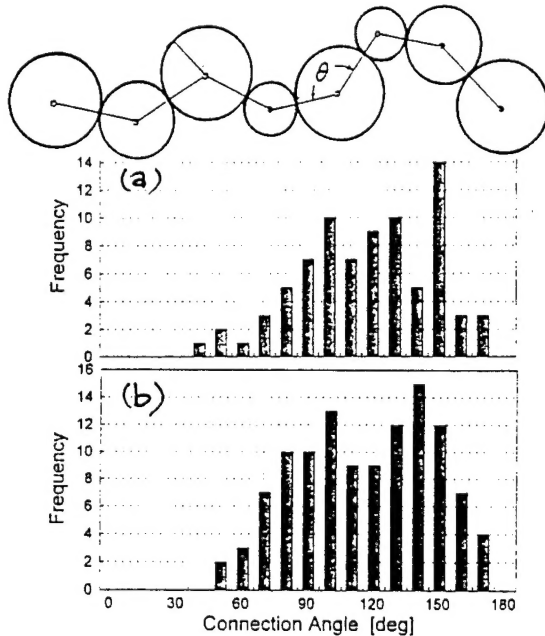
Fig. 3 Distribution of angles (projected) between touching 'primary' particles in sample of 7 multiparticle aggregates thermophoretically extracted from two locations on oxidizer side of laminar CDF seeded with TTIP: a) 5 mm from flame, b) 2 mm from flame (after Albagli, Xing and Rosner, 1994; see, also, Cohen and Rosner, 1993,1994))
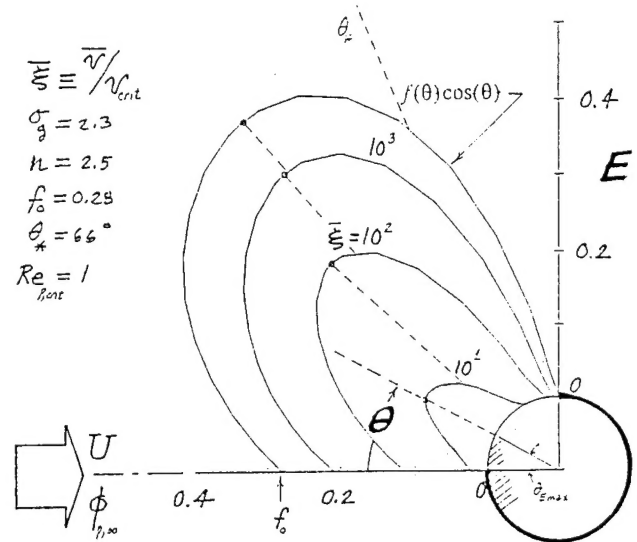
Fig.4 Predicted angular dependence of nondimensional *erosion* rate on an initially circular metal cylinder in high Reynolds number crossflow (after Rosner, Tandon, and Labowsky 1995). Here θ*=66° (incidence angle of maximum erosion yield), f0=0.28 (ratio of erosion yield at normal incidence to that at angle θ* , n=2.5, and log-normal population spread, σ_g, is 2.3)

3
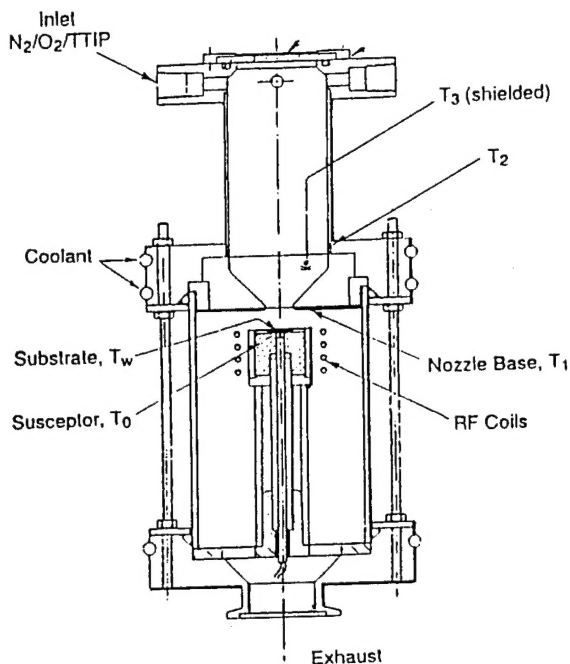
Fig. 5 Axisymmetric impinging jet CVD-flow reactor with inductively heated "pedestal" for studies of vapor + particle co-deposition across laminar BLs (after Rosner, Collins and Castillo, 1993, Collins, 1994, and Gokoglu et.al.,1994)
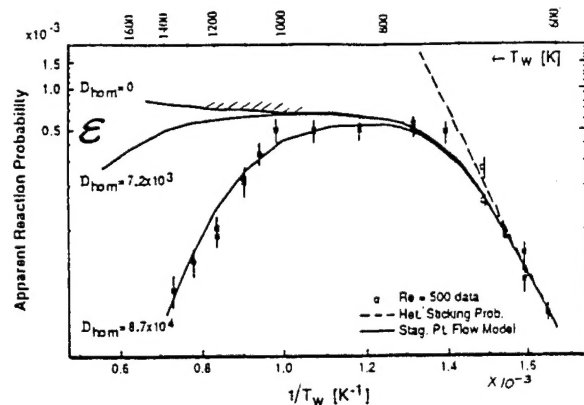
Fig.6 $TiO_2(s)$ deposition rate data (reported as apparent heterogeneous reaction probability ε) from $TTIP/O_2/N_2$ mainstream showing calculated deposition rate behavior in presence of *homogeneous* reactions to form non-depositing species (after Rosner, Collins and Castillo, 1993, Collins, 1994, Collins and Rosner, 1994)
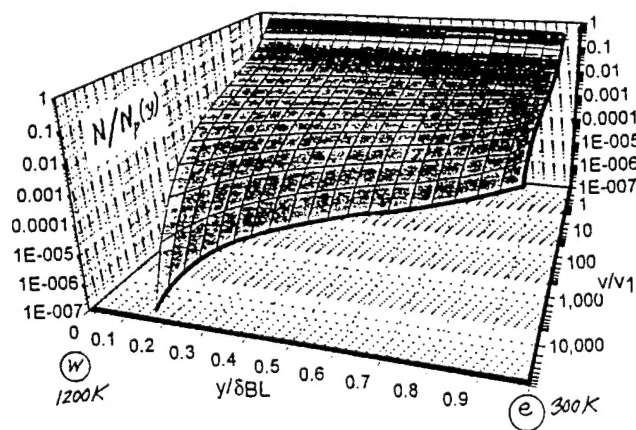
Fig. 7 Predicted local size distributions of particles nucleated within thermal boundary layer near hot deposition surface. y/δ_{BL} = relative position in LBL; v/v_1 = particle volume in monomer volume units (after Tandon and Rosner, 1995)
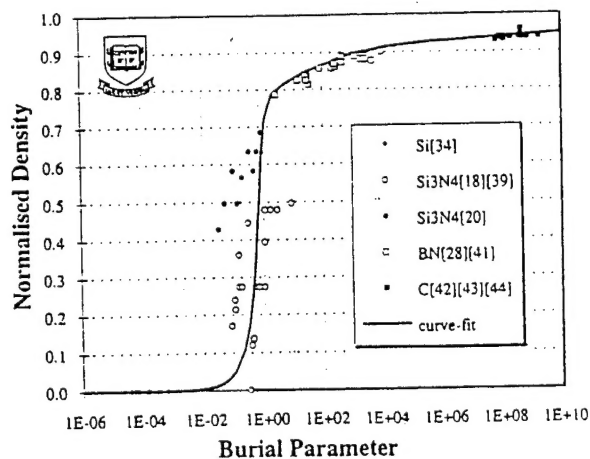
Fig. 8 "Universal" correlation of experimentally reported solid deposit densities based on a Damkohler number ("burial" parameter) comparing the characteristic times for surface reaction and surface diffusion (after Kho, Collins and Rosner, 1994)

4

2.3 EROSION BEHAVIOR OF CERAMIC OR METAL TARGETS IN HIGH-SPEED ABRASIVE STREAMS

By capturing with simple formulae the essential features of available *erosion yield* experiments (carried out using planar targets with suspended particles of a single size), we have developed an efficient method to predict local and total surface *erosion rates* for metal or ceramic targets of simple geometry exposed to a 'polydispersed' population of abrasive particles suspended in a high-speed mainstream (Rosner, Tandon and Labowsky, 1995, Kho, Rosner and Tandon,1995, Khalil and Rosner,1995). For a circular cylinder target over the entire Stokes number range 'universal' graphs have been provided covering the anticipated dimensionless parameter ranges of greatest interest. An example is provided in Fig. 4, which is a polar plot of the *dimensionless local erosion rate* of a metal target over a range of values of the number-mean particle size (volume) to the 'critical' size required to impact under the prevailing conditions. Based on our summary of available experimental data, we also provide representative sets of numerical values of the key phenomenological erosion yield parameters that emerge from our formulation, albeit at $T_w \approx 300K$. To deal with more general, or 'singular' cases of particular interest to the reader, the required correlation formulae and associated quadrature expressions have been provided provided (Rosner, Tandon and Labowsky, 1995, Kho, Rosner and Tandon,1995, Khalil and Rosner,1995).

Among other things, the present model and our results make it clear that erosion rates will be directly proportional to the abrasive particle mass loading in the mainstream, and quite sensitive to mainstream velocity; *viz.*: even more sensitive than U^{n+1} (where, for metals, often, n≈2.5) at intermediate Stokes numbers. Our present results also explain why initially 'blunt'-nosed metal objects tend to become 'wedge-shaped' (sharpened) as a result of erosion (*cf.* Fig4 in the vicinity of the forward stagnation line), whereas blunt ceramic objects tend to become still blunter.

2.4 FORMATION KINETICS AND MORPHOLOGY OF CVD-MATERIALS: THEORY OF MULTI-PHASE BOUNDARY LAYERS WITH NUCLEATION, GROWTH AND THERMOPHORESIS

A small impinging jet (stagnation flow) reactor (Fig. 5) has been used to study the chemical vapor deposition (CVD-) rates of refractory layers on inductively (over-)heated substrates in the presence of complicating homogeneous reactions of the vapor precursor (Collins, 1994). These measurements are being used to understand deposition rates and associated deposit microstructures observed in highly non-isothermal, often particle-containing local CVD environments. Figure 6 shows (logarithmic ordinate) our apparent deposition probability *vs.* reciprocal surface temperature for $TiO_2(s)$ films obtained from TTIP(g) over the broad surface temperature range: 600-1600K. A mathematical model incorporating finite-rate reagent depletion near the hot surface captures the experimentally observed deposition rate trends (Fig. 6; curve marked $Dam_{hom} = A_{hom}\delta^2/D = 8.7 \times 10^4$). A more detailed mathematical model (Tandon and Rosner, 1994) tracks the size distributions of nucleated particles within such BLs (Fig. 7), including the particle+vapor "co-deposition" rate at the surface y=0, and the associated *surface roughness*.

Missing from previous predictions of film deposition rates has been essential information about deposit microstructure and ancillary thermophysical properties. Toward this end we have investigated the possibility of a rational correlation of vapor *deposit* grain *densities* based on the notion that close-packed dense deposits should be possible only when the characteristic time for adatom(molecule) *surface diffusion* is short compared to the time for *surface reaction* and "burial". Our preliminary results (Fig. 8; after Kho, Collins and Rosner,1994) are encouraging and the addition of further relevant characteristic times to our scheme may open the door to the corelation/'anticipation' of other important deposit characteristics.

****

5

In our OSR-sponsored Yale HTCRE Lab research during this program, briefly reviewed here, we have shown that new methods for rapidly measuring particle transport properties and rates, combined with recent advances in boundary layer theory, provide useful means to identify and incorporate important, but often previously neglected, mass transport phenomena in many multiphase propulsion engineering and materials engineering design/optimization calculations.

Despite formidable complexities to be overcome in the design and operation of air-breathing propulsion power plants utilizing a broad spectrum energetic fuels these particular techniques and results are indicative of the potentially useful simplifications and generalizations which have emerged from this program's fundamental AFOSR-funded research studies of combustion-generated particle transport mechanisms, deposition and/or erosion. It is hoped that this Annual Report and its supporting (cited) papers will facilitate the refinement and/or incorporation of some of the present ideas into engineering design procedures of much greater generality and reliability. This work has already helped identify new directions where research results could have a significant impact on engineering practice in both the defense and civilian sectors of the US economy (Section 3.4).

3. ADMINISTRATIVE INFORMATION: PERSONNEL, PRESENTATIONS, APPLICATIONS, "COUPLING' ACTIVITIES

The following sections summarize some pertinent 'non-technical' facets of the abovementioned Yale HTCRE Lab/AFOSR research program during the period: 2/15/94-2/14/95:

3.1 Personnel

The present results (Sections 2 and 5) are due to the contributions of the individuals listed in Table 3.1-1, which also indicates the role of each researcher and the relevant time interval of the activity. It will be noted that, in addition to the results themselves, this program has simultaneously contributed to the research training of a number of students and 2 recent PhDs, who will now be in an excellent position to make future contributions to technologies oriented toward air-breathing chemical propulsion, and high-tech materials processing.

Table 3.1-1 Summary of *Research Participants*[a] on AFOSR Grant : 94-0143
**TRANSPORT PHENOMENA AND INTERFACIAL KINETICS
IN MULTIPHASE COMBUSTION SYSTEMS**

Name	Status[a]	Principal Research Activity[b]
Albagli, D.	PDRA	particle prod/char. in CDFs
Castillo, J.L.	VS	reactions in thermal BLs
Collins, J.	GRA	CVD of ceramic coatings
Garcia-Ybarra, P.	VS	aggregate transport theory
Khalil, Y.F.	RA	erosion of ceramics
Kho, T.	GRA	correl. of density of CVD coatings
Konstandopoulos, A.G.	VS	combined inertia + thermophoresis
Koylu, U.	PDRA	particle prod/char. in CDFs
Labowsky, M. J.	VS	inertial impaction and erosion of metals
Papadopoulos, D	GRA	boundary conditions at G/S interfaces
Rosner, D.E.	PI	program direction-dep. theory/exp
Tandon, P.	GRA	transport phenom. in BLs and CDFs
Xing, Y.	GRA	particle prod/char.exps. in CDFs

[a] PDRA=Post-doctoral Research Asst   GRA= Graduate Research Assistant
   PI = Principal Investigator   VS = Visiting Scholar   RA = Research Affiliate
[b] See Section 5 for specific references cited in text (Section 2)

3.2 Cooperation with US Industry

The research summarized here was supported by AFOSR under Grant 94-0143 (2/15/94-2/14/95). In these fields, the Yale HTCRE Laboratory has also been the beneficiary, over the past decade, of smaller grants from many interested U.S. industrial corporations, including groups within GE, DuPont, Union Carbide (now Advanced Ceramics Corp.) and Shell, as well as the feedback and advice of principal scientists/engineers from each of these corporations and Combustion Engineering-ABB and Textron. We appreciate this level of collaboration, and expect that it will accelerate inevitable applications of our results in areas relevant to their technological objectives (see, also, Section 3.4, below). We also expect these interactions to intensify as a result of the recent formation of an interdisciplinary Combustion Research Center at Yale.

3.3 Presentations and Research Training

Apart from the publications itemized in Section 5 and our verbal presentation (of progress) at the AFOSR Contractors Meeting (June 8-10, Tahoe, NV) , our results over this past year have also been presented at some 10 seminars/conferences--including annual or topical *conferences* of the following professional organizations:

Particle Technology Forum (8/94, Denver CO))
AIChE (11/94, San Francisco CA)
4th Int. Aerosol Conference (Aug.29-Sept.2,1994 @ UCLA, CA)

In addition, during the period: 2/15/94-2/14/95, the PI presented *seminars* at the following Laboratories: ALCOA, PPG, and Technical Universities: Istanbul, Athens, Thessaloniki, ETH-Zurich , Budapest (these were a portion of Prof. Rosner's Fall 1995 Yale Academic Leave itinerary).

This program involved completion of the PhD dissertation research of two Yale ChE Dept. graduate students (Joshua Collins, who defended on 3/4/94, and Pushkar Tandon, who defended on 2/3/95 and will remain at Yale beyond 2/15/95 as a Post-doctoral Research Engineering Scientist (*cf.* Table 3.1-1).

3.4 Some Known *Applications* of Recent Yale-HTCRE Lab Research Results

It has been particularly gratifying to see direct applications of some of this generic AFOSR-supported particle and vapor mass transfer research in more applications-oriented investigations reported in recent years. Indeed, *the writer would appreciate it if further examples known to the reader can be brought to his attention.* Not surprisingly, because of the inevitable "induction period" following publication, our very recent erosion rate studies will be covered in next year's report.

Our AFOSR supported research on *soot deposition rates* from flowing laminar or turbulent combustion gases has been applied by Aerojet Corp. (D. Makel *et.al.*,1990) to develop a model for application to rocket chambers and nozzles (with NASA support). Extensions to jet engine nozzles are currently being made by M.T. Nys at Pratt and Whitney Engine Business in W. Palm Beach FL.

In the area of multicomponent vapor deposition in combustion systems applications of our predictive methods (for "chemically frozen" (Rosner *et.al.*, 1979) and LTCE multicomponent laminar boundary layers) have been made by British Coal Corporation-Power Generation Branch (I. Fantom, contact) in connection with their topping cycles which run gas turbines on the products of fluidized bed coal combustors/gasifiers. Also, in combustion research many groups (*eg.*, Dobbins *et.al.* (Brown U.), Faeth *et.al.* (U. Mich.), Katz *et al.* (J. Hopkins U.)) are now utilizing "thermophoretic sampling" techniques to exploit the size- and morphology-insensitive capture efficiency characteristics that we have proven in our AFOSR research (Section 2.1).

Our AFOSR and NASA fundamental research on chemical element segregation in the CVD of refractory ceramics (*eg.*, SiC and metal borides) (see, *eg.*, Collins and Rosner, 1991, 1992) is evidently of use to AFML contractors synthesizing controlled stoichiometry fibers for light weight/high strength composites (Americom, Textron).

7

For calculating suspended particle concentrations along trajectories outside of aircraft (involved in atmospheric sampling), or inside of CVD reactors, A. S. Geller and D. J. Rader of Sandia-Albuquerque have adopted a method developed in our earlier AFOSR work (Fernandez de la Mora, 1981), and recently applied in our own studies of particle motion in laminar boundary layers with streamwise curvature (Konstandopoulos and Rosner, 1995).

Ongoing work at MIT (Walsh *et.al.* 1992), PSI and Sandia CRF has incorporated our rational correlation of *inertial particle impaction* (*e.g.* a cylinder in cross-flow) in terms of our *effective Stokes number* (Israel and Rosner, 1983, and Konstandopoulos *et. al.* 1993). Recent applications of our AFOSR and DOE-supported research (on the correlation of inertial impaction by cylinders in crossflow) have also been made by the National Engineering Laboratory (NEL) of Glasgow Scotland . NEL is apparently developing mass-transfer prediction methods applicable to waste-heat recovery systems in incinerators, as well as pulverized coal-fired boilers. These applications are somewhat similar to those reported by the Combustion R&D group at MIT and Penn State U, and are now being taken up by VTT-Energy/Aerosol Technology Group, in Finland.

Explicit use of our studies of self-regulated "capture" of incident impacting particles (Rosner and Nagaragan, 1987) is being made in current work on impact separators and ceramic heat exchangers for coal-fired turbine systems in high performance stationary power plants. Other potential applications arise in connection with "candle filters" used to remove fines (sorbent particles,...) upstream of the turbines. A useful summary of work in these interrelated areas (Solar Turbines, Textron Defense Systems, Hague International,...) was presented at the Engineering Foundation Conference *Inorganic Transformations and Ash Deposition During Combustion.*, the proceedings of which appeared in 1992.

Clearly, fruitful *opportunities* for the application of our recent "non-Brownian" convective mass transfer research now exist in many of the programs currently supported by the US Air Force, as well as civilian sector R&D. Indeed, based on the abovementioned 10 papers we have prepared (now in press or submitted (Section 5.3)) as well as our lecture-presentations (Section 3.3) , we expect that these applications will multiply rapidly.

4. CONCLUSIONS

In the OSR-sponsored Yale HTCRE Lab research during the period: 2/15/94-2/14/95, briefly described above, we have shown that new methods for rapidly measuring particle-mass transport properties and rates, combined with our recent advances in mass transport theory, provide useful means to identify and incorporate important, but previously neglected, mass transport phenomena in many chemical propulsion engineering and materials engineering design/optimization calculations. Among our research *results* described in detail in the cited references (Section 5), perhaps the most noteworthy are the development/reporting of:

R1   rational methods to predict the *restructuring kinetics, and transport property evolution* for aggregated 'soot' particles in high pressure combustion gases

R2   rational methods to predict the *erosion rates* of metal and ceramic solid surfaces in abrasive, high-speed streams

R3   Experimental data and quantitative methods for predicting/correlating the effects particle formation in the CVD thermal boundary layer on the rate and quality of vapor-deposited ceramic thin films

R4   Damkohler number-based rational correlation for the density of vapor deposited solid

Despite formidable complexities to be overcome in the design and operation of mobile (and stationary) power plants utilizing a broad spectrum of energetic fuels the abovementioned techniques and results (Sections 2,5) are indicative of the potentially useful simplifications and generalizations emerging from our present fundamental AFOSR-funded research studies of combustion-generated particle transport mechanisms and interfacial reactions relevant to the synthesis of refractory materials. It is hoped that this Annual Report and its supporting papers (Section 5) will facilitate the incorporation of many of the present ideas into design and test procedures of greater generality and reliability. This work has also helped identify new directions where it is anticipated that research results from this AFOSR program have a significant impact on future USA DOD and civilian sector engineering practice.

5. REFERENCES

5.1 CITED BACKGROUND PUBLICATIONS (Predecessor OSR, and ancillary Grants)

Albagli, D., Xing, Y. and Rosner, D.E., "Experimental Studies of the Morphology of Combustion-Generated Ultrafine Inorganic Particles", (in preparation, 1995).

Castillo, J.L., Garcia-Ybarra, P., and Rosner, D.E.,"Morphological Instability of a Thermophoretically Growing Deposit", *J. Crystal Growth* **116**, 105-126, (1992)

Collins, J., Rosner , D. E. and Castillo, J.L., "Onset Conditions for Gas Phase Reaction and Nucleation in the CVD of Transition Metal Oxides", *Materials Research Soc. Symposium Proceedings* Vol. **250**, MRS (Pittsburgh PA) (1992), pp. 53-58

Eisner, A.D. and Rosner, D.E., Experimental Studies of Soot Particle Thermophoresis in Non-Isothermal Combustion Gases Using Thermocouple Response Techniques", *Combustion and Flame* **61**, 153-166(1985); see, also: *J PhysicoChemical Hydrodynamics* (Pergamon) **7** , 91-100 (1986)

Fernandez de la Mora, J. and Rosner, D.E., "Inertial Deposition of Particles Revisited and Extended: Eulerian Approach to a Traditionally Lagrangian Problem", PCH *Physicochemical Hydrodynamics* (Pergamon) **2** (1), 1-21, (1981)

Geller, A.S., Rader, D.J. and Kempka, S.N., "Calculation of Particle Concentration Around Aircraft-Like Geometries", *J. Aerosol Sci.* **24** (6) 823-834 (1993)

Gomez, A., and Rosner, D.E., "Thermophoretic Effects on Particles in Counterflow Laminar Diffusion Flames " *Combustion Science and Technology* **89**, 335-362 (1993)

Gomez, A., Rosner, D.E. and Zvuloni, R., "Recent Studies of the Kinetics of Solid Boron Gasification by $B_2O_3(g)$ and Their Chemical Propulsion Implications", *Proc. 2d Int. Sympos. on Special Topics in Chemical Propulsion*: **Combustion of Boron-Based Solid Propellants and Solid Fuels**, (1992), pp 113-132.

Konstandopoulos, A.G., Labowsky, M J., and Rosner, D.E., "Inertial Deposition of Particles From Potential Flows Past Cylinder Arrays", *J. Aerosol Sci* (Pergamon) **24** (4) 471-483 (1993)

Mackowski, D.W., Tassopoulos, M. and Rosner, D.E.,"Effect of Radiative Heat Transfer on the Coagulation Dynamics of Combustion-Generated Particles", *Aerosol Sci. Technol.(AAAR)* **20** (1) 83-99, (1993))

Rosner, D.E. and Kim, S.S., "Optical Experiments on Thermophoretically Augmented Submicron Particle Deposition From 'Dusty' High Temperature Gas Flows", *The Chemical Engrg. J.*(Elsevier) **29**,[3], 147-157 (1984)

Rosner, D.E. and Nagarajan. R.,"Toward a Mechanistic Theory of Net Deposit Growth from Ash-Laden Flowing Combustion Gases: Self-Regulated Sticking of Impacting Particles and Deposit Erosion in the Presence of Vapor 'Glue'", *Proc. 24th National Heat Transfer Conf.*, AIChE Symposium Series, Vol. **83** [257], 289-296, (1987)

Rosner, D. E. , Chen, B.K., Fryburg, G.C. and Kohl, F.J., Chemically Frozen Multicomponent Boundary Layer Theory of Salt and/or Ash Deposition Rates from Combustion Gases", *Combustion Science and Technology* **20**, 87-106 (1979)

Rosner, D.E., **Transport Processes in Chemically Reacting Flow Systems**, Butterworth-Heinemann, Stoneham MA, 1986; 3d Printing 1990.

5.1 CITED BACKGROUND PUBLICATIONS (Cont.)

Rosner, D.E., Mackowski, D.W and Garcia-Ybarra, P., "Size and Structure-Insensitivity of the Thermophoretic Transport of Aggregated 'Soot' Particles in Gases", *Comb. Sci & Technology* **80** (1-3), 87-101 (1991).

Rosner, D. E., Collins, J. and Castillo, J.L., "Onset Conditions for Gas Phase Reactions and Particle Nucleation/Growth in CVD Boundary Layers", in Proc. *Int. Conf. on CVD (XII)*, 1993, pp 41-47.

Rosner, D.E. and Tassopoulos, M.,"Direct Solutions to the Canonical 'Inverse' Problem of Aerosol Sampling Theory: Coagulation and Size-dependent Wall Loss Corrections for Log-Normally Distributed Aerosols in Upstream Sampling Tubes", *J. Aerosol Sci.* **22** (7) 843-867 (1991).

Rosner, D.E., Mackowski, D.W,. Tassopoulos, M., Castillo, J.L., and Garcia-Ybarra, P., "Effects of Heat Transfer on the Dynamics and Transport of Small Particles in Gases", *I/EC -Research (ACS)* **31**,760-769 (1992)

Rosner, D.E., Konstandopoulos, A.G., Tassopoulos, M., and Mackowski, D.W, "Deposition Dynamics of Combustion-Generated Particles: Summary of Recent Studies of Particle Transport Mechanisms, Capture Rates, and Resulting Deposit Microstructure/Properties", *Proc. Engineering Foundation Conference*: **Inorganic Transformations and Ash Deposition During Combustion**, Engrg. Foundation/ASME, NYC (1992); pp. 585-606

Sung, C. J., Law, C. K., and Axelbaum, R. L., "Thermophoretic Effects on Seeding Particles in LDV Measurements of Flames", *Combustion Science and Technology* (in press, 1994)

Tandon P., and Rosner, D. E., "Simultaneous Vapor- and Particle Deposition Rates at Hot Surfaces; Implications for Deposit Microstructure of Particle Nucleation, Growth, Coagulation and Tarnsport in Boundary Layers", HTCRE Lab # 205; in preparation (1995)

Tandon, P. and Rosner, D.E., "Sintering Kinetics and Transport Property Evolution of Large Multi-particle Aggregates", (to be submitted to *Chem. Eng. Commun.*, March 1995)

Walsh, P.M., Sarofim, A. F., and Beer, J.M., "Fouling of Convection Heat Exchangers by Lignitic Coal Ash", *Energy and Fuels* (ACS) **6** (6) 709-715 (1992)

5.2 PUBLICATIONS WHICH APPEARED* BASED IN PART ON GRANT AFOSR 91-0170

Collins, J., **Effects of Homogeneous Reaction on the Chemical Vapor Deposition of Titanium Dioxide**, PhD Dissertation, Yale University-Graduate School, Dept. Chemical Engineering, 1994

Gokoglu, S.A., Stewart, G.D., Collins, J., and Rosner, D.E.,"Numerical Analysis of an Impinging Jet Reactor for the CVD and Gas Phase Nucleation of Titania", **Mat. Res. Sympos. Proc. Vol. 335**, 171-176 (1994)

Rosner, D.E. and Tandon, P., "Prediction and Correlation of 'Accessible' Area of Large Multi-particle Aggregates ", *AIChE J.* **40** (7), 1167-1182 (1994)

Rosner, D.E., Tandon, P. and Konstandopoulos, A.G., "Rational Prediction of Inertially Induced Particle Deposition Rates for a Cylindrical Target in Dust-Laden Streams",*Proc. 1st Int. Particle Technology Forum*, AIChE , **Vol. II**, 374-381 (1994).

---

*Full papers for this year are reproduced in Section 6 (with Forms 298)

5.3 WORK IN PRESS OR SUBMITTED FOR PUBLICATION

Castillo, J. L. and Rosner, D.E., Role of High Activation Energy Homogeneous Chemical Reactions in Affecting CVD-Rates and Deposit Quality for Heated Surfaces", in press *Chem Eng. Sci.*, 1995)

Cohen, R. D., and Rosner, D. E. , "Kinetics of Restructuring of Large Multiparticle Aggregates" (in preparation, 1995; Preliminary version presented at 10/93 AAAR Mtg.))

Kho, T., Collins, J. and Rosner, D. E., "Development, Preliminary Testing, and Future Applications of a Rational Correlation for the Grain Densities of Vapor-Deposited Materials" (in press *J. Materials Sci.*, 1995)

Kho, T., Rosner, D.E., and Tandon, P., "Simplified Erosion Rate Prediction Technique for Cylindrical Targets in the High Speed Crossflow of Abrasive Suspensions", (submitted to *ASME Trans-J. Engrg. Gas Turbines and Power*, 1994)

Konstandopoulos, A.G. and Rosner, D.E.,"Inertial Effects on Thermophoretic Transport of Small Particles to Walls With Streamwise Curvature---I. Experiment, II. Theory", Accepted 1993 and in press (1995) , *Int. J. Heat Mass Transfer* (Pergamon)

Rosner, D. E., Tandon, A.G., and Konstandopoulos, A.G., "Local Size Distributions of Particles Deposited by Inertial Impaction on a Cylindrical Target in Dust-Laden Streams", (in press *J. Aerosol Sci.*, 1995)

Rosner, D.E., Tandon, P. and Konstandopoulos, A.G., "Rational Prediction of Inertially Induced Particle Deposition Rates for a Cylindrical Target in Dust-Laden Streams", (in preparation, to be submitted to *Chem. Eng. Sci.*, in press, 1995)

Rosner, D.E., Tandon, P. and Konstandopoulos, A.G., "Rational Prediction of Inertially Induced Particle Deposition Rates for a Cylindrical Target in Dust-Laden Streams:Effects of Single-Particle Capture Law and Dust Polydispersity on Deposition Rates and Associated Convective Heat Transfer Reductions", (HTCRE Paper No. 202; *Chem. Eng. Sci.*,in press 1995)

Rosner, D. E., Tandon, P. , and Labowsky, M.J. , "Rapid Estimation of Cylinder Erosion Rates in Abrasive Dust-Laden Streams: Effects of Erosion Rate Law and Dust Polydispersity on Predicted Local and Total Target Wear", (in press, *AIChE J.*, May 1995 issue)

Rosner, D. E. and Tandon, P. , "Effective Surface Area/Volume and Sorptive Capacity of Suspended Populations of 'Micro-porous' Particles (Aggregates) Distributed with Respect to both Size (Volume) and Shape", HTCRE #197, (to be re-submitted, 1995)

Tandon P., and Rosner, D. E., "Translational Brownian Diffusion Coefficient of Large (Multi-particle) Suspended Aggregates", HTCRE Lab # 206; Submitted to *I/EC-Research* (1995)

Tandon P., **Transport Theory for Particles Generated in Combustion Environments**
PhD Dissertation, Yale University-Graduate School, Dept. Chemical Engineering, May 1995

Tassopoulos, M. and Rosner, D.E.,"The Effective Thermal Conductivity of Anisotropic Packings of Spheres" (Part 1."Conduction Through the Solid Phase"; Part 2."Conduction Through the Solid and Void Phases"), *Chem. Eng. Sci.* (in press(1995))

****

LIST OF ABBREVIATIONS

BL	Boundary layer	CDF	Counterflow diffusion flame
CVD	Chemical vapor deposition	CRF	Combustion Research Facility
CSL	Chemical sublayer	CFD	Computational Fluid Dynamics
Dam	Damkohler number	GRA	Graduate research Asst.
G/S	Gas/solid interface	IJHMT	Int. J. Heat/Mass Xfer
LDV	Laser Doppler Velocimetry	LTCE	local thermochem/equilibrium
PC	Pulverized Coal	*pdf*	Probability density function
PI	Principal Investigator	PSD	Particle size distribution
MRS	Materials Research Society	TMA	Trimethyl aluminum
TTIP	Titanium tetra-isopropoxide	VS	Visiting Scholar

6. APPENDICES (Complete Papers Published During 2/15/94-2/14/95 Period; including Form 298 for each)

Gokoglu, S.A., Stewart, G.D., Collins, J., and Rosner, D.E.,"Numerical Analysis of an Impinging Jet Reactor for the CVD and Gas Phase Nucleation of Titania", **Mat. Res. Sympos. Proc. Vol. 335**, 171-176 (1994)

Rosner, D.E. and Tandon, P., "Prediction and Correlation of 'Accessible' Area of Large Multi-particle Aggregates ", *AIChE J.* **40** (7), 1167-1182 (1994)

Rosner, D.E., Tandon, P. and Konstandopoulos, A.G., "Rational Prediction of Inertially Induced Particle Deposition Rates for a Cylindrical Target in Dust-Laden Streams",*Proc. 1st Int. Particle Technology Forum*, AIChE , **Vol. II,** 374-381 (1994).

ABSTRACT:

TRANSPORT PHENOMENA AND INTERFACIAL KINETICS IN MULTIPHASE COMBUSTION SYSTEMS

This *annual technical report* summarizes Yale High Temperature Chemical Reaction Engineering Laboratory research activities (under Grant AFOSR 94-0143) for the one-year period ending 14 February 1995. Among our research *results* described in detail in the cited references (Section 5), perhaps the most noteworthy are the development/reporting of:

R1 rational yet convenient methods to predict the *restructuring kinetics, and transport property evolution* for aggregated 'soot' particles in high temperature combustion gases

R2 rational yet convenient methods to predict the *erosion rates* of metal and ceramic solid surfaces in abrasive, high-speed streams

R3 Experimental data and quantitative methods for predicting/correlating the effects particle formation in the CVD thermal boundary layer on the rate and quality of vapor-deposited ceramic thin films

R4 Damkohler number-based rational correlation for the density of vapor-deposited solids

Ten verbal presentations, 3 archival publications, and two PhDs are associated with this AFOSR-supported research program. Additionally, 10 papers are submitted or in press. Copies of our reprints appearing during this past year are included in the Appendices (Section 6) of this report.

REPORT DOCUMENTATION PAGE

Public reporting burden for this collection of information is estimated to average 1 hour per response, including the time for reviewing instructions, searching existing data sources, gathering and maintaining the data needed, and completing and reviewing the collection of information. Send comments regarding this burden estimate or any other aspect of this collection of information, including suggestions for reducing this burden, to Washington Headquarters Services, Directorate for Information Operations and Reports, 1215 Jefferson Davis Highway, Suite 1204, Arlington, VA 22202-4302, and to the Office of Management and Budget, Paperwork Reduction Project (0704-0188), Washington, DC 20503.

1. AGENCY USE ONLY (Leave blank)	2. REPORT DATE	3. REPORT TYPE AND DATES COVERED
		Reprint

4. TITLE AND SUBTITLE

(U) "Numerical Analysis of an Impinging Jet Reactor for the CVD and Gas Phase Nucleation of Titania"

5. FUNDING NUMBERS

PE - 61102F
PR - 2308
SA - BS
G - F49620-94-1-0143

6. AUTHOR(S)

Gokoglu, S.A., Stewart, G.D., Collins, J., Rosner, D.E.,

7. PERFORMING ORGANIZATION NAME(S) AND ADDRESS(ES)

Yale University
High Temperature Chemical Reaction Engineering Laboratory
Department of Chemical Engineering
PO Box 208286 YS, New Haven, CT 06520-8286 USA

8. PERFORMING ORGANIZATION REPORT NUMBER

9. SPONSORING/MONITORING AGENCY NAME(S) AND ADDRESS(ES)

AFOSR/NA
110 Duncan Avenue, Suite B115
Bolling AFB DC 20332-0001

10. SPONSORING/MONITORING AGENCY REPORT NUMBER

11. SUPPLEMENTARY NOTES

Mat. Res. Sympos. Proc. Vol. 335, 171-176 (1994)

12a. DISTRIBUTION/AVAILABILITY STATEMENT

Approved for public release; distribution is unlimited

12b. DISTRIBUTION CODE

13. ABSTRACT (Maximum 200 words)

We model a cold-wall atmospheric pressure impinging jet reactor to study the CVD and gas-phase nucleation of TiO_2 from a titanium tetra-iso-propoxide (TTIP)/oxygen dilute source gas mixture in nitrogen. The mathematical model uses the computational code FIDAP and complements our recent asymptotic theory for high activation energy gas-phase reactions in thin chemically reacting sublayers. The numerical predictions highlight deviations from ideality in various regions inside the experimental reactor. Model predictions of deposition rates and the onset of gas-phase nucleation compare favorably with experiments. Although variable property effects on deposition rates are not significant (~11% at 1000K), the reduction of rates due to Soret transport is substantial (~75% at 1000K).

14. SUBJECT TERMS

chemical vapor deposition, particle nucleation/growth in BLs, co-deposition of vapors and particles, chemical sublayer theory

15. NUMBER OF PAGES

6

16. PRICE CODE

17. SECURITY CLASSIFICATION OF REPORT	18. SECURITY CLASSIFICATION OF THIS PAGE	19. SECURITY CLASSIFICATION OF ABSTRACT	20. LIMITATION OF ABSTRACT
Unclassified	Unclassified	Unclassified	UL

NUMERICAL ANALYSIS OF AN IMPINGING JET REACTOR FOR THE CVD AND GAS-PHASE NUCLEATION OF TITANIA

SULEYMAN A. GOKOGLU[1], G.D. STEWART[2], J. COLLINS[3] AND D.E. ROSNER[3]
[1]NASA Lewis Research Center, Cleveland, OH 44135
[2]Ohio Aerospace Institute, Brook Park, OH 44142
[3]Chemical Eng. Dept., <u>Yale University</u>, New Haven, CT 06520-8286

ABSTRACT

We model a cold-wall atmospheric pressure impinging jet reactor to study the CVD and gas-phase nucleation of TiO_2 from a titanium tetra-iso-propoxide (TTIP)/oxygen dilute source gas mixture in nitrogen. The mathematical model uses the computational code FIDAP and complements our recent asymptotic theory for high activation energy gas-phase reactions in thin chemically reacting sublayers. The numerical predictions highlight deviations from ideality in various regions inside the experimental reactor. Model predictions of deposition rates and the onset of gas-phase nucleation compare favorably with experiments. Although variable property effects on deposition rates are not significant (~11% at 1000K), the reduction of rates due to Soret transport is substantial (~75% at 1000K).

1. INTRODUCTION

Production of sophisticated materials with superior properties by CVD requires an understanding of coupled transport and chemical processes. This goal can be realized in research programs by combining both experiments and modeling.

Recent Yale University research focused on TiO_2 CVD with simultaneous gas-phase reaction leading to particle nucleation [1-2]. A simple asymptotic theory treated the onset of reactions leading to particle nucleation and reduced CVD rates at high surface temperatures. The theory assumed that all gas-phase reactions are restricted to a thin chemical sublayer adjacent to a hot CVD surface due to their large activation energies. They also developed a lab-scale, cold-wall, impinging jet CVD reactor [3]. Using experiments and appropriate asymptotic and numerical models, we expect to guide future reactor designs and scale-up, resulting in maximum CVD rates while avoiding harmful particle nucleation.

The present axisymmetric, numerical model points to the role of bouyancy and recirculation in the experimental reactor and clarifies the effect of Soret transport in modifying TTIP mass transfer rates. It provides the ability to capture the transition from surface kinetics to gas-phase transport control. Furthermore, it extends the earlier asymptotic theory [1] by removing the restriction that the activation energies of gas-phase reactions should be "large" (i.e. the chemical sublayer should be "thin").

For the case studied at Yale [1-3] for the CVD of TiO_2 from dilute TTIP/O_2 in N_2, the ratio of chemical sublayer to thermal boundary layer thickness is estimated to be 1/5 at the onset of particle nucleation (T≈1050K), which may be too large for the accuracy of the asymptotic theory. Hence, our numerical model may ultimately

be better able to capture the effects of homogeneous chemistry leading to an observed deposition rate fall-off above ~1050K.

2. EXPERIMENT

We use a cold-wall, atmospheric pressure, axisymmetric, imping-ing-jet reactor (Fig. 1). The liquid TTIP source is a constant temperature bubbler. After mixing TTIP vapor with excess oxygen (to "burn away" any co-deposited carbon) and diluting with nitrogen in a short mixing chamber, the gas jet emerges from a converging nozzle and impinges on a polished quartz substrate (diam. 1.3cm). The substrate and the alumina substrate holder are supported from below by an RF-heated graphite susceptor. The susceptor tempera-ture is measured using a Pt-30%Rh/Pt-6%Rh thermocouple just below the substrate. This thermocouple reading is correlated with direct substrate surface temperature measurements made in situ using known melting point lacquers (with ~3-4% accuracy). Gas and surface tem-peratures at several other locations are also measured by thermo-couples. The concentration of water vapor in the reactor is less than 3ppm. Deposition rates are measured by in situ interfero-metry and confirmed by ex situ weight gain. Further details of the experimental system and operating procedure are given in [3].

3. PHYSICO-CHEMICAL/NUMERICAL MODEL

Our modeling study adopts the finite-element-based computational fluid dynamics code FIDAP. The new version of FIDAP incorporates many phenomena relevant to CVD processes, such as temperature dependent fluid density, transport and thermodynamic properties, Soret diffusion, and gas-phase and surface chemical reactions.

We approximate the reactor by using a 2-D axisymmetric geometry (Fig. 2). The inlet and exit are placed sufficiently far from the deposition zone to eliminate numerical uncertainties on rate predictions. The numerical mesh above the substrate is fine enough to resolve the chemical sublayer. Temperature boundary conditions are interpolations of measured surface temperatures in the Yale axisymmetric impinging jet reactor.

We assume that the gas-phase decomposition of TTIP is first or-der with a rate constant of $3.96 \times 10^5 \exp(-8480/T)$ s^{-1} (T is in Kel-vins) [4]. We also assume that the gas-phase products form nonde-positing particles. We fit our low substrate temperature rate data to a Soret-corrected Arrhenius expression, $1.21 \times 10^{0} \exp(-16480/T)$ m/s, to obtain a pseudo-first order surface reaction rate constant. This expression corresponds to a TTIP reactive sticking probability of unity at 987K. For simplicity, the surface reaction rate constant is kept at its 987K value for higher substrate tempera-tures so that the sticking probability does not exceed unity.

The Soret diffusion factor for dilute TTIP in N$_2$ is calculated from kinetic theory (the estimated Lennard-Jones parameters for TTIP are σ=8.13Å and ϵ/k=589K) and fitted to the expression α_T=1.971[1-(223.6)/T]. Unfortunately, FIDAP is currently restricted to constant Soret diffusivities, $D_T = \rho D \omega \alpha_T$, hence we evaluate the gas (N$_2$) density ρ, TTIP Fickian diffusivity D, and α_T at $T_{film} = (T_{nozzle} + T_{surface})/2$, and use the TTIP mass fraction ω at the T_{film} location for the corresponding diffusion limit calculation.
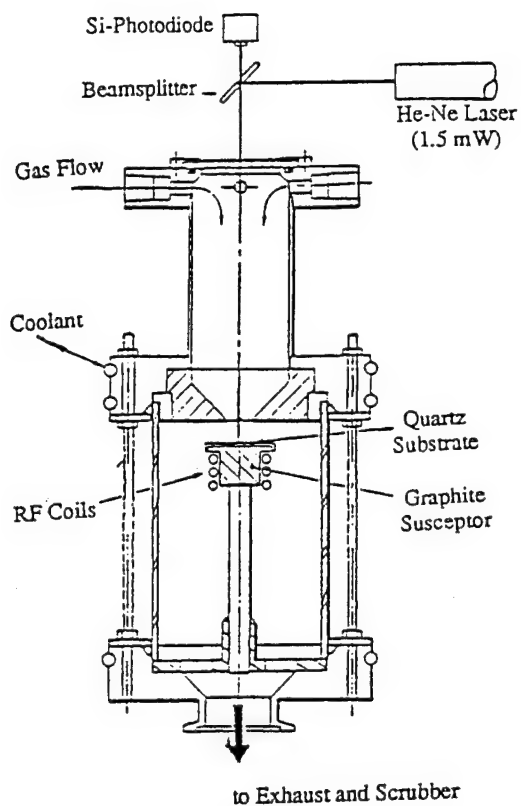
172
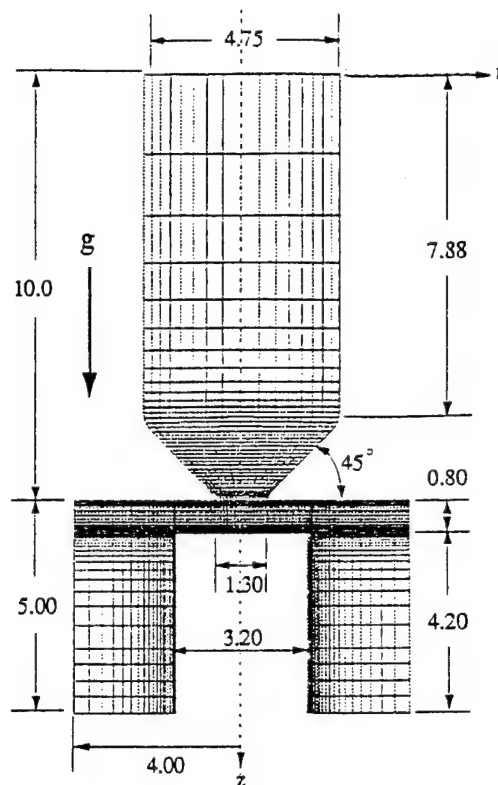
FIGURE 1: Schematic of the experimental reactor; after [1].

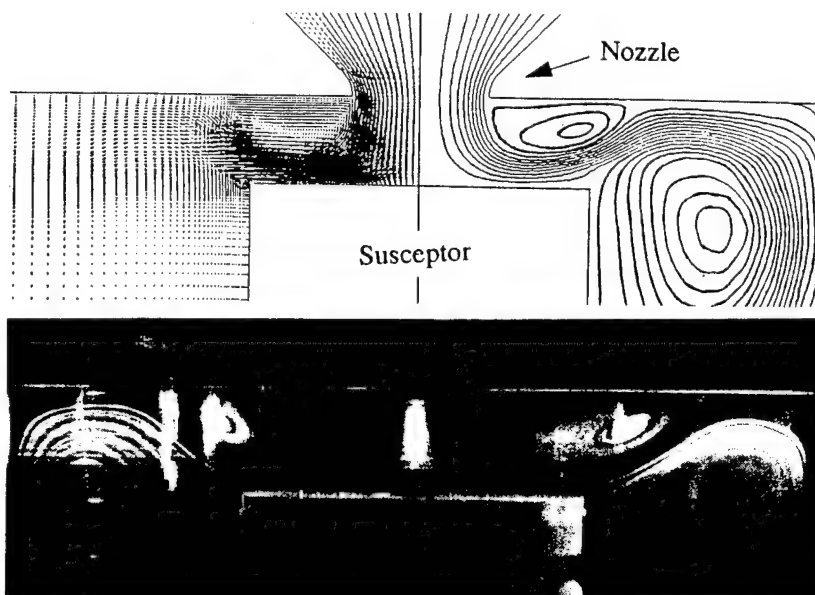FIGURE 2: The computational domain. All dimensions in centimeters, cm.

FIGURE 3: Flow field for argon @ Re=750; $T_{substrate}$=900K.

(a) FIDAP simulation (gas velocity vector/ streamline contours)

(b) experimental visualization with titania seed particles.

4. RESULTS AND DISCUSSION

First, we compare FIDAP predictions to the observed flow field inside the reactor. The experiments use argon seeded with fine titania particles for flow visualization. Figure 3 shows a typical comparison at a Reynolds number of 750 based on nozzle diameter at STP and 900K substrate temperature. Indeed, FIDAP can demonstrate recirculations a) as the jet emerges from the nozzle due to flow separation, and b) on the sides of the hot susceptor due to bouyancy-induced convection. These recirculations are not detrimental because from the photograph one can see that particles trapped in the recirculation regions do not diffuse into the reagent jet, and we estimate that reaction product vapor species are also unable to penetrate appreciably into the jet. The Richardson number based on nozzle to substrate distance is ~0.07 for this case. Lower flow rate (Re<100) measurements at higher substrate temperatures are hampered by buoyancy effects in the jet above the substrate. We discuss elsewhere [5] the operating conditions needed to avoid bouyancy-induced convection in such reactors. Our numerical analysis is capable of handling such non-ideal behavior.

For the results discussed below we fix the gas flow rate at 5160 sccm (Re≈500 for N_2) and the substrate-temperature-based TTIP concentration at $C_s=2.5 \times 10^{-6}$ Kgmol/m^3. Deposition rates are reported as **effective** reaction probabilities ϵ defined as $\epsilon = \dot{n}''/[(1/4)\bar{v}C_s]$, where $\dot{n}''$ and $\bar{v}$ are the molar flux and mean thermal speed of TTIP, respectively, evaluated at the surface.

Figure 4 depicts Soret diffusion and temperature-dependent gas transport-property effects on predicted rates at the stagnation point for transport controlled conditions. The rate reduction due to Soret transport is >75%, whereas the effect of variable properties is <15%, for T>1000K.

The model predicts reasonable deposition rates over the entire regime from surface kinetics to transport control by incorporating the surface kinetics extracted from our experiments (Fig. 5). With the gas-phase kinetics of [4], the model agreement with experiment is less satisfactory, though with similar trends. As the depletion of TTIP by the gas-phase reaction increases (i.e. chemical sublayer gets thicker) at higher substrate temperatures, thereby decreasing the TTIP surface flux (CVD rate), FIDAP's handling of Soret transport becomes more inconsistent. This is because the constant D_T, used by FIDAP as defined above for the calculation of Soret transport, does not exhibit the expected diminishing Soret contribution as TTIP concentration diminishes. Hence, our rate predictions with Soret effect above substrate temperatures of 1200K are not shown. The cause(s) of our underprediction of the steepness of the high temperature rate fall-off is currently under investigation.

The onset of homogeneous nucleation is inferred from a sudden drop in deposition rate at a certain substrate temperature. The reliability of the asymptotic theory prediction of this temperature depends on whether the chemical sublayer is indeed "much" thinner than the thermal boundary layer at the prevailing conditions. Figure 6 depicts the TTIP mass fraction profiles calculated by FIDAP at the stagnation point at a substrate temperature of 1200K with and without gas-phase reaction. We also plot the difference between the two mass fraction curves to demonstrate the extent of gas-phase reaction, as well as the corresponding temperature profile. The predicted rate at this temperature with gas-phase che-

174
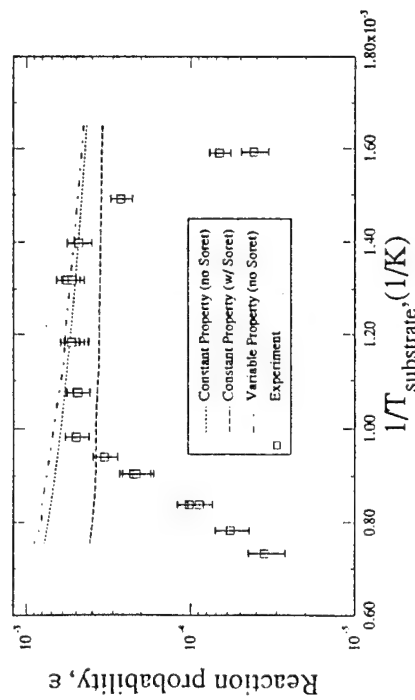
FIGURE 4: Predicted deposition rates with diffusion limitations showing variable property and Soret effects. Experimental data shown for reference.

FIGURE 5: Comparison of predicted deposition rates (including both gas and surface kinetics) with experimental data.
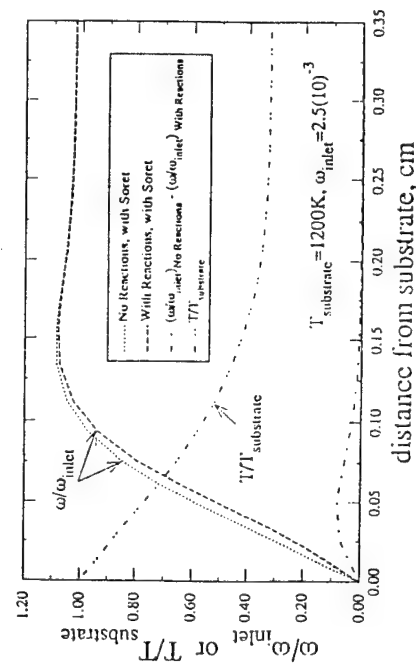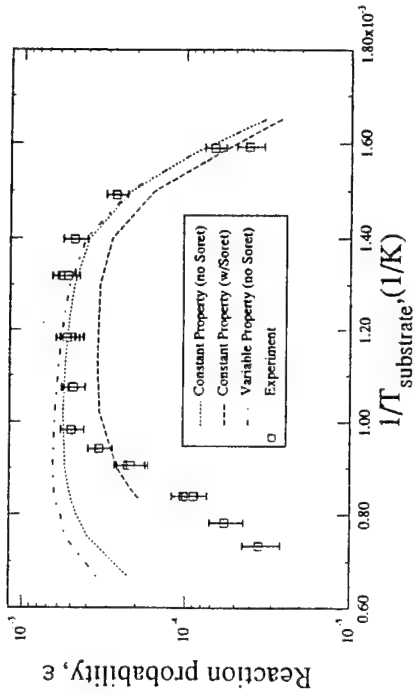

FIGURE 6: The effect of gas phase reaction on mass fraction profile at 1200K. Soret effect is included.
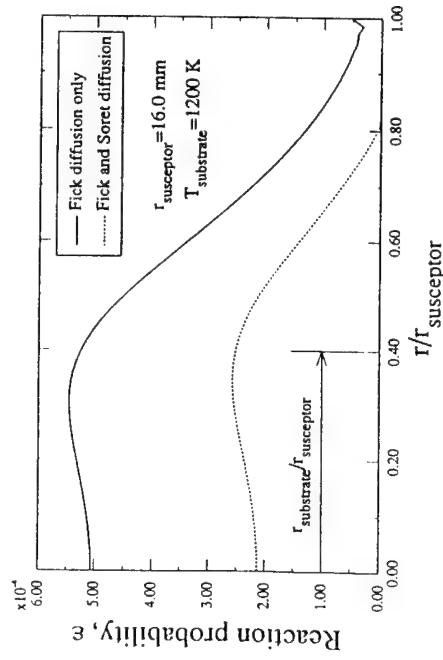
FIGURE 7: Radial variation of predicted deposition rates across susceptor surface.

mistry is observably lower than the one without gas-phase chemistry. If the peak of this curve is taken as a measure of the thickness of the chemical sublayer, it is substantial (30%) compared with the thermal boundary layer thickness. The amplitude and width of the difference curve would be larger at even higher substrate temperatures. Therefore, under such conditions predictions of the full numerical approach are expected to be more reliable than predictions of the simple asymptotic theory. Also noteworthy is the slight "enrichment" in the mass fraction profiles away from the surface due to the Soret effect.

Figure 7 shows that the predicted rates on the susceptor are not uniform in the radial direction beyond the substrate radius (6.35mm vs. 16mm for the susceptor). However, because the deposition rate is roughly uniform across the substrate, we have compared rate measurements to stagnation point rate predictions (Figs. 4 & 5).

5. CONCLUSIONS

Our numerical model can correctly describe the flow field in our experimental atmospheric pressure, impinging jet reactor used for studying the CVD and gas-phase nucleation of titania. The model points to some buoyancy and flow recirculation effects inside the hot substrate reactor affecting the "ideal" stagnation point flow behavior. It can guide the interpretation of deposition rate measurements over a substrate temperature range (600-1400K) covering surface-kinetics-, gas-phase transport-, and gas-phase reaction-governed regimes. Soret transport effects on predicted rates [6] are significant (~75% reduction at 1000K), but variable property effects are modest (<15%). Our numerical model extends the capability of the earlier asymptotic theory to predict the onset temperature of nucleation and the associated reduced deposition rates to include conditions where the chemical sublayer is not "much" thinner than the thermal boundary layer. Future work will include effects of flow rate and TTIP concentration [7], and a more careful examination of the high temperature rate fall-off regime.

6. REFERENCES

1. D.E. Rosner, J. Collins and J.L. Castillo, Proc. Twelfth Int. Symp. on Chemical Vapor Deposition, edited by K.F. Jensen and G.W. Cullen, Proc. Vol. 93-2 (The Electrochem. Soc., Pennington, NJ, 1993), p. 41; also J.L. Castillo and D.E. Rosner, Yale Univ., HTCRE Lab. Publ. #196, June 1993, to be submitted.
2. J. Collins, D.E. Rosner, and J. Castillo, in Chemical Vapor Deposition of Refractory Metals and Ceramics II, edited by T.M. Besmann, B.M. Gallois and J.W. Warren (Mater. Res. Soc. Symp. Proc., 250, 1992) pp. 53.
3. J. Collins, PhD Dissertation, Yale University, Department of Chemical Engineering, in preparation, 1993.
4. K. Okuyama, et al., AIChE J. 36 (3), 409 (1990).
5. G.D. Stewart, et al., in preparation, 1993.
6. Rosner, D.E.,Transport Processes in Chemically Reacting Flow Systems, Butterworth-Heinemann, Stoneham, MA, 3rd Print, 1990.
7. K.L. Siefering and G.L. Griffin, J. Electrochem. Soc. 137 (3), 814 (1990); ibid., 137 (4), 1206 (1990).

REPORT DOCUMENTATION PAGE

Public reporting burden for this collection of information is estimated to average 1 hour per response, including the time for reviewing instructions, searching existing data sources, gathering and maintaining the data needed, and completing and reviewing the collection of information. Send comments regarding this burden estimate or any other aspect of this collection of information, including suggestions for reducing this burden, to Washington Headquarters Services, Directorate for Information Operations and Reports, 1215 Jefferson Davis Highway, Suite 1204, Arlington, VA 22202-4302, and to the Office of Management and Budget, Paperwork Reduction Project (0704-0188), Washington, DC 20503.

1. AGENCY USE ONLY (Leave blank)	2. REPORT DATE	3. REPORT TYPE AND DATES COVERED Reprint

4. TITLE AND SUBTITLE

(U) "Prediction and Correlation of 'Accessible' Area of Large Multi-particle Aggregates "

5. FUNDING NUMBERS

PE – 61102F
PR – 2308
SA – BS
G – F49620-94-1-0143

6. AUTHOR(S)

Rosner, D.E. and Tandon, P.

7. PERFORMING ORGANIZATION NAME(S) AND ADDRESS(ES)

Yale University
High Temperature Chemical Reaction Engineering Laboratory
Department of Chemical Engineering
PO Box 208286 YS, New Haven, CT 06520-8286 USA

8. PERFORMING ORGANIZATION REPORT NUMBER

9. SPONSORING/MONITORING AGENCY NAME(S) AND ADDRESS(ES)

AFOSR/NA
110 Duncan Avenue, Suite B115
Bolling AFB DC 20332-0001

10. SPONSORING/MONITORING AGENCY REPORT NUMBER

12a. DISTRIBUTION/AVAILABILITY STATEMENT

Approved for public release; distribution is unlimited

12b. DISTRIBUTION CODE

13. ABSTRACT (Maximum 200 words)

Aggregates (composed of large numbers of primary particles) are produced in many engineering environments. One convenient characterization is the fractal dimension, the exponent describing how the number of primary particles in each aggregate scales with radial distance from its center of mass. We describe a finite-analytic pseudo-continuum prediction of the normalized accessible surface area of an isothermal quasi-spherical fractal aggregate containing N ($\gg 1$) primary particles, on the surfaces of which a first-order chemical process occurs. Results are displayed for specific fractal dimensions (2.5, 2.18, and 1.8) frequently observed in aggregating systems. An effective Thiele modulus is used to develop an efficient and accurate scheme for predicting/correlating the effectiveness factor for an aggregate containing N primary particles in terms of aggregate fractal dimension, reaction probability, and Knudsen number. Our methods now allow calculations of the accessible surface area of populations of aggregates, provided pdf-$\{N, D_f, \ldots\}$ is known for the populations of interest.

14. SUBJECT TERMS

Soot, aggregated particles, mass transport, accessible surface area Brownian diffusion, nano-particle synthesis in flames, deposit microstructure/properties, Brownian diffusion

15. NUMBER OF PAGES

16

16. PRICE CODE

17. SECURITY CLASSIFICATION OF REPORT	18. SECURITY CLASSIFICATION OF THIS PAGE	19. SECURITY CLASSIFICATION OF ABSTRACT	20. LIMITATION OF ABSTRACT
Unclassified	Unclassified	Unclassified	UL

Prediction and Correlation of Accessible Area of Large Multiparticle Aggregates

Daniel E. Rosner and Pushkar Tandon
Dept. of Chemical Engineering, High Temperature Chemical Reaction Engineering Laboratory,
Yale University, New Haven, CT 06520

Aggregates (composed of large numbers of primary particles) are produced in many engineering environments. One convenient characterization is the fractal dimension, the exponent describing how the number of primary particles in each aggregate scales with radial distance from its center of mass. We describe a finite-analytic pseudo-continuum prediction of the normalized accessible surface area of an isothermal quasi-spherical fractal aggregate containing N (>> 1) primary particles, on the surfaces of which a first-order chemical process occurs. Results are displayed for specific fractal dimensions (2.5, 2.18, and 1.8) frequently observed in aggregating systems. An effective Thiele modulus is used to develop an efficient and accurate scheme for predicting/correlating the effectiveness factor for an aggregate containing N primary particles in terms of aggregate fractal dimension, reaction probability, and Knudsen number. Our methods now allow calculations of the accessible surface area of populations of aggregates, provided pdf{N, D_f, ...} is known for the populations of interest.

Introduction

In many technologies involving suspensions the dispersed phase is comprised of aggregated or agglomerated particles, themselves comprised of a large number, N, of primary particles or spherules which have coagulated (usually as the result of their Brownian motion). While the resulting aggregates may be quasi-spherical and compact, with relatively sharp, if irregular boundaries, more often they are sparse, apparently random clusters of spherules quite permeable to the surrounding solvent and its molecular solutes (Figure 1). Probably the most studied example is that of carbonaceous soot formed deliberately or inadvertently in the combustion of hydrocarbon fuels using air as a gaseous oxidizer (Medalia and Hickman, 1960; Siegla and Smith, 1981). However, qualitatively similar aggregated smokes arise in the vapor phase synthesis of inorganic pigments [for example, $TiO_2(s)$] or viscosity modifiers (for example, fumed silica) (Ulrich, 1984; Megaridis and Dobbins, 1990), and in the combustion of metals (for example, in flares or chemical flash lamps), or the production of catalytic materials (Formenti et al., 1972).

Predictions of the performance of systems containing such

aggregates require a quantitative understanding of the laws governing the exchange of mass-, energy-, and/or momentum between each aggregate and the prevailing host fluid. In particular, we address here the question of what fraction of the surface area of the primary spherules is in fact *accessible* to a diffusing solute molecule in the "continuous" solvent phase—a high temperature combustion gas mixture in the above mentioned examples. For example, in the case of carbonaceous soot aggregates this fundamental question arises in, say, calculating the *growth* rate of the primary particles due to $C_2H_2(g)$ molecule impacts, the *adsorption rate* of possibly carcinogenic condensible molecules, or the ultimate *oxidation rate* of the aggregates due to such combustion gas species as OH(g), O(g), $O_2(g)$, $CO_2(g)$, and so on. For more volatile materials the present theory could also be used to estimate large aggregate *sublimation* rates.

For *small* aggregates, comprised of only a few primary particles (say $2 < N < 20$) in a specified geometrical configuration (for example, linear chain, or quasi-spherical packing of uniform density, and so on) it is no longer impractical to make detailed calculations of transport phenomena in the complex shaped space exterior to the primary particles (Rosner et al.,
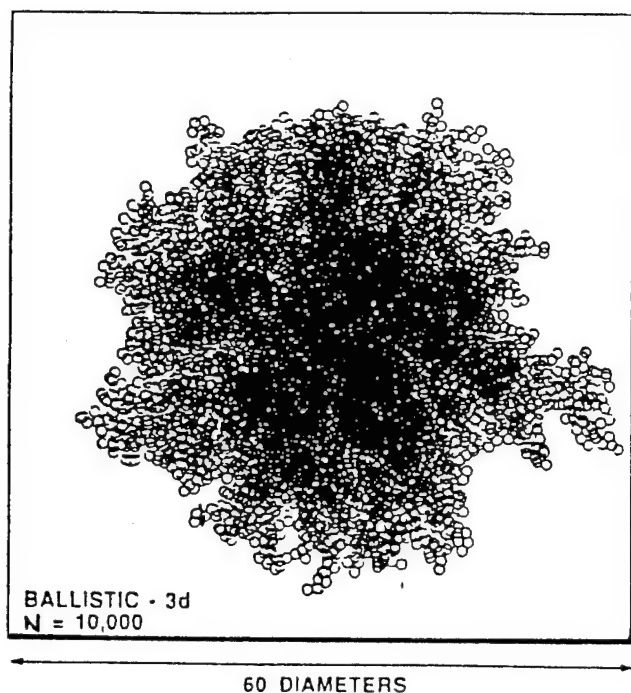
Figure 1. Simulated cluster-monomer ballistically grown three-dimensional aggregate containing 10^4 primary particles.

(After P. Meakin, as reported in Schaefer et al., 1988) ($D_f \approx 2.5$).

Figure 2. Mathematical model of a quasi-spherical aggregate comprised of N-primary spherules showing the important characteristic radii: R_1 (primary particle), R_{gyr} (aggregate), and R_{max} (characteristic aggregate outer radius (Eq. 4)).

1991; Mackowski, 1990, 1994), however, this approach becomes tedious and error-prone for *random* aggregates comprised of rather more particles, perhaps $10^2 < N < 10^6$, as have been observed in *coagulation-aged* systems. It is precisely for populations containing very large aggregates in high-pressure gases or liquids that the above mentioned shielding effects of exterior particles is expected to become appreciable, reducing their *accessible* surface area well below that of the sum of all the primary particles present.

By viewing each large quasi-spherical aggregate as a porous reactive object with a suitable radial variation of effective (pseudo-homogeneous) rate constant and effective reagent diffusion coefficient we seek and provide convenient results for the *accessible area* of large aggregates, suitable for future calculations of mass transfer between populations of such aggregates and the coexisting carrier fluid, here assumed to be a vapor mixture with non-negligible molecular mean-free-path. The general problem is shown to be conceptually identical to that of predicting the effectiveness factor of much larger solid catalyst (support) pellets in a fixed-bed chemical reactor (Aris, 1975; Butt, 1980; Satterfield, 1970; Rosner, 1986, 1990) except that we must now also embrace the possibility of quasi-spherical aggregates that are so sparse as to be essentially transparent to probing molecules traveling on straight line (balllistic) trajectories. Each class of possibilities is conveniently characterized by the so-called *fractal dimension* or *scaling exponent*, D_f, defined by $d \ln N/d \ln r$, where N is the number of primary particles contained in an imaginary sphere of radius r drawn about the aggregate center of mass (Figure 2) (Meakin, 1983; Mountain et al., 1984; Dobbins et al., 1987; Schmidt-Ott et al., 1988a, 1990). In the absence of aggregate restructuring,
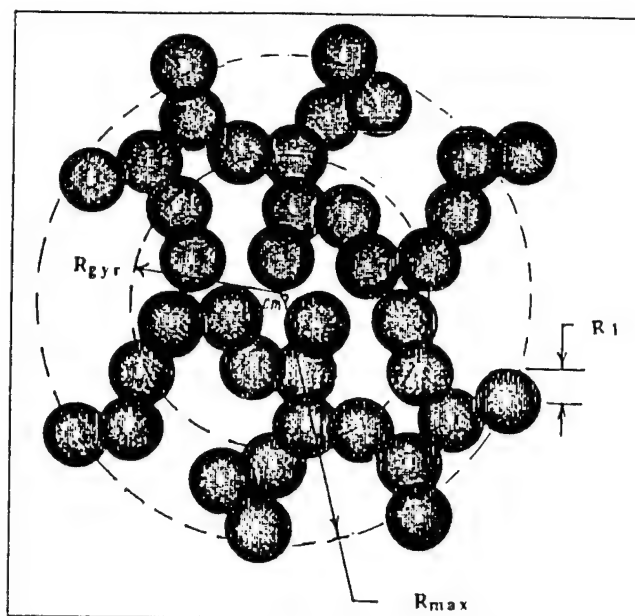
D_f has been observed to be about 1.8 in a wide variety of systems (physically or optically sampled, as well as computer-simulations of aggregate-aggregate encounters), but probably because of partial restructuring, aggregates have been reported with intermediate D_f-values, for example, 2.18 for the silver aggregates experimentally studied by Schmidt-Ott et al. (1988). The value $D_f = 2.5$ has recently been reported for the metal oxides produced by spray precipitation-oxidation in the seeded premixed flame experiments of Matsoukas and Friedlander (1991). In this classification scheme complete restructuring (but without true fusion, which would ultimately obliterate evidence of the primary spheres) is, of course, equivalent to the familiar limiting case $D_f = 3$, corresponding to radially constant properties and a sharply defined outer radius $R_{max}(N)$ larger than the gyration radius R_{gyr} by the familiar factor $(5/2)^{1/2}$, as, for example, in a small virgin charcoal or polycrystalline graphite particle (Dixon-Lewis et al., 1991). [Some authors (for example, Ulrich, 1984) distinguish between physically bound aggregates (easily broken apart) and partially fusion-bonded agglomerates, but this particular distinction will not concern us here.] The goal of the present analysis can then be concisely stated as follows: For a specified aggregate (N, D_f) composed of a large number N of primary spheres of (nearly) uniform radius R_1, on the surface of which a first-order rate process occurs with reaction probability α, in an environment characterized by the mean-free path l_g, what is the ratio of the effective (accessible) surface area to the sum of the primary sphere surface areas? We seek a rational, yet convenient set of quantitative relationships which will permit such calculations over the spectrum of carrier fluid mean free-paths from values so small that continuum (bulk) diffusion occurs even with the gas-filled "pores," to values large enough to not only

lead to Knudsen diffusion within the pores but to also reduce the diffusional resistance of the external fluid layer surrounding the aggregate. The procedures we ultimately recommend are efficient enough to be used to predict the accessible area and transport behavior of *populations* of such aggregates but such applications (Rosner and Tandon, 1993a) are beyond the scope of this article. Some of our methods and results would also be applicable to microporous catalyst supports in fixed-bed reactors, to which Sheintuch and Brandon (1989) have recently applied similar pseudo-continuum methods. These authors treated steady and nonsteady $D_f \geq 2.4$ cases in the absence of external diffusion limitations or noncontinuum (gas kinetic) effects. In the formulation which follows we explicitly deal with a suspended quasi-spherical aggregate comprised of a large number (N) of primary spheres, and develop a convenient rational correlation for our effectiveness factor results in terms of the prevailing reaction probability α, Knudsen number based on primary sphere diameter, Kn_{2R_1}, and the number of primary spheres in the aggregate over a broad range of observed fractal dimensions, D_f.

We present a self-consistent, tractable pseudo-continuum mathematical model for computing the accessible area of a large quasi-spherical fractal aggregate, including the radial distributions of effective pseudo-homogeneous rate constant and reactant molecule effective diffusivity. An efficient finite-analytic method is implemented for the required numerical integrations, and a convenient correlation procedure is developed based on the introduction of an effective Thiele modulus and the well-known relationship valid for the limiting case $D_i = 3$. Results for three particular D_f-values (2.5, 2.18, 1.8) in both Knudsen number limits are discussed as well as those which account for arbitrary Kn and external transport limitations. Tests of the recommended effective Thiele modulus correlation procedure for η_{int} are included. Our principal assumptions and approximations are briefly defended, and several validity criteria and tractable generalizations of current interest are described. Finally, our recommended predictive procedure and its application to coagulation-aged *aggregate populations* are summarized.

Mathematical Model

Basic assumptions

To capture the essential features of simultaneous diffusion and surface reaction in a large aggregate comprised of many ($N \gg 1$) spherical primary particles, our idealized mathematical model is based on the following underlying assumptions:

(A1) The aggregate behaves like a motionless quasi-spherical "porous" granular solid with position-dependent *area per unit volume*, a''', and effective diffusivity for reactant molecules, $D_{A,\text{eff}}$.

(A2) The radial dependence of the effective first-order rate constant and effective diffusivity for reactant molecules are dictated by the aggregate (fractal) exponent D_f defined by $d \ln N/d \ln r$ (see the second section for details).

(A3) A first-order chemical (or physical) process occurs on the external surface of each dense primary spherical particle comprising the aggregate and negligible area is lost at the primary particle contact points. [The second part of this assumption must ultimately be abandoned with the growth of

strong fusion bonds between primary particles (see Koch and Friedlander, 1990, for a recent summary of this rate process), or loss of area as a result of extensive capillary condensation or growth (CVD) from the vapor.]

(A4) Reagent A, of small size compared to the primary particles, is steadily supplied to the intrinsic surfaces of the aggregate by radial diffusion through the gas-filled tortuous pores defined by the void space between the primary particles.

(A5) The aggregate may be approximated as isothermal, that is, each primary particle is at nearly the same steady-state temperature regardless of its position within the aggregate (see, also, the section discussing primary sphere surface roughness).

(A6) When the gas mean-free-path is negligible compared to R_{max}, radial concentration diffusion of reagent also occurs throughout the space $R_{\text{max}} \leq r \leq \infty$ *external* to the aggregate, where it is not appreciably impeded by the presence of primary particles.

We postpone to the fourth section a defence of these idealizations, and provide criteria to define their approximate limits of validity. Several will be seen in the fifth section to be readily generalized to embrace more complex situations that will undoubtedly arise in particular applications. Tentative secondary assumptions introduced to illustrate our *procedures* (for example, the nature of the tortuosity-void fraction relation for Knudsen- or bulk-diffusion) will be introduced, as required, to proceed.

Aggregate structure for $D_f \leq 3$

For an aggregate whose $N(r)$ relation is of the power-law form: $N \sim \beta(r/R_1)^{D_f}$, where β is a dimensionless constant discussed below, we have the basic relation:

$$dN = \beta D_f \left(\frac{r}{R_1} \right)^{D_f - 1} \cdot \frac{dr}{R_1} \qquad (1)$$

describing the (expected) number of primary particles within a shell of thickness dr located at radius r (see Figure 2). [This level of description, in which Eq. 1, in effect, defines an ensemble-averaged radial distribution function for these spatially nonuniform random structures, will prove adequate to our present needs. However, in developing theories of the *restructuring kinetics* of such aggregates (see last section) additional microstructural information *is* needed, and we introduce and track the evolution of the *pdf* of angles between triplets of contacting primary particles (Cohen and Rosner, 1994).] This, in turn, implies that the *local solid fraction, $\phi(r)$*, is given by:

$$\phi(r) \equiv 1 - \epsilon(r) = \frac{\beta D_f}{3} \cdot \left(\frac{r}{R_1} \right)^{-(3 - D_f)} \qquad (2)$$

We now note that when $D_f - 3$, $\phi - \beta = $ const. so that the dimensionless factor β (sometimes called the "filling factor") may be identified with the value of the solid fraction in the uniform porosity limit; that is, $\beta = \phi_{\text{lim}} = 1 - \epsilon_{\text{lim}}$, which, for a random loose packing of uniform size impenetrable spheres, will be about 0.6. Indeed, we visualize that, in general, Eq. 1 applies only outside of a uniform porosity "core" of radius R_i, where:

$$\frac{R_c}{R_1} = \left(\frac{\beta D_f}{3} \cdot \frac{1}{1 - \epsilon_{\lim}}\right)^{1/(3 - D_f)} \qquad (3)$$

This equation indicates that the core radius is necessarily of order R_1, that is, quite small on the scale of the overall aggregate size defined more sharply below.

Whereas most aggregate research has focused attention of the *radius of gyration*, R_{gyr}, we instead introduce the *effective outer radius*, R_{max}, defined by:

$$R_{max} \equiv \left[\frac{3}{2}\left(\frac{D_f + 2}{D_f}\right)\right]^{1/2} \cdot R_{gyr} \qquad (4)$$

which is seen to reduce to the true outer radius of the spherical aggregate in the $D_f - 3$ (uniform porosity) limit. [R_{gyr} is defined such that the actual rotational moment of inertia of the sphere is the same as if all of its mass were concentrated at its gyration radius. Rogak and Flagan (1990), who were primarily concerned with estimating aggregate particle drag in the creeping flow continuum limit, introduce an outer radius similar to that given in Eq. 4 but omitting the factor $(3/2)^{1/2}$. In view of the nature of the $D_f - 3$ limit we recommend Eq. 4 in such future studies. Mulholland et al. (1988) suggested that the *collision radius* of free-molecule clusters (with $D_f = 2$) is about 21% greater than R_{gyr}. Note that $[(3/2)[(2 + 2)/2]]^{1/2} = [(3/2) \cdot (2)]^{1/2} = 1.73$. Thus, the effective collision radius appears to be somewhat less than R_{max}, which is expected on physical (partial penetration) grounds.] Beyond $r = R_{max}$ we treat the domain as primary particle-"free," at least insofar as perimeter-averaged reagent radial diffusion is concerned—that is, we treat $r = R_{max}$ as though it were a "sharp" boundary of the large N aggregate (Figure 2).

Summarizing, if we define the normalized radial variable $\zeta \equiv r/R_{max}$, our idealized model of a large quasi-spherical aggregate containing N primary particles is as follows:

$$\epsilon = \epsilon_{\lim} \approx 0.4 \quad \text{for } (0 \le \zeta \le \zeta_c \ll 1) \qquad (5a)$$

$$\epsilon\{\zeta\} = 1 - \frac{\beta D_f}{3} \cdot \left(\frac{N}{\beta}\right)^{-(3 - D_f)/D_f} \cdot \zeta^{-(3 - D_f)} \quad \text{for } (\zeta_c < \zeta \le 1) \qquad (5b)$$

$$\epsilon = 1 \quad \text{for } (1 \le \zeta < \infty) \qquad (5c)$$

where ϵ is the familiar *void fraction* or *porosity*, $1 - \phi\{\zeta\}$, and $\beta = \phi_{\lim} \approx 0.6$. Whereas higher-order microstructural information (see, for example, Torquato, 1991, or Tassopoulos and Rosner, 1991, 1992) may be needed to increase the accuracy of our Knudsen diffusion coefficient estimates (below), for our present purposes the above level of information will prove to be sufficient—as discussed in the next two subsections.

Bulk diffusion and Knudsen diffusion laws: associated tortuosities

For reagent A diffusion within the aggregate void space we must distinguish between two limiting cases depending upon the ratio of the mean-free-path l_A, to the local mean pore diameter. When this ratio (the local pore Knudsen number) is very small we write:

$$D_{A,eff} = (\epsilon/\tau_c\{\epsilon\}) \cdot D_{A-mix} \qquad (6)$$

where D_{A-mix} is the ordinary Fick diffusion coefficient for species A migration within the prevailing gas mixture and $\tau_c(\epsilon)$ is the continuum-limit tortuosity of the local pore structure with void fraction ϵ. Similarly, in the opposite limit ($Kn_{pore} \gg 1$) we write:

$$D_{A,eff} = (\epsilon/\tau_K\{\epsilon\}) \cdot D_K \qquad (7)$$

where D_K, the Knudsen diffusion coefficient for species A migration down a single straight pore of uniform diameter, is given (for diffuse scattering) by:

$$D_K = (1/3)\bar{c}_A \cdot \{(2/3)[\epsilon/(1 - \epsilon)](2R_1)\} \qquad (8)$$

[Otherwise D_K should contain an additional factor $(2 - f)/f$, where f describes the fraction of scattering events which are "diffuse" (cf. "specular").] Here $\bar{c}_A$ is the mean thermal speed of gas molecule A and the bracketed factor is the mean pore diameter for a random packing of impenetrable spheres of radius R_1 and void fraction ϵ. While recent research (for example, Tassopoulos and Rosner, 1992; Melkote and Jensen, 1992) has indicated that the Knudsen transition is probably somewhat more complex, for arbitrary Kn_{pore} we here adopt the familiar additive resistance relation:

$$D_{A,eff} = \epsilon \cdot \left\{\frac{\tau_c\{\epsilon, \ldots\}}{D_{A-mix}} + \frac{\tau_K\{\epsilon, \ldots\}}{D_K}\right\}^{-1} \qquad (9)$$

(see, for example, Butt, 1980), which correctly recovers the above mentioned limiting formulae, Eqs. 6 and 7. It remains for us to specify the indicated continuum and Knudsen tortuosities for the random packing of impenetrable spheres encountered in such self-similar quasi-spherical aggregates as depicted in Figures 1 and 2.

Recent research has shown that $\tau_c(\epsilon)$ is *microstructure-insensitive* and often adequately described by a power-law in ϵ (Tassopoulos and Rosner, 1992). Imposing the limits $\tau_c\{1\} = 1$ and $\tau_c\{0.4\} = 1.48$ (Huizenga and Smith, 1986), we therefore tentatively adopt (irrespective of D_f):

$$\tau_c\{\epsilon, \ldots\} \approx \epsilon^{-0.416} \qquad (10)$$

Knudsen regime tortuosities $\tau_K\{\epsilon\}$ are known to be more *microstructure-sensitive*, and vary more nearly linearly with the local void fraction ϵ (Tassopoulos and Rosner, 1992). [Elias-Kohav et al. (1991) have recently calculated the tortuosity-porosity relation for a variety of two-dimensional fractal porous media and contrasted them to the behavior of fully random objects. In our future work we plan to probe τ for computer-generated three-dimensional aggregates (cf. the analogous work of Tassopoulos and Rosner (1991) on planar granular deposits.] Imposing the limits: $\tau_K\{1\} = 1$, and $\tau_K\{0.4\} \approx 1.86$ (Olague et al., 1988), we therefore tentatively adopt (irrespective of D_f):

$$\tau_K\{\epsilon\} \approx 1.86 - 1.433(\epsilon - 0.40) \qquad (11)$$

While the *methods* developed below will readily allow the introduction of more complex tortuosity laws should they prove necessary, all specific illustrations contained below (results and

discussion section) will be based on these particular relations for the determination of $D_{A,\text{eff}}\{r\}$.

First-order irreversible sink law for k_{eff}'''

Consider a first-order rate process occurring on the external surface of each primary particle. For a collection of such spheres the available *surface area per unit volume*, a''', can be written:

$$a''' = 3\phi\{r\}/R_1 \tag{12}$$

where $\phi(r)$ is the above mentioned local solid fraction. Therefore, the pseudo-homogeneous rate constant k_{eff}''' will be taken to be:

$$k_{\text{eff}}''' = k_{\text{eff}}'' a''' \tag{13}$$

From a kinetic theory viewpoint k_{eff}'', the *heterogeneous* rate constant (velocity) can be reexpressed:

$$k_{\text{eff}}'' = (1/4)\alpha\bar{c}_A \tag{14}$$

where α is the dimensionless reaction probability ($\alpha \leq 1$) and $\bar{c}_A$ is again the mean thermal speed of species A. [This type of kinetic law can also be used to describe physical *condensation* (with condensation probability α) or *evaporation*, with evaporation sublimation coefficient α, to be discussed later.] While α is not really an elementary rate constant (Rosner, 1972), for our present purposes we will treat α as a specifiable parameter.

Pseudo-homogeneous reaction-diffusion model: spherical symmetry

Using the above information it is possible to derive a simple ODE for the steady-state concentration profile $n_A\{r\}$ established within the aggregate, viewing the latter as a porous sphere with known $D_{A,\text{eff}}\{r\}$ and $k_{\text{eff}}'''\{r\}$-profiles. For example, a species A mass balance for a spherical shell of volume $4\pi r^2 \Delta r$ located at radius r (after division by $4\pi r^2 \Delta r$ and passing to the limit $\Delta r \to 0$) yields the familiar linear second-order ODE:

$$\frac{1}{r^2}\frac{d}{dr}\left[r^2 D_{A,\text{eff}}\{r\}\cdot\frac{dn_A}{dr}\right] = k_{\text{eff}}'''\{r\}n_A\{r\} \tag{15}$$

Introducing the normalized variables:

$$c \equiv n_A\{r\}/n_A\{R_{\max}\}, \quad \zeta \equiv r/R_{\max}, \tag{16a,b}$$

then Eq. 15 can be rewritten in dimensionless form:

$$\frac{1}{\zeta^2}\frac{d}{d\zeta}\left[\zeta^2 \bar{D}\{\zeta\}\frac{dc}{d\zeta}\right] = \Phi^2 \bar{k} c \tag{17}$$

involving the coefficient functions:

$$\bar{D} \equiv D_{A,\text{eff}}\{r\}/D_{A,\text{eff}}\{R_{\max}\} \quad \bar{k} \equiv k_{\text{eff}}'''\{r\}/k_{\text{eff}}'''\{R_{\max}\} \tag{18a,b}$$

and the parameter Φ, the familiar *Thiele modulus*, given explicitly by:

$$\Phi \equiv \frac{R_{\max}}{\left[\dfrac{D_{A,\text{eff}}\{R_{\max}\}}{k'''\{R_{\max}\}}\right]^{1/2}} \tag{19}$$

It is helpful to view Φ as the ratio of the aggregate radius $R_{\max}$ to the characteristic penetration depth defined by the denominator of Eq. 19. Alternatively, the parameter Φ^2 appearing on the righthand side of Eq. 17 may be regarded as the relevant *Damköhler group*—that is, the ratio of the diffusion *time* $R_{\max}^2/D_{A,\text{eff}}\{R_{\max}\}$ to the reaction *time*: $(k_{\text{eff}}'''\{R_{\max}\})^{-1}$ (Rosner, 1986, 1990, Chapter 8). Thus, once the coefficient functions $\bar{D}\{\zeta\}$ and $\bar{k}\{\zeta\}$ and the parameter Φ are specified, it is straightforward to find $c\{\zeta\}$ satisfying the ODE (Eq. 17) and the "split" boundary conditions:

$$c\{1\} = 1 \quad \text{and} \quad (dc/d\zeta)_{\zeta=0} = 0 \tag{20a,b}$$

(See sections on finite-analytic method and inclusion of external boundary layer limitations.) The first of these BCs follows from the definition of c (Eq. 16a); the second follows from the nonsingular behavior of the medium as $r \to 0$, (that is, within the constant porosity inner core), not exclusively "symmetry" (see Rosner, 1986, 1990, Section 6.4.4).

Definition and calculation of the "internal" effectiveness factor

Solution to the boundary value problem (BVP) defined in the previous subsection allows calculation of the single quantity of greatest interest, namely, the actual reaction rate within the aggregate compared to what it would have been had the reagent concentration remained undepleted everywhere within the aggregate. This quantity, hereafter written η_{int}, can also be regarded as the ratio of the effective (or accessible) surface area to the true total primary particle surface area within the aggregate (that is, the sum of the primary sphere areas, Na_1). For this reason this quantity is traditionally referred to as the internal effectiveness factor.

From its definition, we readily find that η_{int} can be calculated from $c\{\zeta\}$ via:

$$\eta_{\text{int}} = \frac{3}{\Phi^2}\cdot\left(\frac{dc}{d\zeta}\right)_{\zeta=1}\cdot\left\{3\int_0^1 \bar{k}\{\zeta\}\zeta^2 d\zeta\right\}^{-1} \tag{21}$$

Thus, once the solution $c\{\zeta\}$ is obtained (see next subsection) the internal effectiveness factor (or normalized accessible area) is readily found from Eq. 21. It is interesting to note that since the core radius makes a negligible contribution to this indicated integral, Eqs. 2, 13, 18, and 21 imply that:

$$\eta_{\text{int}} \approx (D_f/\Phi^2)\cdot(dc/d\zeta)_{\zeta=1} \quad (D_f \leq 3) \tag{22}$$

which is a straightforward generalization of the familiar $D_f = 3$ (constant porosity) result (cf., for example, Rosner, 1986, 1990). However, in developing a compact correlation for all of our computed results, Eq. 21 will prove to be more illuminating (see subsection after next).

Finite-analytic method

While most transport (boundary value) problems do not have

analytic solutions, some, like ODE (Eq. 17) and its BCs, admit analytic solutions if the coefficient functions are assumed to be constant [here $\bar{k}\{\zeta\}$ and $\bar{D}\{\zeta\}$]. In such situations, an attractive scheme to solve the problem is to simply divide the domain into sublayers, each with *piecewise-constant* local coefficients. The BVP over the whole domain can then be solved by applying appropriate continuity conditions at the boundaries of each sublayer. Because we use local analytic solutions applicable within each sublayer this variant of the finite-difference method has been assigned the name: "finite-analytic" method (Chen and Chen, 1984; Rosner et al., 1987; and Rosner, 1986, 1990, p. 484). For any fixed number of sublayers we expect the error involved to be considerably less than that involved in direct discretization of the governing differential equation(s). The finite-analytic approach thus facilitates rapid convergence to the exact solution, allowing division of the domain into fewer sublayers. What follows is a brief account of its implementation for the problem at hand.

For constant $\bar{D}$ and $\bar{k}$, the exact solution to Eq. 17 takes the form:

$$c = [A \exp\{a\zeta\} + B \exp\{-a\zeta\}]/\zeta \qquad (23)$$

where $a \equiv (\bar{k}/\bar{D})^{1/2}\Phi$.

With the boundary conditions @ $\zeta = \bar{\zeta}_1$, $C = \hat{c}_1$ and $\zeta = \bar{\zeta}_2$ $C = \hat{c}_2$, the constants A and B are:

$$A = [\hat{c}_1 \bar{\zeta}_1 \cdot \exp\{a\bar{\zeta}_1\} - \hat{c}_2 \bar{\zeta}_2$$
$$\cdot \exp\{a\bar{\zeta}_2\}]/[\exp\{2a\bar{\zeta}_1\} - \exp\{2a\bar{\zeta}_2\}]$$

$$B = [\hat{c}_1 \bar{\zeta}_1 \cdot \exp\{a\bar{\zeta}_1\} - \hat{c}_2 \bar{\zeta}_2 \cdot \exp\{-a\bar{\zeta}_2\}]/$$
$$[\exp\{-2a\bar{\zeta}_1\} - \exp\{-2a\bar{\zeta}_2\}] \qquad (24)$$

and

$$dc/d\zeta = [A \exp\{a\zeta\}(a\zeta - 1) - B \exp\{-a\zeta\}(a\zeta + 1)]/\zeta^2$$

For a porous medium with fractal exponent $D_f < 3$, the coefficient functions $\bar{D}$ and $\bar{k}$ are not constant and depend on ζ through the local porosity $\epsilon\{\zeta\}$ of the medium, as discussed earlier. Thus, to solve the problem of diffusion and reaction in the "fractal" aggregate we assume that the porous medium consists of a central core with constant porosity enveloped by successive concentric annular shells. The porosity (and therefore $\bar{k}$ and $\bar{D}$) is assumed to be constant within each of these shells but differs from shell to shell (in accord with ϵ evaluated at each shell arithmetic mean radius), as given by Eq. 5. The analytic solution as given by Eq. 23 holds within each of these shells for the local values of $\bar{k}$ and $\bar{D}$. As illustrated in Figure 3, the outer region has been divided into n zones (shells) and $n + 1$ nodes. Defining c_i and ζ_i as dimensionless concentration and distance from center at node i, respectively, (cf. Figure 3a) the following condition should be satisfied at each node i:

$$\left(\bar{D}\left(\frac{dc}{d\zeta}\right)_{\zeta = \zeta_i}\right)_{zone = i-1} = \left(\bar{D}\left(\frac{dc}{d\zeta}\right)_{\zeta = \zeta_i}\right)_{zone = i}^{i} \qquad (25)$$

Substituting from Eqs. 23 and 24 we get a linear algebraic relationship between c_{i-1}, c_i, and c_{i+1}. Writing Eq. 25 for $i = 2$,
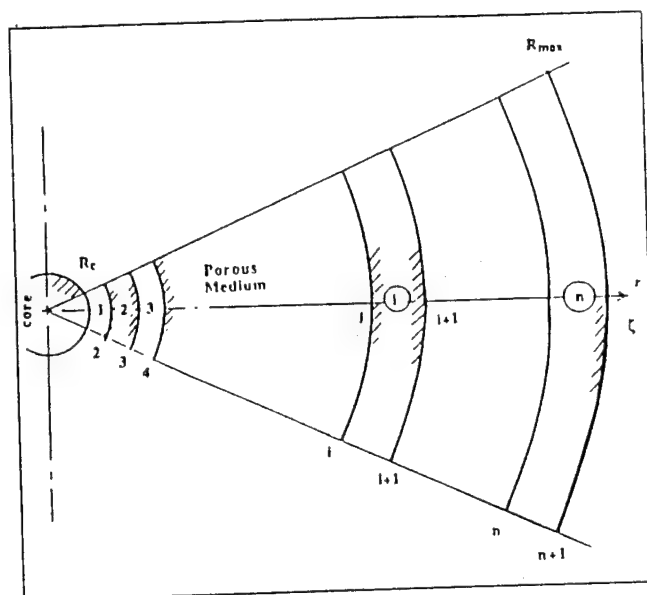

Figure 3a. Discretization nomenclature for implementation of a finite-analytic method (FAM) to solve numerically the present radial diffusion/pseudohomogeneous reaction model for the accessible area of a large, quasi-spherical multiparticle aggregate of nonuniform porosity.
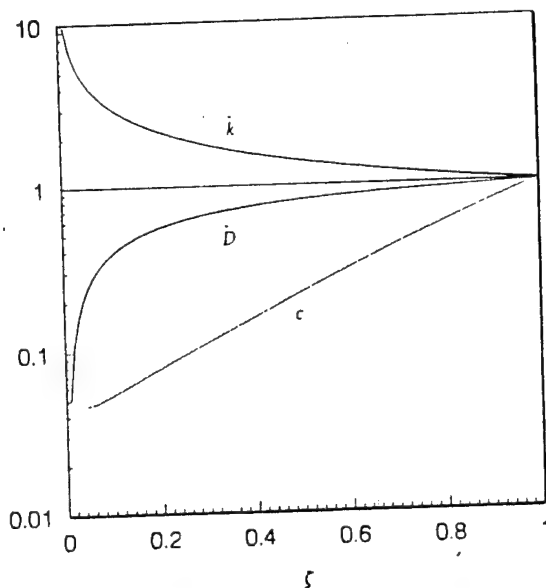
Figure 3b. Typical radial profiles of normalized pseudohomogeneous reaction rate coefficient ($\bar{k}$), reagent diffusion coefficient ($\bar{D}$), and corresponding steady-state normalized composition profile (c).

Logarithmic ordinate; case shown: $D_f = 2.5$, $N = 10^1$, $\alpha = 10^{-1}$, and $Kn_{3R_1} = 10$.

3, ... n we have $n - 1$ linear algebraic equations in $n + 1$ variables (c_i, $i = 1, \ldots n + 1$). The two other required equations are:

$$c_{n+1} = 1 \qquad (26)$$

and species A flux continuity condition at $\zeta = \zeta_{core}$.

$$\left(\bar{D}\left(\frac{dc}{d\zeta}\right)_{\zeta=\zeta_{core}}\right)_{core} = \left(\bar{D}\left(\frac{dc}{d\zeta}\right)_{\zeta=\zeta_{core}}\right)_{zone=1} \quad (27)$$

Inside the core the concentration profile is again given by Eq. 23 with the following boundary conditions:

$$c = c_1 \quad @ \quad \zeta = \zeta_{core} \quad (28)$$

$$(dc/d\zeta)_{\zeta=0} = 0$$

From Eqs. 23 and 28 we obtain:

$$c = c_1 \sinh\{\Phi_{core}\zeta\}/(\zeta \sinh\{\Phi_{core}\}) \quad (0 \leq \zeta \leq \zeta_{core}) \quad (29)$$

where $\Phi_{core} = R_{core}/(D_{eff,Rcore}/k_{eff,Rcore}''')^{1/2}$.

This system of $n+1$ linear equations can be rapidly solved for the concentration profile (see, for example, Figure 3b) using Thomas' algorithm for tridiagonal matrices. The internal effectiveness factor, η_{int}, can then be calculated as Eq. 21, or, alternatively:

$$\eta_{int} = \frac{\int_0^1 \bar{k}c\{\zeta\}\zeta^2 d\zeta}{\int_0^1 \bar{k}\zeta^2 d\zeta} \quad (30)$$

where the indicated integrals are replaced by their equivalent algebraic sums.

In a typical $D_f = 1.8$ numerical calculation we used $n = 10$ sublayers, having determined that at even this level of subdivision our η_{int} results are quite insensitive to n. A typical Sun Sparc II station run time was less than 5 s. As a useful check on the computer program, in the special case $D_f = 3$ we recover the well known constant property result for η_{int} (see the next subsection and Figure 7).

Correlation strategy for η_{int} ($D_f \leq 3$)

Despite the computational efficiency of the finite-analytic numerical method described in the previous subsection for accurately calculating η_{int} for any particular combination of the parameters N, D_f, Kn, ... and choice of laws for $\bar{D}\{\zeta\}$ and $\bar{k}\{\zeta\}$, it would be desirable to have available a compact, rational correlation formula which could be used to rapidly predict η_{int} with acceptable accuracy (say $< 3\%$ rms error) over the entire range of aggregate/environmental parameters of engineering interest. This is especially important for solving problems involving the presence of *populations* of aggregates, for which N covers a "spectrum" of values and we again wish to calculate the total accessible surface area per unit volume represented by this population (see second to last subsection and Rosner and Tandon, 1993a). At the outset, we should comment that while this calculation requires an overall factor $\eta_{overall}$ which is the product of η_{int} and a corresponding factor, η_{ext}, describing the effect of an external diffusion layer, we show in the next section that, once η_{int} is known it is straight-

forward to calculate both η_{ext} and $\eta_{overall}$ via simple explicit algebraic formulae.

Just as our finite-analytic strategy (previous subsection) for the solution of the BVP defined earlier was based on the familiar analytic behavior of the constant property ($D_f = 3$) special case, our proposed correlation for η_{int} will be based on the well-known properties of the function:

$$\eta_3\{x\} = (3/x)[(\tanh x)^{-1} - x^{-1}] \quad (31)$$

which (with $x = \Phi$) describes η_{int} in the $D_f = 3$ limit, and which behaves like $1 - (2/5)x^2 + \ldots$ for small x and $3/x$ for large x.

Inspection of the ODE (Eq. 17) suggests that when Φ is sufficiently small (to allow "deep penetration" of the reagent) the principal effect of the $D_f < 3$ terms [which lead to $\bar{D}\{\zeta\} < 1$ and $\bar{k}\{\zeta\} > 1$] will be to cause the solution to be similar to the $D_f = 3$ case but with an effective value of Φ "stretched" by the factor:

$$[\langle\bar{k}\rangle/\langle\bar{D}\rangle]^{1/2} \quad (32)$$

where $\langle\ \rangle$ is some appropriate average value of the indicated quantity over the domain $0 \leq \zeta \leq 1$. We postpone for the moment the question of which average is most successful and will empirically consider below members of the subclass:

$$\langle\Psi\rangle_q \equiv (1+q) \cdot \int_0^1 \Psi\{\zeta\} \cdot \zeta^q d\zeta \quad (33)$$

where Ψ is $\bar{k}$ or $\bar{D}$ and $q > 0$.

In the large Φ limit we know that the reagent penetration will be shallow so that $\bar{k} = 1$ and $\bar{D} = 1$ within this outer "boundary layer." Thus, in this limit, Eq. 21 reveals that the solution to our BVP must be:

$$\lim_{\Phi \gg 1} \eta_{int} = (3/\Phi) \cdot \left\{3 \int_0^1 \bar{k}\{\zeta\}\zeta^2 d\zeta\right\}^{-1} = 3[\langle\bar{k}\rangle_2\Phi]^{-1} \quad (34)$$

in which the relevant effective-Φ is seen to be "stretched" by the factor $\langle\bar{k}\rangle_2$. Summarizing, we expect that $\eta_3\{\Phi_{eff}\}$ will be an acceptable approximation to η_{int} provided Φ_{eff} is chosen such that the stretching factor $[\langle\bar{k}\rangle/\langle\bar{D}\rangle]^{1/2}$ is applied for "small" Φ and the stretching factor $\langle k\rangle_2$ is applied for "large" Φ. For these reasons we simply investigate the choices:

$$\Phi_{eff}\{\Phi\} \equiv \left[\left(\frac{\langle\bar{k}\rangle_q}{\langle\bar{D}\rangle_q}\right)^{1/2}\right]^{1/(1+\Phi)} \cdot \Phi \cdot [\langle\bar{k}\rangle_2]^{\Phi/(1+\Phi)} \quad (35)$$

For each such choice we compared values of η_{int} (correlation) with η_{int} (FAM). We found that *all* of our $D_f < 3$ η_{int}-results were quite acceptable for the choice $q = 1$. This is readily demonstrated in the "correlation" plots Figures 4, 5, and 6 for cases involving continuum (bulk) pore diffusion (Figure 4), Knudsen pore diffusion (Figure 5), and transitional Knudsen numbers (Figure 6).

One sees that the rms errors are only about 3%, with the acceptably small local errors peaking (ca. 4%) at intermediate η_{int}-values (near 0.8). Thus, to rapidly predict η_{int} for large aggregates to within about ca. 3% error one merely uses the

Figure 4. Test of the effective Thiele modulus correlation (Eqs. 31 and 35) for the internal effectiveness factor η_{int} of large $(N \geq 10^2)$ fractal aggregates in the continuum (bulk-) pore diffusion limit.

For unshaded points $Kn_{2R_1} = 10$; for shaded points: $Kn_{2R_1} = 1$.

well-known $\eta_3\{x\}$ function with a suitably calculated (nonlinearly stretched) *effective Thiele modulus*, Φ_{eff} (Eq. 35) with $q = 1$. [We suggest that this rational correlation strategy can be implemented for a wide class of engineering problems. Ear-
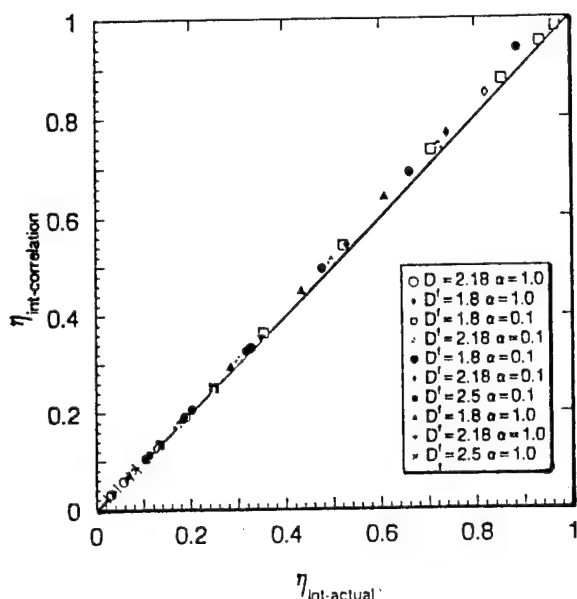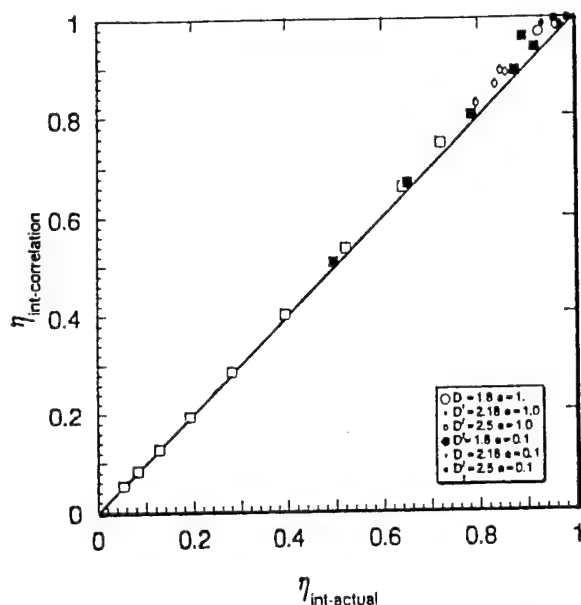

Figure 5. Test of the effective Thiele modulus correlation (Eqs. 31 and 35) for the internal effectiveness factor η_{int} of large $(N \geq 10^2)$ fractal aggregates in the Knudsen pore diffusion limit.
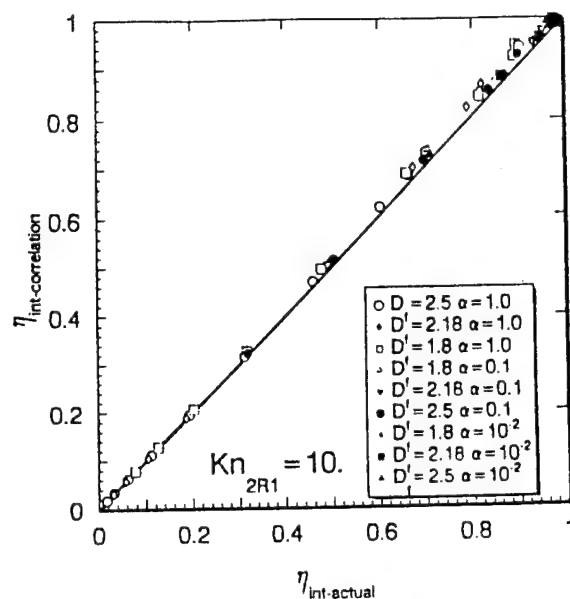

Figure 6. Test of the effective Thiele modulus correlation (Eqs. 31 and 35) for the internal effectiveness factor η_{int} of large $(N \geq 10^2)$ fractal aggregates in the transition pore diffusion regime; $Kn_{2R_1} = 10$.

lier, closely related examples from the author's research (DER) may be found in Israel and Rosner (1983) and Rosner and Feng (1974).] Since, in this case $\langle \bar{k} \rangle_q$ can be evaluated in closed form (for any q) this recommended procedure only requires the calculation of $\langle \bar{D} \rangle_1$, which is a trivial numerical integration for the present class of tortuosity laws (second section), or any other choice of tortuosity laws deemed (via future research on aggregate microstructure) to be more appropriate (fourth section).

In closing this section, we remark that the acceptably small local errors of the present recommended correlation appear to be systematically positive (see Figures 4, 5, 6). This implies that a slight modification of the exponents appearing in Eq. 35 could easily reduce them further. However, the present simple version (the first we investigated!) is acceptable for our present purposes. We remark that this procedure should also be useful for estimating η_{int} for ordinary catalyst pellets ($D_f = 3$) which, because of their manufacture (pelleting, impregnation, and so on), have *spatially nonuniform* $D_{A,eff}$ and k''_{eff} properties.

Results and Discussion

Inclusion of external boundary layer limitations

If the gas mean-free-path is small on the scale of $2R_{max}$ (Eq. 4), then, even though the aggregate may be *internally* accessible (as when $D_f = 1.8$ and Knudsen diffusion prevails within the aggregate) the steady-state reagent concentration established at $r = R_{max}$ will be systematically less than that in the ambient, contributing to an apparent reduction in accessible surface area. This effect of the "resistance in series" represented by the external gas boundary layer is easily included in our analysis via introduction of the additional factor:

$$\eta_{ext} = n_{A,w}/n_{A,\infty} \qquad (36)$$

which is explicitly calculated below. The overall effect of internal and external diffusional resistance on the normalized accessible surface area of the aggregate will then be given by the product:

$$\eta_{overall} = \eta_{int} \cdot \eta_{ext} \qquad (37)$$

where the calculation and correlation of η_{int} have already been dealt with earlier.

Our idealized mathematical model to account for the *external* diffusion layer makes use of earlier results for the dimensionless (Nusselt-Sherwood) mass-transfer coefficient for diffusional transfer to/from a motionless, isolated solid sphere, viz.

$$Nu_m = 2 \cdot \{1 + fct\{Kn\}\}^{-1} \qquad (38)$$

where $Kn = l/(2R_{max})$. Note that $fct(0) = 0$ in order to recover the familiar continuum limit value 2, but $fct\{\infty\} = \infty$ to eliminate this diffusional resistance in the free-molecule limit. Several authors have calculated and/or measured the important function $fct\{Kn\}$ appearing in Eq. 38. For our present purposes we adopt the following corrected form of the Fuchs-Sutugin approximation (Friedlander, 1977):

$$fct(Kn) = 2Kn \cdot \left\{\frac{1.33 + 1.42(2Kn)^{-1}}{1 + (2Kn)^{-1}}\right\} \qquad (39)$$

[The coefficient of $(2Kn)^{-1}$ in the numerator of Eq. 39 has been increased (from 0.71) to force agreement with independent $Kn \ll 1$ results.] Then a steady-state analysis in which the reagent A flow rate into the quasi-spherical aggregate is balanced against the steady-state rate of its consumption within the aggregate yields the explicit algebraic result:

$$\eta_{ext} = \left\{1 + \frac{\frac{\alpha}{4}\bar{c}_A a_1 N \cdot \eta_{int}}{2\pi R_{max} Nu_m D_{A\text{-mix}}}\right\}^{1} \qquad (40)$$

where a_1 ($= 4\pi R_1^2$) is the surface area of a primary spherule.

For the illustrative calculations given below we will assume that reagent A has a molecular mass and collision cross-section similar to that of the background gas mixture, so that $l_g = l_A$. We will also make use of the corresponding molecular theory estimate:

$$D_{A\text{-mix}} \approx (1/3)l_A \cdot \bar{c}_A \qquad (41)$$

These (unnecessary) assumptions will simply reduce the number of parameters that must be specified in the examples below, and thereby help us focus on the essential trends. With these simplifications we find that $\eta_{overall}$ can be expressed:

$$\eta_{overall} \cong \left\{\frac{1}{\eta_{int}} + \frac{\frac{3}{4}\alpha\beta\left(\frac{R_{max}}{R_1}\right)^{D_f-1}}{Nu_m \cdot Kn_{2R_1}}\right\}^{-1} \qquad (42)$$

where Kn_{2R_1} is the Knudsen number based on primary sphere diameter $2R_1$, a quantity specified explicitly in the aggregate transport calculations illustrated below. Thus:

$$Kn \equiv l/(2R_{max})$$
$$= Kn_{2R_1} \cdot (R_{max}/R_1)^{-1} = Kn_{2R_1} \cdot (N/\beta)^{-1/D_f} \qquad (43)$$

which fixes Kn (cf. Eq. 39) for every choice of aggregate size N and Knudsen number based on primary sphere diameter.

Illustrative results and implications

Before examining representative results for $\eta_{overall}$ it is interesting to examine the sensitivity of η_{int} to the structural exponent D_f and aggregate size N. One such set of results is shown in Figure 7, which reveals that even for a reaction probability of unity, and for aggregates containing very many primary particles, if D_f is less than 2 and Kn_{2R_1} is large enough (here $Kn_{2R_1} = 10$) essentially the entire aggregate area is "accessible" ($\eta_{int} \approx 1$). [Indeed, for $D_f < 2$ one finds that for Knudsen pore diffusion the *penetration depth* $[D_{A,eff}\{R_{max}\}/k_{eff}'''\{R_{max}\}]^{1/2}$ increases more rapidly with N than R_{max} itself, that is, the relevant Thiele modulus Φ actually *decreases* with increasing N! However, even for $D_f < 2$ this remarkable behavior does not occur in the continuum pore diffusion limit ($Kn_{pore} < 1$).] However, for a given N-value (say, $N = 10^5$) one sees that η_{int} falls off rapidly at higher values of the exponent D_f. Thus, if for any reason restructuring of an initially $D_f = 1.8$ aggregate containing N primary particles occurred, η_{int} would drop accordingly, even if primary sphere *fusion* did not occur.

In Figure 8, which serves as one check on our general computer program (incorporating the pore diffusion transition between continuum and Knudsen), we show how η_{int} relates to its (separately computed) continuum- and Knudsen-pore diffusion asymptotes. Note that, in the "small" N domain, because of the reduced average pore size, one approaches the Knudsen diffusion asymptote, whereas for $N \gg 1$ more of the aggregate pores fall in the continuum (bulk) diffusion regime.
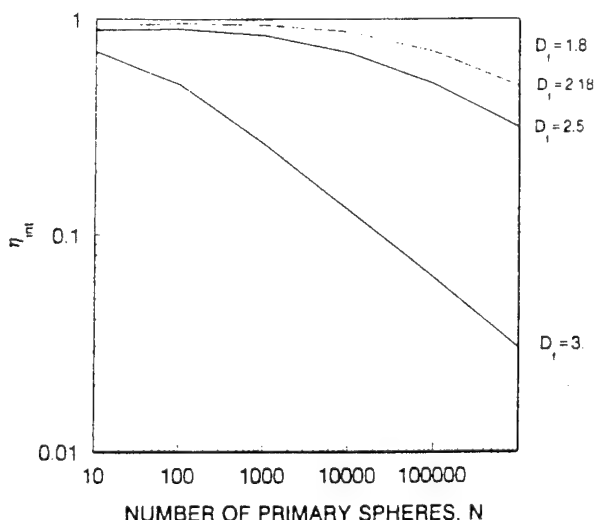

Figure 7. **Predicted dependence of the internal effectiveness factor, η_{int}, on a aggregate size N and fractal dimension D_f for $\alpha = 10^{-1}$; $Kn_{2R_1} = 10$.**
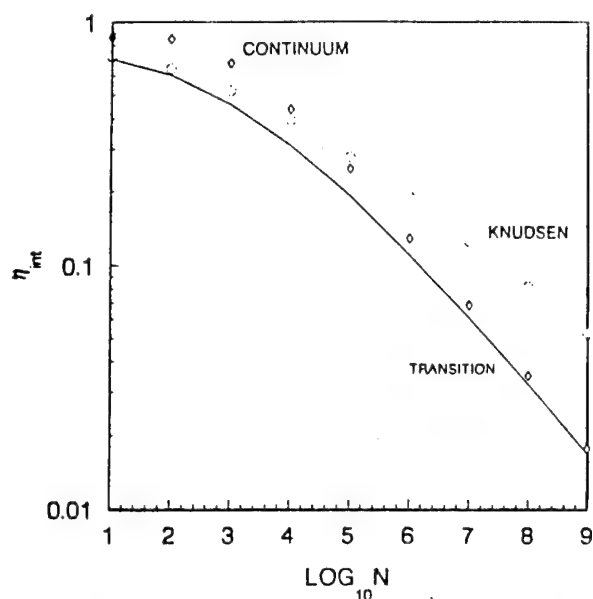
Figure 8. Nature of the η_{int} transition from obstructed continuum (bulk·) diffusion to Knudsen pore diffusion for large quasi-spherical aggregates ($D_f = 2.5$, $Kn_{2R_1} = 10$, $\alpha = 1$).

This particular graph applies to the parameter combination: $D_f = 2.5$, $\alpha = 1$, $Kn_{2R_1} = 10$. However, as commented above, even for $D_f = 1.8$ low values of η_{int} result at small enough ambient mean free paths (high enough pressures).

For the same value of Kn_{2R_1}, Figures 9 and 10 reveal the sensitivity of the overall normalized accessible surface area, $\eta_{overall}$, to aggregate size N and reaction (or "trapping") probability α, for the important special cases $D_f = 1.8$ (open aggregates) and $D_f = 2.5$ (more compact aggregates). We remark that the exponent $D_f = 1.8$ (± 0.1) has been observed or inferred for aggregate smokes in many combustion environments (see
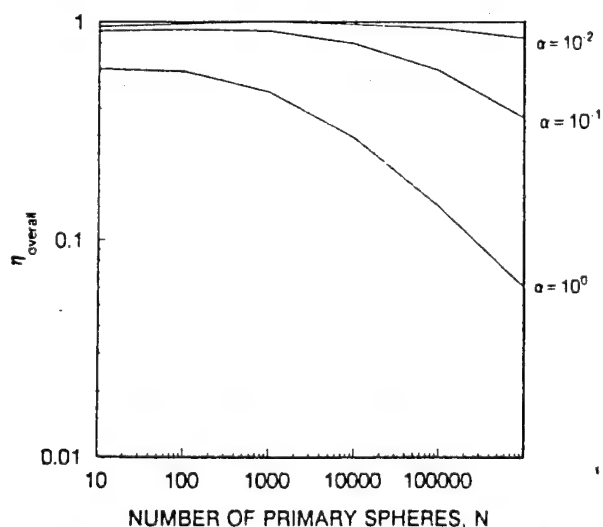

Figure 10. Predicted dependence of the overall effectiveness factor, $\eta_{overall}$, on aggregate size N and reaction probability α for $D_f = 2.5$ ($Kn_{2R_1} = 10$).

the useful summaries of Megaridis and Dobbins (1990) and Puri et al. (1993). [Megaridis and Dobbins (1990) have also called attention to the narrow size *range* (spread) of the primary particle diameters in particular laminar flow environments. Primary particle diameters reported are often of the order of tens of nanometers, which accounts for the very high specific surface areas of these materials.] The value $D_f = 2.5$ was recently observed for aggregated metal oxide smokes produced by spray pyrolysis-oxidation of aqueous metal salts in laminar, atmospheric pressure premixed flames (Matsoukas and Friedlander, 1991). Monte Carlo simulation studies in 3 dimensions (Meakin, 1983, 1984) reveal that the D_f-values near 1.8 result from cluster-cluster agglomeration whereas D_f-values near 2.5

Figure 9. Predicted dependence of the overall effectiveness factor, $\eta_{overall}$, on aggregate size N and reaction probability α for $D_f = 1.8$ ($Kn_{2R_1} = 10$).
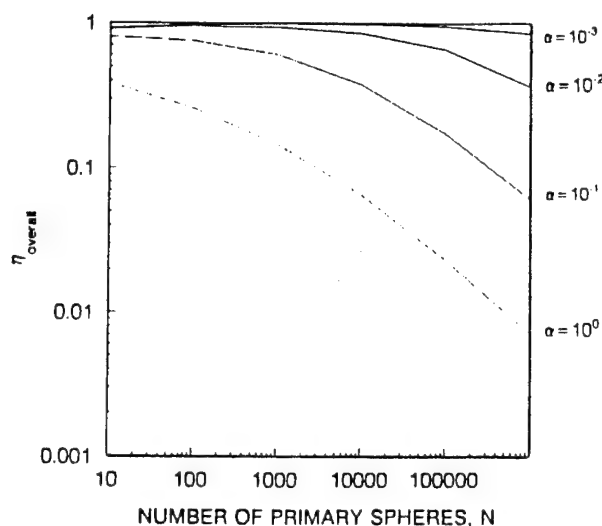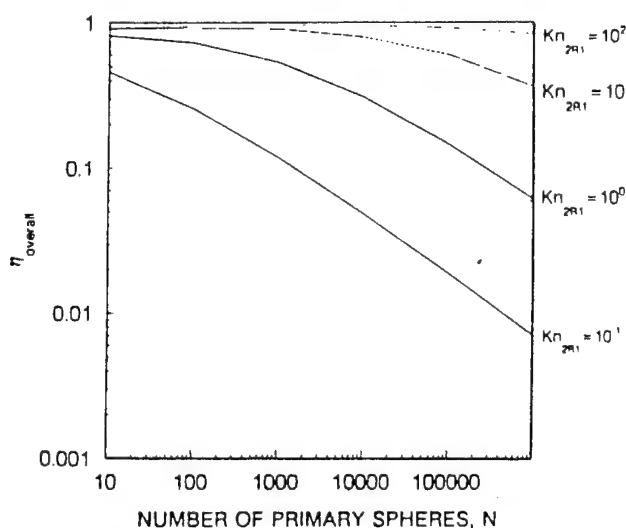

Figure 11. Predicted dependence of the overall effectiveness factor, $\eta_{overall}$, on aggregate size N and gas mean free path (in multiples of $2R_1$) for a reaction probability α of 10^{-1} ($D_f = 1.8$).

result from cluster-monomer aggregation in the absence of further restructuring (Figure 1). Whatever the prevailing D_f value, our procedure is seen to facilitate rational predictions of the accessible surface area of large quasi-spherical aggregates as a function of both reaction probability and Knudsen number.

Whereas some authors have stated or implied that aggregates with $D_f \leq 2$ are always "totally accessible" this will clearly *not* be the case at pressure levels large enough to cause the mean-free-path to be comparable with the average pore diameter $\{(2/3)[\epsilon/(1-\epsilon)](2R_1)\}$, or, certainly, the primary particle diameter. Moreover, unless l_g is large compared to $2R_{max}$, the external boundary layer limitation is not escapable. This is clearly illustrated in Figure 11 for the case of $D_f = 1.8$ with a reaction probability of 10^{-1}. We remark that reaction probabilities of approximately this order of magnitude have been reported for the *oxidation* of suspended carbonaceous soot by OH(g) or O(g) (Neoh et al., 1981; Roth et al., 1990). In contrast, inferred reaction probabilities for the growth of "young" soot via $C_2H_2(g)$ impacts are of the order of 10^{-3} (Harris and Weiner, 1984). Our approach and results may therefore be of special interest in high-pressure devices—such as modern aircraft gas turbine combustors (which operate at ca. 30 atm, Correa and Shyy, 1987), or flame-produced $TiO_2(s)$ (chloride-process) pigment reactors (Ulrich, 1984). In this respect, re-examination of Eq. 41 used above indicates that, provided assumptions 1–6 (second section) are satisfied, our present results could also be used to estimate the accessible area of such aggregates in supercritical vapors (Mohamed et al., 1989) or true liquids (Matijevic, 1981; Zukoski et al., 1990) by setting $Nu_m = 2$, and reinterpreting Kn_{2R_1} as a dimensionless solute diffusion coefficient (inverse Peclet number):

$$Kn_{2R_1} = (D_{A\cdot mix})_{exp}/\{((1/3)\bar{c}_A)\cdot(2R_1)\} \qquad (44)$$

where $(D_{A\cdot mix})_{exp}$ is the experimental solute A Fick (or Brownian-) diffusion coefficient in the prevailing fluid, and the mean molecular speed $\bar{c}_A$ is formally calculated using gas kinetic theory. In this respect the effective reaction probability, α_{eff}, should be calculated from:

$$\alpha_{eff} = (k'')_{exp}/[(1/4)\bar{c}_A] \qquad (45)$$

Clearly, however, these results would have to be generalized to deal with ("hindered" diffusion) situations in which the effective size of a (macro-) solute A is not negligible compared to the prevailing spherule diameter (cf. A4). Indeed, Hagenlock and Friedlander (1989) have carried out Monte Carlo simulations of finite size gas molecules striking $D_f = 2.5$ aggregates of spheres with $N \leq 10^3$, keeping track of collision frequency (assuming diffuse reflection) as a function of aggregate size and gaseous Knudsen number $l_g/(2R_1)$. Remarkably, they report steady-state collision frequencies less than that expected for N isolated spheres even in the *nonreactive* limit ($\alpha \to 0$) and point molecule limit ($\sigma_A/(2R_1) \to 0$), a paradoxical result evidently at variance with the predictions of our present pseudo-continuum model (for which $\eta_{int} \to 1$ when $\alpha \to 0$ and $\sigma_A/(2R_1) \to 0$ for any fixed N, Kn).

Discussion

Equations 15–43 will clearly permit rapid estimates for many parameter combinations of particular interest to the reader. Moreover, as mentioned in the fifth section and will be explicitly illustrated in Rosner and Tandon (1993a), they are readily applied to predict the accessible area of, say, log-normal *populations* of aggregates frequently observed in coagulation-aged systems (Matsoukas and Friedlander, 1991).

It is noteworthy that, whereas Meakin and Whitten (1983), using Monte Carlo simulation methods, have implied that the accessible area (or interface) of an aggregate will scale as a simple power (near 0.74 in 3 dimensions) of the total aggregate size, our pseudo-continuum relations, which also include external boundary layer effects, reveal that the actual relationship will not be so simple. This is readily seen by examining the range of values of $1 + (d \ln \eta_{overall}/d \ln N)$ revealed in Figures 9, 10, and 11. (Note that the logarithmic coordinates of these figures allow direct visualization/computation of the required local logarithmic derivative.)

It is also interesting to note that the present approach can shed useful light on the meaning of recent experimental measurements suggested to characterize aggregates *in situ*. One such measurement recommended and illustrated by Schmidt-Ott (1988) is the so-called *attachment coefficient* for aggregate scavenging of, say, radioactive $^{211}Pb(g)$-atoms. In our notation this quantity (called β by Schmidt-Ott) is equivalent to:

$$\beta_{S \cdot O} = (1/4)\alpha \bar{c}_A a_1 \cdot N \eta_{overall} \qquad (46)$$

where the important *product* $N \cdot \eta_{overall}$ may be regarded as the accessible (or "exposed") number of primary particles, and, in this case, $A \equiv ^{211}Pb(g)$. In the near free-molecular limit ($Kn \gg 1$) this coefficient has been shown to be approximately proportional to the *photoelectron yield* (Burtscher and Schmidt-Ott, 1985) of small ($N \leq 40$, $D_f \approx 2.18$, $R_1 \approx 7.5$ nm) aggregates of silver illuminated by *uv* radiation ($\lambda \approx O\{200 \text{ nm}\}$). [This is already an example for which l_A should be distinguished from the gas *mixture* mean-free-path, and Eq. 41 for $D_{A\cdot mix}$ suitably generalized (Rosner, 1986, 1990).] However, inspection of Eq. 42 and the laws of *electron* scattering in gases suggests that this linearity is not likely to be preserved in the continuum (high-pressure) limit.

It is also noteworthy that there may be a sort of "Reynolds analogy" relation (Rosner, 1986) between the mass-transfer (scavenging) behavior of aggregates and their momentum transfer behavior. Indeed, a near equality between the effective scavenging radius and the mobility equivalent radius has been reported and discussed by Meakin et al. (1989), Schmidt-Ott et al. (1990), and Rogak et al. (1991) (who report agreement within ca. 15% for $Kn \leq O(1)$). This implies that our scavenging rate formalism for aggregates, at least in the high α limit, provides some insight as to the mobility and hence Brownian diffusivity, of such aggregates over a wide range of sizes and Kn_{2R_1}-values. In view of the simplicity and computational efficiency of our methods these implications certainly warrant future investigation.

Defence of Approximations, Generalizations

It would be prudent to briefly reconsider some of our fundamental approximations, indicating their expected domain of validity and suggesting possible generalizations of likely future interest.

Continuum approximation for small N and D_f

Even though the simple scaling law: $d \ln N/d \ln r = \text{const.} \equiv D_f$ has been found to apply down to remarkably small aggregate sizes (Schmidt-Ott et al., 1988, 1990; Megaridis and Dobbins, 1990) clearly, our pseudo-continuum mathematical model (in which each aggregate is treated as a quasi-spherical porous object) should not be expected to apply to aggregates containing, say, less than about 30 primary particles. While the extent to which such pseudo-continuum results match small N detailed particle-level diffusional simulations (Rosner et al., 1991; Mackowski, 1994) remains to be investigated, we should therefore not expect our present results to be quantitatively accurate for aggregate sizes much below about 10^2, especially when D_f is less than 2. [The situation here is quite similar to our earlier theoretical studies of the evaporative combustion of a "cloud" containing N dispersed fuel droplets (Labowsky and Rosner, 1978). In anticipation of relevant "small N" results we have deliberately started our graphs at $N=10$, in order to embrace some of the expected "matching" domain.]

Tortuosity-porosity laws over the spectrum of pore Knudsen numbers

Current research (extensions of Tassopoulos and Rosner, 1992; Melkote and Jensen, 1992; Elias-Kohav et al., 1991) may reveal that our presently used tortuosity laws are not sufficiently accurate, especially in the Knudsen pore diffusion limit (where higher-order microstructural information characterizing the likely primary sphere positions may need to be added) or in the transition regime (where the pore Knudsen number dependence of the tortuosity may not quite be monotonic and, accordingly, depart too much from the behavior tentatively assumed here). Whatever the outcome of such studies, however, the present pseudo-continuum *procedures* should remain useful to (re-)compute and correlate the accessible surface area of such aggregates as a fraction of the total area of the primary spheres present. Indeed, in the near future it would be interesting to compare the present η_{int} estimates with much more computationally-intensive Brownian simulations on computer-generated fractal aggregates in 3 dimensions.

In closing this section it should be remarked that unusual Knudsen diffusion conditions would occur deep inside such an aggregate since, as one approaches the "core" one can show that the local characteristic radial length over which the porosity changes by an appreciable fractional amount, that is, $(d \ln \epsilon/dr)^{-1}$ will no longer be large on the scale of the local average pore diameter! We should also comment that the limit $\alpha \to 1$, while formally included here, should also be expected to be singular for Knudsen diffusion (when $\alpha = 1$ no reagent molecule survives *one* collision with the pore wall!). This implies that corrections to Eq. 8 should be introduced in the high reaction probability limit (Verhoff and Streider, 1971).

Nonspherical aggregate shapes

It has been reported that "small" aggregate-aggregate encounters lead to larger aggregates for which the gyration radii are not the same in all directions. Botet and Jullien (1986) and Hentschel (1984) report an asymptotic gyration radius ratio of ca. 2. Moreover, electron micrographs of soots sampled from diverse systems usually reveal a wide variety of nonspherical aggregate morphologies, often somewhat stringy in character (Ulrich, 1984; Lahaye and Prado, 1981). While there is ample precedent for treating the effectiveness of nonspherical porous catalyst pellets (with $D_f = 3$) using the notion of an *equivalent sphere* of effective radius:

$$R_{eff} = 3 \cdot (V/A)_{outer\ envelope} \qquad (47)$$

(See Aris, 1957). If increased accuracy were needed the present model could readily be generalized to deal with, say, prolate spheroidal porous media which are fractal-like in each principal direction. Moreover, external diffusion layer transport could be dealt with using the dimensionless transfer coefficient for such spheroids (Yovanovich, 1987) but preferably based on the characteristic length $(A_{ext}/\pi)^{1/2}$. These generalizations would allow for the fact that the characteristic Brownian *rotation* time of such large aggregates, for example, $(6D_{N,rot})^{-1}$, would be much larger than the characteristic time $((A_{ext}/\pi)/Nu_m)^2/D_{A \cdot mix}$ for reactant molecule diffusion across the external boundary layer, especially at small Knudsen numbers based on the length $(A_{ext}/\pi)^{1/2}$. Thus, the often-quoted notion that Brownian rotation would *ensure* the reasonableness of a quasi-spherical aggregate approximation even for large elongated aggregates is probably illusory. However, we leave such generalizations to the future, noting only that some of the features of porous suspended particles which are distributed with respect to both size N and *aspect ratio* R are treated in Rosner and Tandon (1994).

Kinetic laws other than first-order irreversible

As mentioned earlier, the present treatment for η_{int} and $\eta_{overall}$ can be generalized to apply equally well to simple *physical* phenomena such as reversible *condensation* or *evaporation* in which the interfacial rate process (sink strength) is proportional to $\alpha [n_A - n_{A,eq}\{T_w; p\}]$ where α is now the condensation or evaporation coefficient. However, in some systems the dependence of α and $n_{A,eq}\{T_w; p\}$ on the radius (of curvature) of the primary particles may have to be explicitly taken into account. More complex *nonlinear* kinetic laws will require separate treatment and will inevitably reveal a dependence on additional dimensionless parameters, as is already familiar in the field of heterogeneous catalysis (Aris, 1975; Satterfield, 1970; Froment and Bischoff, 1979; Engasser and Horvath, 1973).

Primary sphere surface roughness and/or internal porosity

Using X-ray scattering or adsorption techniques some aggregated soot systems have been reported to exhibit significant primary particle surface roughness and/or porosity within the primary spherules (Lahaye and Prado, 1981; Hurd et al., 1987). If necessary, such behavior could be modeled by imagining the primary particles to consist of an outer microporous layer covering an impermeable core, or containing micropores throughout. Indeed, in the spirit of self-similarity (Feder, 1988; Dimotakis, 1991), what we have called the primary particles could themselves be viewed as fractal microspheres, thereby making direct use (on a smaller scale) of the concepts described here. From this vantage point our present treatment (As-

sumption A3) is therefore seen to be equivalent to assuming that the primary spheres are themselves characterized by an effective primary sphere Thiele modulus so large that *their* internal effectiveness factors are very small, corresponding to reaction or trapping on their outer surfaces.

Nonisothermal behavior

Since most of the interfacial processes mentioned above (physical condensation/evaporation, reactive growth from the vapor phase, oxidation (gasification) by one or more reagents in the vapor phase) are not ergoneutral; in general there will be a tendency for the aggregate to overheat or undercool relative to the surrounding gas mixture. Moreover, if the effective *Biot number*, Bi_h, for radial energy transfer defined by:

$$Bi_h \equiv (k_g/k_{agg,eff}) \cdot (Nu_h/2) \qquad (48)$$

(Rosner, 1986, 1990) is not sufficiently small, then temperature nonuniformities *within* the aggregate may play a role in determining both η_{int} and $\eta_{overall}$, especially when the reaction probability α is low and sharply (Arrhenius-) temperature dependent, and the mole fraction of the reagent is not very small. [In this case it might also be necessary to account for the tendency, due to radiative energy loss, for the larger aggregates to be systematically cooler than the smaller ones (Mackowski et al., 1991, 1994; Rosner et al., 1992).]

At the moment, not enough is known about the local effective radial thermal conductivity, $k_{agg,eff}$, within such aggregates, including the Rayleigh-limit *radiative* contribution, to realistically assess these nonisothermal effects. However, we remind the reader that, under thermophysical conditions such that $Bi_h \ll 1$, then our *isothermal* η_{int}-results (Figures 7 and 8) *could* be taken over to find $\eta_{overall}$ even under nonisothermal conditions, since the dominant temperature nonuniformities would then occur only in the external (thermal) gaseous boundary layer.

Conclusions

Principal conclusions for $D_f < 3$ aggregates

A simple pseudo-continuum method has been developed, described and illustrated for calculating the accessible surface area of a large open aggregate containing N primary spherical particles ($N \gg 1$) suspended in a gas at pressures such that the mean-free-path is not necessarily negligible or appreciable compared to the overall aggregate radius. For this purpose, the N-particle aggregate has been treated as a porous granular solid characterized by the scaling exponent $D_f = d \ln N/d \ln r$, and the primary sphere diameter $2R_1$. A simple yet rational correlation scheme has been developed, based on the more familiar $D_f = 3$ case and the notion of an effective (stretched) Thiele modulus Φ_{eff}, which can predict to within about 3% the numerically calculated normalized accessible surface area of such an aggregate over the entire range of parameters of physical interest, viz.: primary particle number, N; structural exponent, D_f; reaction probability, α; and Kn_{2R_1}, the ambient gas mean-free-path (measured in primary particle diameters). As a byproduct, valuable insight has been provided on recent experimental techniques for *in situ* probing of the accessible area of fractal aggregates, for example, the scavenging of radioactive lead atoms and photoelectron emission.

Application of correlations to a_{eff}''' calculations for coagulation-aged suspensions

This formulation and the above-mentioned correlation open the door to calculations of the accessible area per unit volume for coagulation-aged *populations* of aggregates, as observed in many technologies, and in natural environments. Thus, if there are a total of N_p aggregates per unit volume, with specified normalized *size distribution pdf{N}*, we can now rapidly calculate (at least for, say, $N \geq 30$) the most difficult part of the integrand appearing in:

$$a_{eff}''' = N_p \cdot \int_1^\infty a_1 N \cdot \eta_{overall}\{N; D_f, \alpha, Kn_{2R_1}\} \cdot pdf\{N\} dN \qquad (49)$$

and compare the result of this integration to the total area per unit volume, a_{max}''', associated with the sum of all primary particles present *irrespective of their state of aggregation*. Indeed, this a_{eff}'''/a_{max}'''-ratio, which can be considered an *overall effectiveness factor for the aggregate population*, will be seen to dictate aggregated particle/carrier fluid exchange processes in many applications involving flocculated suspensions (Rosner and Tandon, 1993a), including physical- and chemical-vapor deposition (Castillo and Rosner, 1988; Rosner and Liang, 1987) and "particle-modified" chemical vapor deposition (Komiyama et al., 1991).

Future work on transport to/from large aggregates

A number of the generalizations outlined in the fourth section may prove to be necessary and ultimately valuable, building on the effective porous object results and approach outlined here. Indeed, to better understand the large N-limit this approach is being extended to *all* interesting mass-, momentum-, and energy exchange properties of aggregates, including their thermophoretic "propulsion" (Rosner et al., 1991) and radiative properties (Dobbins and Megaridis, 1991; Mackowski, 1992b). It would also be interesting to investigate the vapor nucleating ability of such aggregates, including uptake rates by capillary condensation in the singular "pores" created where primary particles touch. These investigations of aggregates containing many primary spherical particles, including their rearrangement (restructuring) kinetics (Cohen and Rosner, 1994) are now underway, using some of the results of this article and analogous pseudo-continuum methods (Rosner, Cohen, and Tandon, 1993).

Notation

a_1 = surface area of one primary sphere (Figure 2)
a''' = surface area per unit volume
A = reactant species [OH(g), C₂H₂(g), ²¹¹Pb(g)], or area
R = aspect ratio (of prolate spheroid)

Bi_h = Biot number for heat-transfer (ratio of internal- to external heat-transfer resistance)

c = normalized species A local concentration variable

$\bar{c}_A$ = mean thermal speed of molecules A, $[8k_BT/(\pi m_A)]^{1/2}$

D = normalized effective diffusion coefficient; Eqs. 2–18

$D_{A,\text{eff}}$ = effective diffusion coefficient for species A in local porous medium

$D_{A\cdot\text{mix}}$ = coefficient for diffusion of species A through prevailing vapor mixture

D_f = fractal dimension, exponent $d\ln N/d\ln r$

D_K = Knudsen diffusion coefficient (single straight pore of average diameter)

f = fraction of incident molecules scattered diffusely (by surface)

k_{eff}''' = effective pseudo-homogeneous first-order rate constant $(k''a''')$

k'' = first-order heterogeneous rate constant

k_B = Boltzmann constant

Kn = Knudsen number (ratio of gas mean-free-path to characteristic dimension)

l = gas mean-free path

m_a = molecular mass of species A

n_A = local number of density of species A

N = total number of primary spheres in aggregate (see Figure 2)

Nu_m = Nusselt (Sherwood) number for mass transfer to/from sphere

r = radius (measured from aggregate center-of-mass); Figure 2

R_1 = radius of primary spheres; Figure 2

R_c = inner core radius; Eq. 3

R_{gyr} = radius of gyration; Figure 2

R_{max} = maximum (outer) radius defined by Eq. 4

T_w = absolute temperature of solid at $r = R_{\text{max}}$

V = volume

x = argument (of the indicated function): $\eta_3\{x\}$

Greek letters

α = reaction probability, condensation coefficient, and so on $(0 \leq \alpha \leq 1)$

β = filling factor (Eq. 2) = $\phi_{\text{lim}} = 1 - \epsilon_{\text{lim}}$

ϵ = local void fraction $(1 - \phi)$

ζ = normalized radial position variable, r/R_{max}

η = "effectiveness" factor: accessible area as a fraction of Na_1

$\eta_3\{x\}$ = function defined by Eq. 31

λ = radiation wavelength

τ = tortuosity of local pore structure defined by Eqs. 6 and 7

Φ = Thiele modulus (reciprocal of dimensionless reactant penetration depth)

ϕ = solid fraction $(1 - \epsilon)$

Miscellaneous

BC = boundary condition

cm = center of mass; Figure 2

FAM = finite-analytic method

ODE = ordinary differential equation

$O\{\ \}$ = order of magnitude "operator"

S-O = Schmidt-Ott

$\tanh\{\ \}$ = hyperbolic tangent function

^{211}Pb = radioactive isotope of the element lead

$(\bar{\ })$ = normalized by conditions at $r = R_{\text{max}}$

$\langle\ \rangle_q$ = average value defined by Eq. 33

$\{\ \}$ = argument of indicated function

$fct\{\ \}$ = function of indicated argument

$pdf\{\ \}$ = probability density function of indicated random variable

Subscripts

agg = pertaining to aggregate

A = pertaining to species A

c = pertaining to core or to continuum (high-pressure limit) conditions

eff = effective

eq = pertaining to local equilibrium

exp = experimental

ext = external

f = fractal

gyr = gyration

h = pertaining to heat transfer

int = internal

K = Knudsen

$\lim$ = limiting value

m = pertaining to mass transfer

mix = pertaining to local vapor mixture

max = maximum value

$pore$ = based on (mean) pore diameter

q = index appearing in Eq. 33; $q \geq 0$

rot = rotational

$2R_1$ = based on diameter of primary particles

1 = primary particle (spherule); Figure 2

∞ = evaluated at $r = \infty$ (far from aggregate center-of-mass)

Literature Cited

Abbasi, M. H., J. W. Evans, and I. S. Abramson, "Diffusion of Gases in Porous Solids: Monte Carlo Simulations in the Knudsen and Ordinary Diffusion Regimes," *AIChE J.*, **29**(4), 617 (1983).

Aris, R., "On Shape Factors for Irregular Particles—I. The Steady State Problem. Diffusion and Reaction," *Chem. Eng. Sci.*, **6**, 262 (1957).

Aris, R., *The Mathematical Theory of Diffusion and Reaction in Permeable Catalysts—Volume 1*, Clarendon, New York (1975).

Botet, R., "Aerodynamics of 'Filigree' Objects," in preparation (1992).

Botet, R., and R. Jullien, "Intrinsic Anisotropy of Clusters in Cluster-Cluster Aggregation," *J. Phys. A: Math. Gen.*, **19**, L907 (1986).

Burtscher, H., and A. Schmidt-Ott, "Experiments on Small Particles in Gas Suspension," *Surface Sci.*, **156**, 735 (1985).

Butt, J. B., *Reaction Kinetics and Reactor Design*, Prentice-Hall, Englewood Cliffs, NJ (1980).

Castillo, J. L., and D. E. Rosner, "Nonequilibrium Theory of Surface Deposition from Particle-Laden, Dilute Condensible Vapor-Containing Stream, Allowing for Particle Thermophoresis and Vapor Scavenging Within the Laminar Boundary Layer," *Int. J. Multiphase Flow*, **14**(1), 99 (1988).

Charalampopoulos, T. T., and H. Chang, "Agglomerate Parameters and Fractal Dimension of Soot Using Light Scattering—Effects on Surface Growth," *Combustion and Flame*, **87**, 89 (1991).

Chen, C. J., and H. C. Chen, "Finite Analytic Numerical Method for Unsteady Two-Dimensional Navier-Stokes Equations," *J. Computational Physics*, **53**, 209 (1984).

Cohen, R. D., and D. E. Rosner, "Restructuring Kinetics of Multi-Particle Aggregates," in preparation (1994).

Coniglio, A., and H. E. Stanley, "Screening of Deeply Invaginated Clusters and the Critical Behavior of the Random Superconducting Network," *Phys. Rev. Lett.*, **52**(13), 1068 (1984).

Correa, S. M., and W. Shyy, "Computational Models and Methods for Continuous Gaseous Turbulent Combustion," *Prog. in Energy and Combust Sci.*, **13**(4), 249 (1987).

Dickenson, E., "Short-Range Structure in Aggregates, Gels and Sediments," *J. Colloid Interface Sci.*, **118**(1), 286 (1987).

Dimotakis, P. E., "Fractals, Dimensional Analysis and Similarity, and Turbulence," *Nonlinear Sci. Today*, **1**(2), 1 (1991).

Dixon-Lewis, G., D. Bradley, and S. El-Din Habik, "Oxidation Rates of Carbon Particles in Methane-Air Flames," *Combustion and Flame*, **86**, 12 (1991).

Dobbins, R. A., and C. M. Megaridis, "Morphology of Flame-Generated Soot as Determined by Thermophoretic Sampling," *Langmuir*, **3**, 254 (1987).

Dobbins, R. A., and C. M. Megaridis, "Absorption and Scattering of Light by Polydisperse Aggregates," *Appl. Optics*, **30**(33), 4747 (1991).

Elias-Kohav, T., and M. Sheintuch, "Steady-State Diffusion and Reactions in Catalytic Fractal Porous Media," *Chem. Eng. Sci.*, 46(11), 2787 (1991).

Engasser, J. M., and C. Horvath, "Effect of Internal Diffusion in Heterogeneous Enzyme Systems: Evaluation of True Kinetic Parameters and Substrate Diffusivity," *J. Theor. Biol.*, 42, 137 (1973).

Feder, J., "The Cluster Fractal Dimension," in *Fractals*, Plenum Press, New York, pp. 31-40 (1988).

Feng, H., and D. E. Rosner, "Energy Transfer Effects of Excited Molecule Production by Surface-Catalyzed Atom Recombination," *Faraday Trans. I.—Phys. Chem.*, 70, 884 (1974).

Formenti, M., M. Juillet, P. Meriaudeau, S. J. Teichner, and P. Vergnon, "Aerosol Route to Metal Oxide Catalysts," *J. Colloid Interface Sci.*, 39(1), 79 (1972).

Friedlander, S. K., *Smoke, Dust and Haze—Fundamentals of Aerosol Behavior*, John Wiley, New York (1977).

Froment, G. F., and K. B. Bischoff, *Chemical Reactor Analysis and Design*, John Wiley, New York (1979).

Gomez, A., and D. E. Rosner, "Thermophoretic Effects on Particles in Counterflow Laminar Diffusion Flames," *Combust. Sci. and Tech.*, 89, 335 (1993).

Hagenlock, R., and S. K. Friedlander, "Numerical Calculations of Collision Frequency of Molecules With DLA Clusters," *J. Colloid Interface Sci.*, 133(1), 185 (1989).

Harris, S. J., and A. M. Weiner, "Soot Particle Growth in Premixed Toluene/Ethylene Flames," *Combust. Sci. and Tech.*, 38, 75 (1984).

Hentschel, H. G. E., "The Structure and Fractal Dimension of Generalized Diffusion-Limited Aggregates," in *Kinetics of Aggregation and Gelation*, F. Family and D. P. Landau, eds., Elsevier, pp. 165-168 (1984).

Huizenga, D. G., and D. M. Smith, "Knudsen Diffusion in Random Assemblages of Uniform Spheres," *AIChE J.*, 32(1), 1 (1986).

Hurd, A. J., D. W. Schaefer, and J. E. Martin, "Surface and Mass Fractals in Vapor-Phase Aggregates," *Phys. Rev.*, A35(5), 2361 (1987).

Israel, R., and D. E. Rosner, "Use of a Generalized Stokes Number to Determine the Aerodynamic Capture Efficiency of Non-Stokesian Particles from a Compressible Gas Flow," *Aerosol Sci. Tech.*, 2, 45 (1983).

Julien, R., M. Kolb, and R. Botet, "Scaling Properties of Growth by Kinetic Clustering of Clusters," in *Kinetics of Aggregation and Gelation*, F. Family and D. P. Landau, eds., Elsevier, New York (1984).

Koch, W., and S. K. Friedlander, "The Effect of Particle Coalescence on the Surface Area of a Coagulating Aerosol," *J. Colloid Int. Sci.*, 140, 419 (1990).

Komiyama, H. T., and L. S. Hong, "Chemical Vapor Deposition of CuO_x Films by CuI and O_2: Role of Cluster Formation on Film Morphology," *J. Amer. Ceram. Sci.*, 74(7), 1597 (1991).

Labowsky, M., and D. E. Rosner, "Group Combustion of Droplets in Fuel Clouds: I. Quasi-Steady Predictions," *Evaporation—Combustion of Fuels: ACS Advances in Chem. Series*, 166, 63 (1978).

Lahaye, J., and G. Prado, "Morphology and Internal Structure of Soot and Carbon Blacks," in *Particulate Carbon: Formation During Combustion*, D. C. Siegla and G. W. Smith, eds., Plenum Press, New York, pp. 33-55 (1981).

Mackowski, D. W., "Phoretic Behavior of Asymmetric Particles in Thermal Nonequilibrium with the Gas: Two Sphere Aggregate," *J. Colloid Int. Sci.*, 140(1), 138 (1990).

Mackowski, D. W., M. Tassopoulos, and D. E. Rosner, "Effect of Radiative Heat Transfer on the Coagulation Rates of Combustion-Generated Particles," *Aerosol Sci. Tech.*, 20(1), 83 (1994).

Matijevic, E., "Monodispersed Metal (Hydrous) Oxides—A Fascinating Field of Colloid Science," *Acc. Chem. Res.*, 14, 22 (1981).

Matsoukas, T., and S. K. Friedlander, "Dynamics of Aerosol Agglomerate Formation," *J. Colloid Interface Sci.*, 146(2), 495 (1991).

Meakin, P., and T. A. Witten, Jr., "Growing Interface in Diffusion-Limited Aggregation," *Phys. Rev.*, A28(5), 2985 (1983).

Meakin, P., "Particle-Cluster Aggregation With Fractal Particle Trajectories and On Fractal Substrates," in *Kinetics of Aggregation and Gelation*, F. Family and D. P. Landau, eds., Elsevier, pp. 91-99 (1984).

Meakin, P., B. Donn, and G. W. Mulholland, "Collisions Between Point Masses and Fractal Aggregates," *Langmuir*, 5, 510 (1989).

Medalia, A. I., and F. A. Heckman, "Morphology of Aggregates—II. Size and Shape Factors of Carbon Black Aggregates from Electron Microscopy," *Carbon*, 7, 567 (1969).

Megaridis, C. M., and R. A. Dobbins, "Morphological Description of Flame-Generated Materials," *Combust. Sci. Tech.*, 71, 95 (1990).

Melkote, R. R., and K. F. Jensen, "Computation of Transition and Molecular Diffusivities in Fibrous Media," *AIChE J.*, 38(1), 56 (1992).

Mohamed, R. S., P. G. Debenedetti, and R. K. Prud'homme, "Effects of Process Conditions on Crystals Obtained from Supercritical Mixtures," *AIChE J.*, 35(2), 325 (1989).

Mountain, R. D., and G. W. Mulholland, "Stochastic Dynamics Simulation of Particle Aggregation," in *Kinetics of Aggregation and Gelation*, F. Family and D. P. Landau, eds., Elsevier, pp. 83-86 (1984).

Mountain, R. D., G. W. Mulholland, and H. R. Baum, "Simulation of Aerosol Agglomeration in the Free-Molecular and Continuum Flow Regimes," *J. Colloid Interface Sci.*, 114(1), 67 (1986).

Mountain, R. D., and G. W. Mulholland, "Light Scattering from Simulated Smoke Agglomerates," *Langmuir*, 4, 1321 (1988).

Mulholland, G. W., R. J. Samson, R. D. Mountain, and M. H. Ernst, "Cluster Size Distribution for Free-Molecular Agglomeration," *Energy and Fuels*, 2, 481 (1988).

Neoh, K. G., J. B. Howard, and A. F. Sarofim, "Soot Oxidation in Flames," in *Particulate Carbon: Formation During Combustion*, D. C. Siegla and G. W. Smith, eds., Plenum Press, New York, pp. 261-282 (1981).

Olague, N. E., D. M. Smith, and M. Ciftcioglu, "Knudsen Diffusion in Ordered Sphere Packings," *AIChE J.*, 34(11), 1907 (1988).

Puri, R., T. F. Richardson, R. J. Santoro, and R. A. Dobbins, "Aerosol Dynamic Processes of Soot Aggregates in a Laminar Ethene Diffusion Flame," *Combustion and Flame*, 92(3), 320 (1993).

Rogak, S. N., and R. C. Flagan, "Stokes Drag on Self-Similar Clusters of Spheres," *J. Colloid Interface Sci.*, 134(1), 206 (1990).

Rogak, S. N., U. Baltensperger, and R. C. Flagan, "Measurement of Mass Transfer to Agglomerate Aerosols," *Aerosol Sci. Tech.*, 14, 447 (1991).

Rogak, S. N., H. V. Nguyen, and R. C. Flagan, "The Mobility and Structure of Aerosol Agglomerates," *Aerosol Sci. Tech.*, 18, 25 (1993).

Rosner, D. E., and M. Tassopoulos, "Deposition Rates from 'Polydispersed' Populations of Arbitrary Spread," *AIChE J.*, 35(9), 1497 (1989).

Rosner, D. E., "High Temperature Gas-Solid Reactions," *Ann. Rev. of Mat. Sci.*, 2, 573 (1972).

Rosner, D. E., *Transport Processes in Chemically Reacting Flow Systems*, Butterworths-Heinemann, Stoneham, MA (1990).

Rosner, D. E., R. D. Cohen, and P. Tandon, "Development of Pseudo-Continuum Theories of the Restructuring Kinetics of Large Multi-Particle Aggregates in Combustion Systems," Abstract 8D4, p. 331, AAAR Annual Meeting, Oak Brook, IL (Oct. 11-15, 1993).

Rosner, D. E., and B. Liang, "Laboratory Studies of Binary Salt CVD in Combustion Gas Environments," *AIChE J.*, 33(12), 1937 (1987).

Rosner, D. E., D. W. Mackowski, and P. Garcia-Ybarra, "Size- and Structure-Insensitivity of the Thermophoretic Transport of Aggregated 'Soot' Particles in Gases," *Combust Sci. Tech.*, 80(1-3), 87 (1991).

Rosner, D. E., D. W. Mackowski, M. Tassopoulos, and P. Garcia-Ybarra, "Effects of Heat Transfer on the Dynamics and Transport of Small Particles in Gases," *Ind./Eng. Chem.-Research*, 31, 760 (1992).

Rosner, D. E., R. Nagarajan, M. Kori, and S. A. Gokoglu, "Maximum Effect of Vapor Phase Chemical Reactions on CVD-Rates and Deposition Onset Conditions in the Absence of Interfacial Chemical Kinetic Barriers," *Proc. 10th Inf. Conf. on CVD*, G. W. Cullen, ed., The ElectroChem Soc., 87-8, pp. 61-80 (1987).

Rosner, D. E., and P. Tandon, "Effective Area/Volume and Sorptive Capacity of Populations of 'Microporous' Aerosol Particles Distributed With Respect to Both Size (Volume) and Shape," *AIChE J.*, submitted (1994).

Rosell, J., "Vapor Scavenging Ability of a Fractal Aggregate," *Yale University, ChE 620a Course Report* (1990).

Roth, P., O. Brandt, and S. Von Gersum, "High Temperature Oxidation of Suspended Soot Particles Verified by CO and CO_2 Measurements," *23rd Int. Symposium on Combustion*, Orleans, France, The Combustion Institute, pp. 1485-1491 (1990).

Satterfield, C. N., *Mass Transfer in Heterogeneous Catalysis*, MIT Press, Cambridge, MA (1977).

Schaefer, D. W., E. J. Martin, P. Wiltzins, and D. S. Cannell, "Fractal Geometry of Colloidal Aggregates," *Phys. Rev. Lett.*, 52, 2371 (1984).

Schaefer, D. W., "Fractal Models and Structure of Materials," *MRS Bulletin*, 8(2), 22 (1988).

Schaefer, D. W., A. J. Hurd, D. K. Christen, S. Spooner, and J. S. Lin, "Growth and Structure of Pyrogenic Silica," *Mat. Res. Sci. Symp. Proc.*, 121, 305 (1988).

Schmidt-Ott, A., "*In Situ* Measurement of the Fractal Dimensionality of Ultrafine Aerosol Particles," *Appl. Phys. Lett.*, 52(12), 954 (1988).

Schmidt-Ott, A., "New Approaches to *In Situ* Characterization of Ultrafine Agglomerates," *J. Aerosol Sci.*, 19(5), 553 (1988).

Schmidt-Ott, A., U. Baltensperger, H. W. Gaggeler, and D. T. Jost, "Scaling Behaviour of Physical Parameters Describing Agglomerates," *J. Aerosol Sci.*, 21(6), 711 (1990).

Sheintuch, M., and S. Brandon, "Deterministic Approaches to Problems of Diffusion, Reaction and Adsorption in a Fractal Porous Catalyst," *Chem. Eng. Sci.*, 44(1), 69 (1989).

Siegla, D. C., and G. W. Smith, eds., *Particulate Carbon: Formation During Combustion*, Plenum Press, New York (1981).

Smith, D. M., "Knudsen Diffusion in Constricted Pores: Monte-Carlo Simulations," *AIChE J.*, 32(2), 329 (1986).

Tassopoulos, M., and D. E. Rosner, "Simulation of Vapor Diffusion in Anisotropic Particulate Deposits," *Chem. Eng. Sci.*, 47(2), 421 (1991).

Torquato, S., "Thermal Conductivity of Disordered Heterogeneous Media from the Microstructure," *Rev. in Chem. Eng.*, 4, 151 (1984).

Torquato, S., "Random Heterogeneous Media; Microstructure and Improved Bounds on Effective Properties," *Appl. Mech. Rev.*, 44(2), 37 (1991).

Ulrich, G. D., "Flame Synthesis of Fine Particles," *Chem. Eng. News* (*ACS*), 22 (1984).

Verhoff, F. H., and W. Streider, "Numerical Studies of Knudsen Diffusion and Chemical Reaction in Capillaries of Finite Length," *Chem. Eng. Sci.*, 26, 245 (1971).

Wu, M. K., and S. K. Friedlander, "Enhanced Power-Law Agglomerate Growth in the Free-Molecule Regime," *J. Aerosol Sci.*, 24(3), 273 (1993).

Yovanovich, M. M., "New Nusselt and Sherwood Numbers for Arbitrary Isopotential Bodies at Near Zero Peclet and Rayleigh Numbers," Paper No. AIAA-87-1643, *AIAA 22nd Thermophysics Conf.*, Honolulu (June, 1987).

Zukoski, C. F., M. K. Chow, G. H. Bogush, and J. L. Look, "Precipitation of Uniform Particles—The Role of Aggregation," *Mat. Res. Soc. Symp. Proc.*, 180, 131 (1990).

**HIGH TEMPERATURE CHEMICAL REACTION
ENGINEERING LABORATORY**
YALE UNIVERSITY
BOX 2159, YALE STATION
NEW HAVEN, CONNECTICUT 06520 U.S.A.

REPORT DOCUMENTATION PAGE

Public reporting burden for this collection of information is estimated to average 1 hour per response, including the time for reviewing instructions, searching existing data sources, gathering and maintaining the data needed, and completing and reviewing the collection of information. Send comments regarding this burden estimate or any other aspect of this collection of information, including suggestions for reducing this burden, to Washington Headquarters Services, Directorate for Information Operations and Reports, 1215 Jefferson Davis Highway, Suite 1204, Arlington, VA 22202-4302, and to the Office of Management and Budget, Paperwork Reduction Project (0704-0188), Washington, DC 20503.

1. AGENCY USE ONLY (Leave blank)	2. REPORT DATE	3. REPORT TYPE AND DATES COVERED Conf. Proc.

4. TITLE AND SUBTITLE

(U) "Rational Prediction of Inertially Induced Particle Deposition Rates for a Cylindrical Target in Dust-Laden Streams"

5. FUNDING NUMBERS

PE – 61102F
PR – 2308
SA – BS
G – F49620-94-1-0143

6. AUTHOR(S)

Rosner, D.E., Tandon, P. and Konstandopoulos, A.G.

7. PERFORMING ORGANIZATION NAME(S) AND ADDRESS(ES)

Yale University
High Temperature Chemical Reaction Engineering Laboratory
Department of Chemical Engineering
PO Box 208286 YS, New Haven, CT 06520-8286 USA

8. PERFORMING ORGANIZATION REPORT NUMBER

9. SPONSORING/MONITORING AGENCY NAME(S) AND ADDRESS(ES)

AFOSR/NA
110 Duncan Avenue, Suite B115
Bolling AFB DC 20332-0001

10. SPONSORING/MONITORING AGENCY REPORT NUMBER

11. SUPPLEMENTARY NOTES

12a. DISTRIBUTION/AVAILABILITY STATEMENT

12b. DISTRIBUTION CODE

13. ABSTRACT (Maximum 200 words)

We review here results of our recent research on the *deposition dynamics of combustion-generated particles* in power production and materials synthesis/processing technologies. In this brief summary, which emphasizes the capture of inertially impacting particles , we outline and illustrate the results of recently developed methods to predict total surface *deposition rates and associated convective heat transfer reductions* for targets exposed to a distribution of particles suspended in a mainstream. Our methods combine the essential features of recently developed *single particle sticking probability laws* with correlations of the *inertial impaction* of particles on targets in high Reynolds number cross-flow, to develop formulae and 'universal' graphs which provide the dependence of particle deposition rates, and associated reductions in convective heat transfer, on such system parameters as mainstream velocity, mean suspended particle size and target size. The deposition rate/deposit microstructue/properties prediction and correlation procedures illustrated here [R 9,10] can be used in many ways; *eg.* incorporated into improved 'fouling propensity indices', to motivate, evaluate and implement "ruggedization" and/or *fouling reduction strategies*, and/or to optimize the "harvesting" of tailored particles for subsequent processing.

14. SUBJECT TERMS

Soot, aggregated particles, mass transport, thermophoresis, particle inertia, Brownian diffusion, deposit microstructure/properties, Brownian diffusion,

15. NUMBER OF PAGES

8

16. PRICE CODE

17. SECURITY CLASSIFICATION OF REPORT	18. SECURITY CLASSIFICATION OF THIS PAGE	19. SECURITY CLASSIFICATION OF ABSTRACT	20. LIMITATION OF ABSTRACT
Unclassified	Unclassified	Unclassified	UL

Standard Form 298 (890104 Draft)
Prescribed by ANSI Std. 239-18
298-01

PREDICTION/CORRELATION OF PARTICLE DEPOSITION RATES FROM DILUTE POLYDISPERSED FLOWING SUSPENSIONS AND THE NATURE/PROPERTIES OF RESULTING DEPOSITS*

D. E. Rosner, P. Tandon, A.G. Konstandopoulos and M. Tassopoulos

Yale University, Department of Chemical Engineering
High Temperature Chemical Reaction Engineering Laboratory
New Haven, CT 06520-8286 USA

SUMMARY

We review here results of our recent research on the *deposition dynamics of combustion-generated particles* in power production and materials synthesis/processing technologies. In this brief summary, which emphasizes the capture of inertially impacting particles*, we outline and illustrate the results of recently developed methods to predict total surface *deposition rates and associated convective heat transfer reductions* for targets exposed to a distribution of particles suspended in a mainstream. Our methods combine the essential features of recently developed *single particle sticking probability laws* with correlations of the *inertial impaction* of particles on targets in high Reynolds number cross-flow, to develop formulae and 'universal' graphs which provide the dependence of particle deposition rates, and associated reductions in convective heat transfer, on such system parameters as mainstream velocity, mean suspended particle size and target size. The deposition rate/deposit microstructue/properties prediction and correlation procedures illustrated here [R 9,10] can be used in many ways; *eg.* incorporated into improved 'fouling propensity indices', to motivate, evaluate and implement "ruggedization" and/or *fouling reduction strategies*, and/or to optimize the "harvesting" of tailored particles for subsequent processing.

Details on our theoretical studies, and their immediate laboratory antecedents [L1,R4,5,16], will be found in our archival references (Section 8). A judicious blend of (numerical and physical) experiments, theory, and intuition will continue to be necessary to economically arrive at methods/results to improve the generality and accuracy of particle-deposition-related design calculations for a wide variety of equipment/fuel types. Our computational and correlation methods are being extended to treat more complex situations of practical importance in power generation and materials synthesis/processing applications.

1. INTRODUCTION, BACKGROUND

Initially clean heat exchanger, containment, or target surfaces exposed to high temperature flowing suspensions---*eg.*, ash or soot particles in fossil fuel (oil or coal-) combustion products, can acquire a sufficient fraction of this solid material to cause a noticeable decline in heat transfer or aerodynamic performance. This decline is associated with the local growth of microgranular insulating layers, often undesired and creating the need for periodic shutdown for cleaning. To answer such questions as: required maintainence intervals for a particular (class of) fuel(s) ; assess the most economical degree of fuel 'cleaning'; or, in particle synthesis/processing applications, to select optimum conditions for harvesting desirable particles or coatings,... a quantitative understanding of *deposition rates /deposit microstructure/properties* is clearly necessary. From the viewpoint of capturing a non-negligible fraction of the mainstream particle flow rate, *inertial impaction* is usually the mechanism responsible for most of the deposited mass and volume. However, by far the greatest uncertainty in making such deposition rate predictions is associated with the appropriate single impacting particle *capture fraction* , or sticking probability s [R10]. In general, s is a function of both incident velocity and angle, but not yet fully understood even for particle impaction on 'dry' granular deposits [K3, R 10]. Moreover, in most applications s will be determined in part by the simultaneous rates of *vapor* and much *smaller particle (non-inertial)* deposition [R6]*. As summarized below, we have extended/applied *inertial impaction* theory [F1, I1,K2, R13] and applied what we now know about *single particle capture behavior* [K3 , R10] to predict the sensitivity of deposition rate to system parameters (*eg.*, mainstream velocity, particle mass loading, rebound velocity, mean

---

*For a review of multi-component *vapor* convective-diffusion and *thermophoretic particle mass transfer* in chemically reactive flow systems, see. *e.g.*, [R8,15,17]. Our prior experimental and theoretical studies of alkali *vapor deposition* are conveniently summarized in [R 4]. For a useful overview of heat exchanger fouling research as of *ca.* 1989 see: [M 1].

particle size, target diameter, *etc.*). This capability can clearly be used to motivate, evaluate and implement "ruggedization" and/or *fouling reduction strategies*, or optimize the 'harvesting' of tailored particles for subsequent processing.

2. PREDICTION of PARTICLE DEPOSITION RATES

We have developed a convenient formalism [R9] for making rational engineering predictions of deposition rates in high-gas velocity particle-laden environments, based, in part, on recently developed single particle sticking capture laws [K3,R10] for impaction on granular deposits. Exploiting such information, even when available for the particular materials combinations of interest, to anticipate deposition rates in realistic engineering environments was previously thought to be a computationally demanding task since it is necessary to track the impingement frequency, velocity and incidence angles of all the different size particles in the mainstream capable of striking the target locations of interest, invoking the abovementioned *sticking (or 'rebound') laws* at each such point to predict the corresponding cumulative local deposition rate. However, by focusing our attention on specific canonical geometries (*eg.*, circular-cylindrical targets in cross-flow (Fig.1)) and introducing a modest number of defensible approximations (Section 3) to summarize the predicted and/or measured rebound behavior on the solid surfaces of interest, we have shown that the tedious portion of such deposition rate predictions can be efficiently carried out 'once-and-for-all', thereby reducing the engineering problem of predicting target deposition rates, and the associated reduction in convective heat transfer rate, to that of multiplying a readily calculated *reference deposition rate* by a set of 'universal' dimensionless deposition rate functions, some of which are illustrated here. Our reference deposition rate is that which would be expected in the prevailing environment if all mainstream particles had the mean size and were captured upon impacting the target surface without experiencing aerodynamic deceleration or deflection due to the carrier gas flow. For convenience and generality, our results are cast in terms of the following *dimensionless* parameters: ratio of mainstream velocity U to the reference critical velocity, $V_{p,crit}$(v_{crit}), for particle rebound from the solid surface, ratio of mean abrasive particle size, $\bar{v}$, to the threshold ('critical') size, v_{crit}, required for impaction on the target in the prevailing flow environment [R3], spread, σ_g , of the mainstream particle size distribution $C_\infty(v)$ (here assumed 'log-normal'[R3]), and the characteristic 'slip' Reynolds number for the critical size particles in the mainstream [I1]. In this way we have shown that many previously observed characteristics of granular deposits (*eg.*, fouling layers layers) including their frequent "lobular" appearance (Fig. 3), can be understood theoretically.

3. PRINCIPAL ASSUMPTIONS

To incorporate the essential physical phenomena without making unrealistic idealizations, most work to date has been based on the following *basic assumptions*:

A1   Local particle impaction frequencies, velocities, and angle-of-incidence can be calculated with sufficient accuracy from recent correlations summarizing the results of individual suspended non-Brownian particle trajectories calculated for steady, inviscid flow past the target , including non-Stokesian drag corrections (*cf.* [I 1](Fig. 1)

A2   Even for impaction on *granular* deposits [R10], single particle capture probability laws at particular velocities and incidence angles can be invoked to predict average deposition rates in engineering applications where suspended particles of different sizes arrive over a broad range of impact velocities and incidence angles.

A3.   'Rebounding' particles donot appreciably influence incoming particles, nor deposit in appreciable numbers upon re-impaction on the same target

A4   Predicted 'initial' deposition rate trends (spatial distributions) determined on an initially smooth target can be used to anticipate longer time deposition rate trends on inevitably roughened targets which ultimately depart from their original shape due to localized deposit growth.

A5   The mainstream population of suspended particles is approximately log-normal with respect to particle volume [R3] and, while the particle *mass loading*, ω_p, in the mainstreamneed *not* be very small [R1 , P1], the *volume fraction*, ϕ_p, corresponding to the total particle number density N_p and mean particle volume $\bar{v}$ *is* negligible.

Subject to these assumptions, as noted above actual local deposition rates at any position x/L_t (=polar angle θ for a circular cylinder (Fig 1) if L_t is taken to be $d_t/2$) can be expressed as the product of an easily calculated *reference deposition rate*, $(DR)_{ref}$ and a universal dimensionless function $D(x/L_t,...)$ introduced, calculated(Section 4) and plotted (Fig. 3) over the interesting range of mean suspended particle diameters (expressed as a multiple of critical diameter required for inertial impaction in the prevailing environment [R3]) and a dimensionless velocity ratio characterizing the *rebound behavior* of the particles on the surface of interest. An attractive feature of this type of formulation is that the dimensionless function D, and its average value D over the 'upwind-facing' surface of the target, can be calculated 'once-and-for-all' *via* straightforward numerical quadratures in terms of an acceptably small number of dimensionless parameters defining the system (application). Indeed, the availability of such results dramatically simplifies the task of predicting local and total deposition rates for, say, heat exchanger tubes in the cross-flow of ash-laden combustion products [R9] . Moreover, by introducing a modified (heat transfer coefficient-weighted-) average value of D, designated D_h (Eq.2(below),Fig.4),the prediction of the associated *convective heat transfer reduction.* has also been dramatically simplified [R9].

4 SINGLE PARTICLE CAPTURE PROBABILITY LAWS
and the CALCULATION of $D(x/L_t, ...)$

We have *applied* the micromechanical theory of particle *capture sticking fraction* (which provides the functional form of s when particular projectile particles are directed at particular target materials (including granular deposits) at a known velocity V_p and angle of incidence θ_i (*cf.* the target outward normal) to predict local and total particle capture rates for specific cases of practical importance; *eg.* a cylindrical target immersed in a polydispersed suspension of such particles[R3,9]. Three distinct classes of single particle capture laws have been considered, as follows: constant capture fraction, "on-off" (Fig.2a) capture behavior (expected on a 'clean' (particle-free) smoothe surface), and capture by a 'granular' *deposit* (above the particle critical velocity, the sticking probability does not fall abruptly to zero but, rather, exhibits an exponential 'tail' ([K3,R10] see Fig. 2b).

The *dimensionless* local deposition rate function $D(x/L_t)$ is explicitly given by an integral of the form:

$$D\left(x/L_t,...\right) = \frac{1}{\overline{v}} \int_0^\infty s\left(v, x/L_t\right) \cdot \eta_{local}\left(v, x/L_t\right) \cdot v \cdot C_\infty(v) \cdot dv \qquad (1)$$

To complete the calculation of $D(x/L_t,...)$ in any particular situation (see, *eg.*, Fig.3) we must specify the three inertial impaction functions: impact velocity,$V_p(v, x/L_t)/U$, angle-of-incidence (Fig.1) $\theta_i(v, x/L_t)$ (these determine the local capture fraction) and the local dimensionless particle impingement frequency $\eta_{local}(v, x/L_t)$. Our primary goal has often been the mean value $\overline{D}$ of D over the upwind-facing surface of the target. For a circular cylinder it is interesting to note that $\overline{D}$ so defined is merely $2/\pi$ times the conventionally defined *total capture (efficiency) fraction*, η_{cap} based on target 'frontal area' [R15].

5. ASSOCIATED REDUCTION in CONVECTIVE HEAT TRANSFER RATE

One frequent reason for interest in deposition dynamics is the consequence of even a thin deposit for *heat transfer* performance. Accordingly, we derived the following interesting explicit relation between fractional convective heat transfer reduction and the abovementioned local deposition rate function. An important result of our analysis is the relevance of the ($Nu_h(x/L_t)$-'weighted'-) integral :

$$\overline{D_h} \equiv \frac{L_t}{x_m} \cdot \int_0^{x_m/L_t} \left[\frac{Nu_h\left(x/L_t\right)}{Nu_h(0)} \right] \cdot D\left(x/L_t,...\right) \cdot d\left(x/L_t\right) \qquad (2)$$

where the integrand contains the position dependence of the *local convective heat transfer coefficient.* and x_m is the maximum value of x capable of experiencing particle impacts for a symmetrical target. The relevance of $\overline{D}_h$ to heat transfer reduction is clearly understood when it is recognized that equal thickness local deposits will have greater effect on overall convective heat transfer if located near the position of maximum Nu_h; *eg.* the forward stagnation point region (where $Nu_h(\theta;Re)$ maximizes in the Re-range of interest) than if located near $\theta=\pi/2$ radians (*cf.* Figs. 1,3). The *fractional reduction of convective heat transfer rate* $\dot{q}'$ with time t on stream is found to be given by [R9]:

$$\frac{-\Delta\dot{q}'_w}{\left(\dot{q}'_w\right)_{t=0}} \cong \frac{1}{1-\langle\varepsilon\rangle} \cdot \frac{\int_0^t (DR)_{ref}\,dt}{d_t} \cdot \frac{k_g}{k_{dep}} \cdot \left|\frac{\frac{1}{2}Nu_h(0)}{\overline{Nu_h}}\right| \cdot \overline{D}_h \tag{3}$$

To summarize, for the canonical case of say, a circular cylinder in $Re_t^{1/2}\gg1$ crossflow, our 'universal' results for $D(\theta)$ and $\overline{D}_h$, coupled with Eq.(3) and a rational estimate of $(1-\langle\varepsilon\rangle)\cdot k_{dep}$ appropriate to the granular deposit in question, can be used to predict the time-on-stream corresponding to, say, a specified fractional loss of convective heat transfer rate of $-\Delta\dot{q}'_w/\dot{q}'_w$ (*eg.*,10%). Under conditions for which the deposits are not necessarily confined to the forward stagnation region (*eg.*, for impact/rebound on a bare surface at large values of $(\overline{v}/v_{crit})^{1/3}$ and $U/V_{p,cr}$), then $\overline{D}_h$ is found to be noticeably smaller than $\overline{D}$.

Figure 3 is a representative polar plot of dimensionless deposition rates on the upwind surfaces of the cylinder in crossflow for one of the sticking laws considered (Fig. 2). The rebound parameter $(U/V_{cr}(v_{cr}))$ is only 0.1 for the case (shown) of capture on clean solid surfaces. The calculated contours are for different values of dimensionless mean volume, $\overline{\xi}$, defined as the ratio of $\overline{v}$ of the mainstream distribution and the critical particle volume, v_{crit}. For the case of clean solid surfaces, an impacting particle is captured only if the normal velocity component, $V_{p,n}$, is less than the size-dependent critical velocity, $V_{p,crit}(v)$. Therefore, as the dimensionless mean size of the particles increases, a larger fraction of these particles rebound in the forward stagnation region but somewhat smaller particles are captured at larger angles, θ, leading to the formation of deposits with off-axis 'lobes' (Fig. 3), which *have* been frequently observed.

Figure 4 summarizes representative results for the function $\overline{D}_h$ needed to predict *convective heat transfer reductions* (*via* Eq(3)). Trends for $\overline{D}_h$ are the same as those for $\overline{D}$ but, as expected, there is a systematic decrease below $\overline{D}$ in those cases for which there is appreciable off-axis deposition.

A valuable byproduct of this approach is the ability to evaluate the local *sensitivity* of deposition rates to key system parameters [R9], such as gas velocity, mean particle size in the mainstream and target dimension. Our results indicate the presence of interesting opposing tendencies----for example, an increase in gas velocity increases the particle impingement rate but also increases the fraction of impacts leading to *rebound*. Similarly, an increase in target dimension would reduce the frequency of impacts but increase the likelihood of capture upon each (lower velocity) impact. Clearly, an understanding of these 'tradeoffs' is necessary to evaluate, say, the efficacy of rival strategies for reducing heat exchanger fouling rates.

6. DEPOSIT MICROSTRUCTURE/THERMOPHYSICAL PROPERTIES

In many applications it is necessary to embrace phenomena explicitly missing from the 'baseline' analysis outlined above (*eg.*, larger particle capture effects associated with the simultaneous presence and capture of condensible *vapor* and/or *submicron* (subcritical) *particles* (see, *eg.*, [C1,R6,10]). For example, we would expect systematic shifts in the critical velocity for particle rebound, $V_{p,crit}(v)$, based on the relative amount of vapor and/or sub-micron (supercritical) particle deposition, locally.

Additionally, it is clearly necessary to understand the interesting links between deposit microstructure/properties and particle deposition mechanism [T1,5]. Thus, in comparing such deposition rate predictions with experiments, it should be borne in mind that, for 'thick' granular deposits, one must incorporate information on the *microstructure* including, at least, the void fraction $<\varepsilon>$ of such deposits (see, *eg.*,[T1,4,R10]). We know from these ancillary studies that the local deposit *thickness* and associated local *thermal resistance* at any given time on-stream are not determined only by the history of the local particle volume fluxes due to impaction/capture.

The particle-level dynamical simulations which led to our currently used capture fraction laws for particle impact on dry mono-sized deposits (Section 4, Fig. 2, and [K1, R10]) also lead to particular microstructures [R10] which have been characterized using a number of distribution functions [T4] including 'pore'-size and contact normals. These statistical descriptors have also been used for deposits grown using simpler 'algorithms' regarding arrival mechanism and 'rolling events' prior to incident particle 'arrest' (Fig. 5, after [T1-5]). Using accelerated random-walk (Brownian mass- or heat- 'tracer') simulation methods we have also developed and illustrated methods to predict the anisotropic effective 'diffusivities' of these deposits, including the *effective thermal conductivity* $k_{dep,eff}$ (Fig. 6, after [T3]) and the effective Fick diffusivity for vapor diffusion through the gas-filled interstitial spaces between the spheres. We are currently generalizing these methods to include the effects of particle 'polydispersity', capillary condensation, and partial sintering ('consolidation').

7. CONCLUSIONS

Despite the daunting complexities remaining to be overcome in the design and operation of power plants (*eg.*, utilizing a broad spectrum of ash-bearing fuels, including refuse-based 'fuels'), as well as combustion-derived particle synthesis/processing devices (*eg.*, optical wave guide manufacture [R1]), these recent methods and results are indicative of the potentially useful simplifications and generalizations emerging from current fundamental research studies of suspended particle deposition mechanisms and their connection to microparticulate *deposit formation*. Long-range investigations should continue in each of the underlying theoretical areas summarized above, as well as others beyond the scope of this brief paper (see,*eg.*,[C4,G1,2, R7,8,11,13,14]. Only then will it be possible to provide engineers with significantly better "tools" for making rational assessments of particulate deposition phenomena in future, high-performance equipment. We hope this brief overview and the reasonably complete bibliography of our work (including titles; Section 8) will accelerate this process *via* the requisite and timely exchange of R&D information among PTF-participants.

8. LITERATURE CONTRIBUTIONS: DEPOSITION/DEPOSIT FUNDAMENTALS

[C1] Castillo, J.L., and Rosner, D.E. "Non-equilibrium Theory of Surface Deposition from Particle-Laden, Dilute Condensible Vapor -Containing Streams, Allowing for Particle Thermophoresis and Vapor Scavenging within the Laminar Boundary Layer", *Int. J. Multiphase Flow*, **14** (1), 99-120(1988)

[C2] Castillo, J.L. and Rosner, D.E., "Surface Deposition from a Binary Dilute Vapor-Containing Stream, Allowing for Equilibrium Condensation within the Laminar Boundary Layer", *I. J. Multiph Flow*, **15**, [1], 97-118 (1989)

[C3] Castillo, J.L., Garcia-Ybarra, P. and Rosner, D.E., "Morphological Instability of a Thermophoretically Growing Deposit", *J. Crystal Growth* **116**, 105-126,(1991)

[C4] Castillo, J.L., Mackowski, D.W., and Rosner, D.E., "Photophoretic Contribution to the Transport of Absorbing Particles Across Combustion Gas Boundary Layers", ACS Symposium Issue: **Ash Deposition**, *Prog. Energy and Comb. Sci.* **16**, 253-260 (1989)

[E1] Eisner,A. and Rosner, D.E., "Experimental Studies of Soot Particle Thermophoresis in Non-isothermal Combustion Gases Using Thermocouple Response Techniques", *Comb. & Flame* **61**, 153-166 (1985)

[F1] Fernandez de la Mora, J., and Rosner, D.E.,"Inertial Deposition of Particles Revisited and Extended: Eulerian Approach to a Traditionally Lagrangian Problem", *J. Physicochemical Hydrodynamics (PCH)* (Pergamon) **2**, 1-21 (1981); see, also *J. Fluid Mech* **125**, 379-395 (1982)

[G1] Garcia-Ybarra, P. and Rosner, D.E., "Thermophoretic Properties of Non-spherical Particles and Large Molecules", *AIChE J.* **35** (1), 139-147 (1989)

[G2] Gokoglu, S. A. and Rosner, D.E., "Correlation of Thermophoretically-Modified Small Particle Diffusional Deposition Rates in Forced Convection Systems with Variable Properties, Transpiration Cooling and/or Viscous Dissipation", *Int. J. Heat Mass Transfer* **27**, 639-645 (1984)

[G3] Gomez, A. and Rosner D. E. (1991) "Thermophoretic Effects on Particles in Counterflow Laminar Diffusion Flames", *Comb. Sci. Tech.* **89** 335-362 (1993)

[I1] Israel, R. and D. E. Rosner, "Use of Generalized Stokes Number to Determine the Aerodynamic Capture Efficiency of Non-Stokesian Particles from a Compressible Gas Flow", *Aerosol Sci. Tech.*, **2**, 45-51 (1983)

[K1] Konstandopoulos, A.G., and Rosner, D.E., "Studies of Combined Effects of Particle Inertia and Thermophoresis on Deposition Rates Across Laminar Combustion Gas Boundary Layers" *Int. J. Heat Mass Transfer* (in press,1994)

[K2] Konstandopoulos, A.G., Labowsky, M.J. and Rosner, D.E.,"Inertial Deposition of Particles from Potential Flows Past Cylinder Arrays" *J. Aerosol Science* (Pergamon) **24** (4) 471-483 (1993)

[K3] Konstandopoulos, A. G. "A Micro-Mechanical Approach to Particle Capture and Deposit Growth" (Ch.5, PhD Dissertation: **Effects of Particle Inertia on Aerosol Transport and Deposit Growth Dynamics**, Yale University ChE, ME Depts. (1991)

[L1] Liang, B. and Rosner, D.E., " Laboratory Studies of Binary Salt CVD in Combustion Gas Environments", *AIChE J.* **33** (12) , 1937-1948 (1987)

[L2] Liang B., Gomez, A., Castillo J. and Rosner D.E., "Experimental Studies of Nucleation Phenomena within Thermal Boundary Layers-Influence on CVD Rate Processes", *Chem. E Commun* **85**,113-133 (1989)

[M1] Marner, W.J.,"Progress in Gas-Side Fouling of Heat Exchanger Surfaces", in **Proc. A.L. London Symposium on Compact Heat Exchangers**, pp 421-489, Hemisphere, Washington DC.(1989); also available as: ASME Book # AMR069 or *Appl. Mech Rev* **43** (3), 35-66 March (1990)

[P1] Park, H. M. and Rosner D. E., "Combined Inertial and Thermophoretic Effects on Particle Deposition Rates in Highly Loaded Dusty Gas Systems", *Chem. Eng. Sci.*, **44** (10), 2233-2244 (1989)

[R1] Rosner, D.E. and Park, H. M., "Thermophoretically-Augmented Mass-, Momentum- and Energy-Transfer Rates in High Particle Mass-Loaded Forced Convection Systems", *Chem. Engng. J.*, **43**(10) 2689-2704 (1988).

[R2] Rosner, D.E., "Total Mass Deposition Rates from 'Polydispersed' Aerosols"; *AIChE J.* **35**, [1], 164-167 (1989)

[R3] Rosner D.E. and Tassopoulos M., "Mass Deposition Rates from Streams Containing 'Polydispersed' Particle Populations of Arbitrary Spread", *AIChE J.* **35** (9) 1497-1508 (1989)

[R4] Rosner, D.E., "Experimental and Theoretical Research on the Deposition Dynamics of Inorganic Compounds from Combustion Gases"; *J. PhysicoChem Hydrodynamics* (PCH) (Pergamon) **10**, [5/6], 663-674 (1988)

[R5] Rosner, D. E. and Kim, S. S. "Optical Experiments on Thermophoretically Augmented Submicron Particle Deposition from 'Dusty' High Temperature Gas Flows", *Chem. Engng. J.*, **29**, pp. 147-157 (1984).

[R6] Rosner, D.E., and Nagarajan, R., "Toward a Mechanistic Theory of Deposit Growth from Ash-Laden Flowing Combustion Gases: Self-Regulated Sticking of Impacting Particles and Deposit Erosion in the Presence of Vapor 'Glue'", in *AIChE Symposium Series*, **83**, No. 257, **Heat Transfer-Pittsburgh 1987** (R.W. Lyczkowski, ed.) 289-296 (1987)

[R7] Rosner, D.E., Mackowski, D.W., and Garcia-Ybarra, P., "Size- and Structure-Insensitivity of the Thermophoretic Transport of Aggregated 'Soot' Particles in Gases", *Combustion Science and Technology* **80**,(1-3),87-101(1991)

[R8] Rosner, D.E., Mackowski, D.W., Tassopoulos, M., Castillo, J., Garcia-Ybarra, P., "Effects of Heat Transfer on the Dynamics and Transport of Small Particles Suspended in Gases", *Ind/Engrg. Chem-Res* (ACS) **31**,760-769 (1992)

[R9] Rosner, D.E. and Tandon, P., "Rational Prediction of Inertially-Induced Particle Deposition Rates on a Cylindrical Target in Dust-Laden Streams: Effects of Single-Particle Capture Law and Dust Polydispersity on Deposition Rates and Associated Convective Heat Transfer Reductions" , HTCRE Paper No. 202 , March 1994

[R10] Rosner, D.E., Konstandopoulos, A., Tassopoulos, M. and Mackowski, D.W., "Deposition Dynamics of Combustion-Generated Particles: Summary of Recent Studies of Particle Transport Mechanisms, Capture Rates and Resulting Deposit Microstructure/Properties", in **Inorganic Transformations and Ash Deposition During Combustion**, (S.A.Benson, ed)., Engineering Foundation/ASME, (1992); pp 585-606

[R11] Rosner, D. E. and Fernandez de la Mora J. , "Correlation and Prediction of Thermophoretic and Inertial Effects of Particulate Deposition from Non-Isothermal Turbulent Boundary Layers", in **Particulate Laden Flows in Turbomachinery**, (W. Tabakoff, C. T. Crowe and D. B. Cale, eds.), ASME, NY, 85-94 (1982)

[R12] Rosner, D. E. and Fernandez de la Mora J. , "Boundary Layer Effects on Particle Impaction and Capture", *ASME Trans.--J. Fluid Engrg.*, **106**, 113-114 (1984)

[R13] Rosner, D. E., Gunes D., and Anous N. , "Aerodynamically-Driven Condensate Layer Thickness Distributions on Isothermal Cylindrical Surfaces", *Chem. Engrg. Comm.*, **24**, 275-287 (1983)

[R14] Rosner, D. E., Gokoglu, S. and Israel, R., "Rational Engineering Correlations of Diffusional and Inertial Particle Deposition Behavior in Non-Isothermal Forced Convection Environments", in **Fouling and Heat Exchanger Surfaces**, Engrg. Foundation, NY, 235-256 (1983)

[R15] Rosner, D. E., **Transport Processes in Chemically Reacting Flow Systems**, Butterworth-Heinemann Publishers, Stoneham, MA (1986); 3d Printing Dec 1990, 4th Printing (Contact Author Directly)

[R16] Rosner, D.E. and Atkins, R.M., "Experimental Studies of Salt/Ash Deposition Rates from Combustion Products Using Optical Techniques", in **Fouling and Slagging Resulting From Impurities in Combustion Gases** (Bryers, R. W., ed.), Engineering Foundation, NYC, Publication No. 81-18 (1983), pp.469-492; in particular: Rosner, D.E., Appendix: "Recent Advances in the Theory of Deposition From Combustion Gases", pp. 486-492

[R17] Rosner, D.E., Chen, B.K., Fryburg, G., Kohl, F.J. ,"Chemically Frozen Multi-component Boundary Layer Theory of Salt and/or Ash Deposition Rates From Combustion Gases", *Comb. Sci. Tech.* **20**, 87-106 (1979)

[T1] Tassopoulos, M., **Relationships Between Particle Deposition Mechanism and Resulting Deposit Microstructure/Effective Transport Properties**, PhD Dissertation, Yale University, Dept. ChE (1991)

[T2] Tassopoulos, M. and Rosner, D.E., "Simulation of Vapor Diffusion in Anisotropic Particulate Deposits", *Chem. Eng. Sci.* **47**(2) 421-443 (1991)

[T3] Tassopoulos, M. and Rosner, D.E.,"The Effective Thermal Conductivity of Anisotropic Packings of Spheres" (Part 1."Conduction Through the Solid Phase"; Part 2."Conduction Through the Solid and Void Phases"), *Chem. Eng. Sci.* (in press(1994))

[T4] Tassopoulos, M. and Rosner, D.E., "Microstructural Descriptors Characterizing Granular Deposits", *AIChE J.* **38**(1) 15-25 (1991)

[T5] Tassopoulos, M., O' Brien, J. A. and Rosner D. E., "Simulation of Microstructure-Mechanism Relationships in Particle Deposition, *AIChE J.* **35** (6) 967-980 (1988)
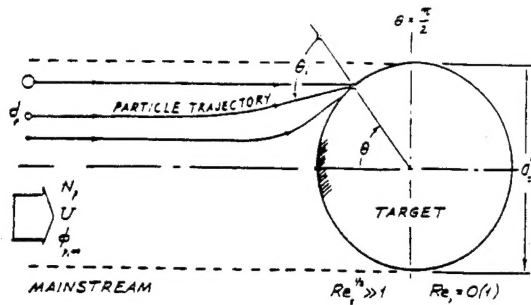
Fig. 1 'Fouling' of a heat exchanger surface (here circular cylinder in high Reynolds number crossflow) in response to the arrival of impacting particles log-normally distributed with respect to size. Particle *capture fraction s* dependent on incident velocity (Fig. 2) and angle θ_i [R 9]
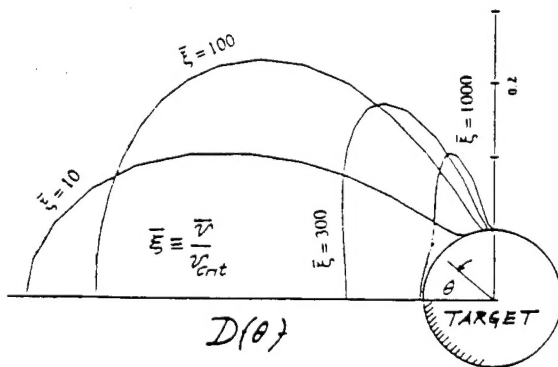

Fig. 2 Single particle *capture probability laws* (particle velocity dependence) considered [R9]. Cases shown: capture on a clean solid surface; and incident particle capture by a *granular deposit* (after [K3])

Fig. 3 Polar plot of local dimensionless *deposition rate* on a circular cylinder in crossflow for several values of the particle population size parameter $\bar{v}/v_{crit}$; Cases shown: Threshold velocity for critical size particle *rebound* equal to ten times the mainstream velocity, U (after [R9]).Note tendency to form off-axis 'lobes' when $\bar{v}/v_{crit}$ exceeds about 100.

Fig. 4 Upwind cylinder surface-averaged deposition rate function dictating convective *heat transfer reductions* (*via* Eq. (3)). Dependence on mean particle size (volume) in the mainstream population for each class of particle sticking fraction law (Fig. 2). (after [R 9])
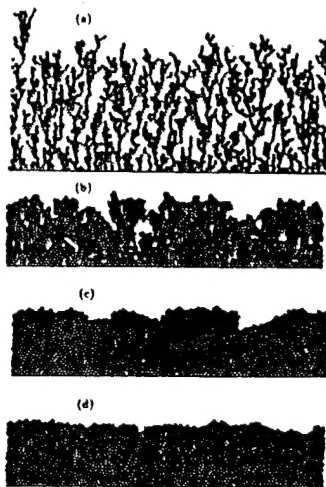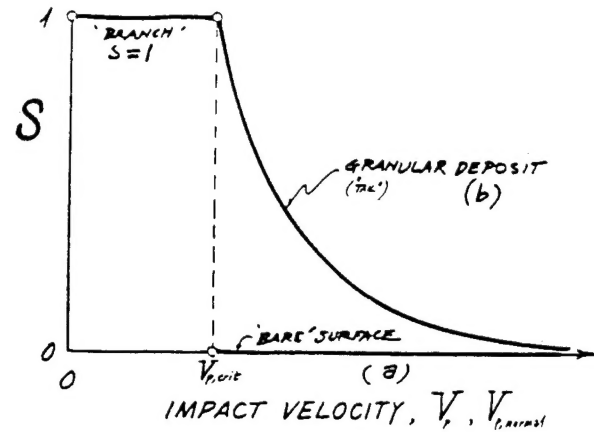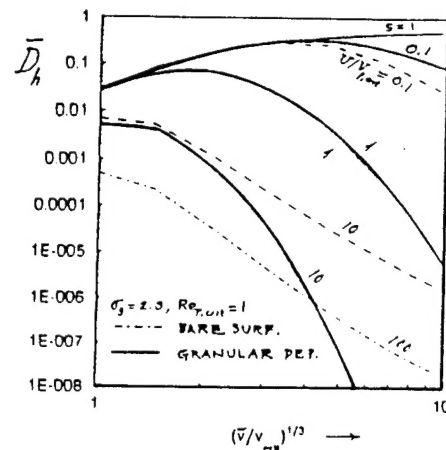

Fig.5 Particle-level computer simulation (2D) of microstructures for granular deposits of uniform size spoherical particles (after [T1,4]). Cases shown: "algorithmic" deposits with various degrees of "restructuring" (0-,1-,2-,3-"rolling" events after initial impact; normal 'ballistic' incidence)
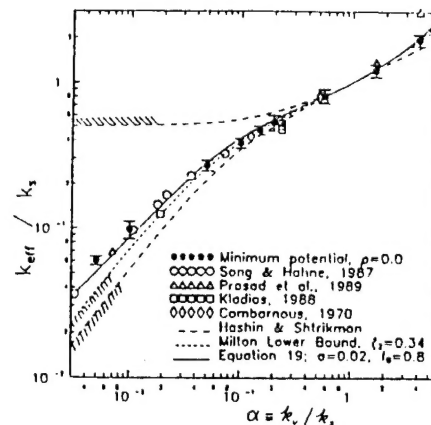

Fig. 6 Effective orientation-averaged thermal conductivity of anisotropic computer-simulated granular deposits comprised of uniform-sized spherical particles (after Refs. [T1,3]). Brownian 'heat tracer' simulation results as a function of 'void'/particle thermal conductivity ratio. Also shown: experimental data and rigorous theoretical bounds.